

AD-A054 161

SOUTHERN METHODIST UNIV DALLAS TEX DALLAS GEOPHYSICAL LAB F/G 8/11
GEOPHYSICAL MODEL STUDIES OF THE TULAROSA BASIN, NEW MEXICO.(U)
DEC 77 R E REINKE, E HERRIN

AFOSR-76-2890

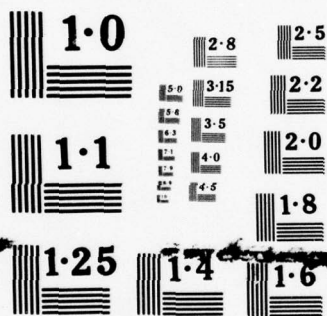
UNCLASSIFIED

AFOSR-TR-78-0779

NL

1 OF 2
ADA
054161





NATIONAL BUREAU OF STANDARDS
MICROCOPY RESOLUTION TEST CHART

AFOSR-TR- 78 - 0779

FOR FURTHER TRAN *11.11*

(2)

5c

AD A 054161

AD NO.

DDC FILE COPY

See 1473

DDC
RECEIVED
MAY 17 1978
B

DISTRIBUTION STATEMENT A
Approved for public release;
Distribution Unlimited

AIR FORCE OFFICE OF SCIENTIFIC RESEARCH (AFSC)
NOTICE OF TRANSMITTAL TO DDC
This technical report has been reviewed and is
approved for public release IAW AFR 190-12 (7b).
Distribution is unlimited.
A. D. BLOSE
Technical Information Officer

UNCLASSIFIED

SECURITY CLASSIFICATION OF THIS PAGE (When Data Entered)

19 REPORT DOCUMENTATION PAGE		READ INSTRUCTIONS BEFORE COMPLETING FORM
1. REPORT NUMBER AFOSR-TR-78-0779	2. GOVT ACCESSION NO.	3. RECIPIENT'S CATALOG NUMBER
4. TITLE (and Subtitle) GEOPHYSICAL MODEL STUDIES OF THE TULAROSA BASIN, NEW MEXICO		5. TYPE OF REPORT & PERIOD COVERED Scientific Final
		6. PERFORMING ORG. REPORT NUMBER
7. AUTHOR(s) Robert E Reinke Eugene Herrin		8. CONTRACT OR GRANT NUMBER(s)
9. PERFORMING ORGANIZATION NAME AND ADDRESS Dallas Geophysical Laboratory Southern Methodist University Dallas, TX 75275		10. PROGRAM ELEMENT, PROJECT, TASK AREA & WORK UNIT NUMBERS 2309/A1 61102F
11. CONTROLLING OFFICE NAME AND ADDRESS AFOSR/NP Bolling AFB, Bldg. #410 Wash DC 20332		12. REPORT DATE DECEMBER 1977
14. MONITORING AGENCY NAME & ADDRESS (if different from Controlling Office) Final technical rept.		13. NUMBER OF PAGES 171
15. SECURITY CLASS. (of this report) Unclassified		15a. DECLASSIFICATION/DOWNGRADING SCHEDULE
16. DISTRIBUTION STATEMENT (of this Report) Approved for public release; distribution unlimited.		
17. DISTRIBUTION STATEMENT (of the abstract entered in Block 20, if different from Report)		
18. SUPPLEMENTARY NOTES		
19. KEY WORDS (Continue on reverse side if necessary and identify by block number)		
20. ABSTRACT (Continue on reverse side if necessary and identify by block number) <p>The Tularosa and Jornada del Muerto Basins are two prominent north-south valleys in southern New Mexico. In 1975 two one hundred ton TNT equivalent tests were conducted in the Tularosa Basin by the Defense Nuclear Agency as part of the Dice Throw high explosive test series. In 1976, 620 tons of explosive were detonated in the Jornada del Muerto. Seismic records of these events revealed apparent anomalous surface wave propagation within the basins. Results of a shear wave refraction profile as well as reflection, gravity, and magnetic data have been used as input for theoretical computation of Rayleigh wave</p>		

DD FORM 1 JAN 73 1473 EDITION OF 1 NOV 65 IS OBSOLETE

UNCLASSIFIED

SECURITY CLASSIFICATION OF THIS PAGE (When Data Entered)

407 712

characteristics within the basins. The theoretically predicted group and phase velocities, as well as ellipticities, correlate well with those measured from seismic records of the surface waves excited within the basin. In general, the slowest surface wave group corresponds to the fundamental mode of the Rayleigh wave, while the earlier surface wave arrival can be correlated with the higher modes of the Rayleigh wave. The observed surface wave behavior has placed additional constraints upon the interpretation of the geophysical surveys of the basins.

UNCLASSIFIED
 SECURITY CLASSIFICATION OF THIS PAGE(When Data Entered)

2

FINAL TECHNICAL REPORT

to the

AIR FORCE OFFICE OF SCIENTIFIC RESEARCH

from

Robert E. Reinke

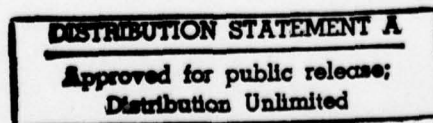
and

Eugene Herrin

Dallas Geophysical Laboratory
Southern Methodist University
Dallas, Texas 75275

Name of Contractor: Southern Methodist University
Effective Date of Contract: July 1, 1975
Contract Expiration Date: February 28, 1977
Total Amount of Contract Dollars: \$26,513
Contract Number: AFOSR-76-2890
Principal Investigator and Phone Number: Eugene Herrin
AC 214 692-2760
Program Manager and Phone Number: Truman Cook, Director of
Research Administration
AC 214 692-2031
Title of Work: Geophysical Model Studies of the
Tularosa Basin, New Mexico
University Account Number: 80-78

Sponsored by
Air Force Office of Scientific Research



SURFACE WAVE PROPAGATION
IN THE TULAROSA AND JORNADA DEL MUERTO BASINS,
SOUTH CENTRAL NEW MEXICO.

ACCESSION for		
NTIS	White Section	<input checked="" type="checkbox"/>
DOC	Buff Section	<input type="checkbox"/>
UNANNOUNCED		<input type="checkbox"/>
JUSTIFICATION _____		
BY _____		
DISTRIBUTION/AVAILABILITY CODES		
Dist.	AVAIL.	and/or SPECIAL
A		

Robert Edward Reinke
Geophysical Laboratory
Southern Methodist University
December 1977

Reinke, Robert Edward

B. A. University of Dallas,
1972

SURFACE WAVE PROPAGATION IN THE TULAROSA AND JORNADA DEL
MUERTO BASINS, SOUTH CENTRAL NEW MEXICO.

Advisor: Professor Eugene T. Herrin

The Tularosa and Jornada del Muerto Basins are two prominent north-south valleys in southern New Mexico. In 1975 two one hundred ton TNT equivalent tests were conducted in the Tularosa Basin by the Defense Nuclear Agency as part of the Dice Throw high explosive test series. In 1976 620 tons of explosive were detonated in the Jornada del Muerto. Seismic records of these events revealed apparent anomalous surface wave propagation within the basins. Results of a shear wave refraction profile as well as reflection, gravity, and magnetic data have been used as input for theoretical computation of Rayleigh wave characteristics within the basins. The theoretically predicted group and phase velocities, as well as ellipticities, correlate well with those measured from seismic records of the surface waves excited within the basin. In general, the slowest surface wave group corresponds to the fundamental mode of the Rayleigh wave, while the earlier surface wave arrival can be correlated with the higher modes of the Rayleigh wave. The observed surface wave behavior has placed additional constraints upon the interpretation of the geophysical surveys of the basins.

TABLE OF CONTENTS

	Page
ACKNOWLEDGEMENTS.....	iv
LIST OF ILLUSTRATIONS.....	vi
INTRODUCTION.....	1
THE SEISMIC REFRACTION SURVEY.....	13
GRAVITY AND MAGNETIC DATA.....	41
SURFACE WAVE PROPAGATION IN THE TULAROSA BASIN.....	55
SURFACE WAVE PROPAGATION IN THE JORNADA DEL MUERTO....	124
CONSIDERATIONS FOR PREDICTION OF SURFACE WAVE GROUND MOTION LEVELS IN ALLUVIAL VALLEYS.....	145
DISCUSSION AND CONCLUSIONS.....	151
REFERENCES CITED.....	157

ACKNOWLEDGEMENTS

Funds for this research were provided by the U. S. Air Force Office of Scientific Research under contract AFOSR-76-2890 monitored by Mr. William J. Best. The author was partially supported during the study by a National Science Foundation traineeship under NSF Grant 85-52 to Southern Methodist University. This grant also provided partial funding of computer expense.

The work could not have been completed without the encouragement and assistance of Professor Eugene Herrin. The author benefitted greatly from many discussions with Dr. Tom Goforth. Nancy Cunningham assisted in computer operation and software development.

Lou Karably, Steve Melzer, and Al Schenker of the Air Force Weapons Laboratory made available much of the data used in the study in addition to providing many valuable suggestions.

Dr. Roger Turpening of ERIM made available the records of the P and SH refraction surveys. Abby Liskow of ERIM made the first break picks and plotted the travel times.

Dr. John Hoffman of the Albuquerque Seismological Labora-

tory made available digital tape records of the ASL stations.

Dr. Jack Murphy of Computer Sciences Corporation made some valuable suggestions.

Karl Thomason and John Farris assisted in the operation of the SMU seismic stations. Betty Sielert of Universal Security and Don Duquette of DynaElectron Corp., Stallion Range Center, White Sands Missile Range, also provided assistance during the SMU field operations.

Liebe Purnell patiently assisted in manuscript preparation.

The author's wife, Susan, also assisted in manuscript preparation and provided constant support and encouragement throughout the course of the study.

LIST OF ILLUSTRATIONS

Figure		Page
1	Index map of Tularosa Basin area.	2
2	Cross section through the southern portion of the San Andres Mountains.	5
3	Test area in Jornada del Muerto. Solid contours indicate complete Bouguer anomaly; dotted lines, residual anomaly.	6
4	Test area of Tularosa Basin. Solid contours indicate complete Bouguer anomaly; dotted lines, residual anomalies.	7
5	Vertical component, SMU station, pre-Dice Throw, August 12, 1975.	9
6	Vertical component, SMU station, Dice Throw, October 6, 1976.	11
7	Seismogram recorded by Leet at Trinity test, July, 1945.	12
8	Location of ERIM survey line.	14
9	Location of reflection line. Contours indicate elevation in feet of base of Tertiary(?).	15
10	Section of SH record from Salt Flats shotpoint.	16
11	Section of SH record from Road shotpoint.	17
12	SH travel time curves.	18
13	Field example of low velocity layer in a P wave refraction profile.	21

Figure		Page
14	P wave travel time curves.	22
15	Idealized SH velocity-depth structure.	24
16	Travel time curves in the presence of a low velocity layer.	25
17	Idealized P velocity-depth structure.	27
18	Comparison of P and S travel time curves for a simple layered model.	28
19	Cross section from reflection profile along ERIM survey line.	31
20	Lower section of pre-Tertiary strata in San Andres Mountains.	35
21	Upper section of pre-Tertiary strata in San Andres Mountains.	36
22	Cross section interpreted from gravity data in the Tularosa Basin.	43
23	Location of cross section and gravity survey points.	45
24	Elevation of top of consolidated rock in the Tularosa Basin.	46
25	Stratigraphic section showing formation densities.	48
26	Elevation in feet of base of Tertiary(?) in Dice Throw test area.	51
27	IGRF map of northern portion of Tularosa Basin.	52
28	Corrected residual magnetic map.	53
29	ASL station locations for August, 1975, pre-Dice Throw event.	57
30	Recording from L-7 system at station E-9000. August, 1975, event.	58

Figure		Page
31	Recording from station E-16000. August, 1975, event.	59
32	Recording from station E-24000. August, 1975, event.	60
33	Recording from station E-35000. August, 1975, event.	61
34	Recording from station E-LAVA. August, 1975, event.	62
35.	Recording from station W-12000. August, 1975, event.	63
36	Recording from station W-15000. August, 1975, event.	64
37	ASL station locations for August, 1975, event.	65
38	L-7 system recording from station E-16000. September, 1975, event.	66
39	Recording from station E-24000. September, 1975, event.	67
40	Recording from station OR-1. September, 1975, event.	68
41	Recording from station OR-2. September, 1975, event.	69
42	Recording from station OR-3. September, 1975, event.	70
43	Recording from station W-9000. September, 1975, event.	71
44	Recording from station W-15000. September, 1975, event.	72
45	Recording from SMU station south of the Malpais. September, 1975, event.	76
46	Comparison of spectra of first and second surface wave groups received at SMU sta- tion. August, 1975, event.	74

Figure		Page
47	Particle motion of first surface wave group. E-16000. August, 1975.	78
48	Particle motion of second surface wave group. E-16000. August, 1975.	79
49	Particle motion of first surface wave group. E-35000. August, 1975.	80
50	Particle motion of second surface wave group. E-35000. August, 1975.	81
51	Particle motion of first surface wave group. E-LAVA. August, 1975.	82
52	Particle motion of second surface wave group. E-LAVA. August, 1975.	83
53	Particle motion of surface wave group. W-12000. August, 1975.	84
54	Particle motion of first surface wave group. W-15000. August, 1975.	85
55	Particle motion of second surface wave group. W-15000. August, 1975.	86
56	Particle motion of surface wave group. (two wave groups not distinct). W-9000. September, 1975.	87
57	Particle motion of first surface wave group. W-15000. September, 1975.	88
58	Particle motion of second surface wave group. W-15000. September, 1975.	89
59	Particle motion of first surface wave group. E-24000. August, 1975.	90
60	Particle motion of second surface wave group. E-24000. August, 1975.	91
61	Particle motion of first surface wave group. E-24000. September, 1975.	92
62	Particle motion of second surface wave group. E-24000. September, 1975.	93

Figure		Page
63	Comparison of observed phase velocities at SMU station with those computed for model 1.	96
64	Comparison of observed group velocities at SMU station with those computed for model 1.	100
65	Layered models for Tularosa Basin.	98
66	Comparison of observed group velocities at E-35000 and E-LAVA with those computed for model 2.	103
67	Comparison of observed group velocities at SMU station with those computed for model 3.	104
68	Theoretical ellipticity for model 1.	109
69	Theoretical ellipticity for model 2.	110
70	Theoretical ellipticity for model 3.	111
71	Theoretical ellipticity for model 4.	112
72	Characteristic particle motion from OR-1.	114
73	Particle motion of first beat in surface wave group. SMU station south of the Malpais.	116
74	Particle motion of second beat in surface wave group. SMU station south of the Malpais.	117
75	Comparison of group velocities observed at SMU station south of the Malpais with those computed for model 4.	120
76	Comparison of spectra of first and second beats in surface wave group. SMU station south of the Malpais.	122
77	Recording from ERIM 16000 station.	126

Figure		Page
78	Recording from ERIM 25000 East station.	127
79	Recording from ERIM 25000 South station.	128
80	Recording from ERIM 35000 station.	129
81	Recording from ERIM 43000 station.	130
82	Recording from ERIM 62000 station.	131
83	Particle motion of first surface wave group. SMU station. October, 1976.	132
84	Particle motion of second surface wave group. SMU station. October, 1976.	133
85	Comparison of observed phase velocities at SMU station with Jornada model.	135
86	Layered model for Jornada del Muerto.	138
87	Comparison of observed group velocities at SMU station with those computed for Jornada model.	139
88	Theoretical ellipticity computed for Jornada model.	141
89	Theoretical spectral ratios. model 2/ model 1.	147
90	Theoretical spectral ratios. model 3/ model 1.	148
91	Theoretical spectral ratios. model 4/ model 1.	149
92	Generalized east-west cross section through the Tularosa Basin.	152

INTRODUCTION

The Tularosa Basin is a prominent north-south valley in southern New Mexico extending 125 miles (201 kilometers) southward from the vicinity of Carrizozo to the New Mexico-Texas border (Figure 1). Bounded on the east by Sierra Blanca and the Sacramento mountains and on the west by the Sierra Oscura, the San Andres, and Organ mountains, the basin has an average width of 30 miles (48 kilometers). In August and September, 1975, two one hundred ton TNT equivalent explosive tests were conducted in the Tularosa Basin by the Defense Nuclear Agency as part of the Dice Throw high explosive test series. Preliminary examination of seismic records from these events revealed apparent anomalous seismic wave propagation within the basin. In October of 1976, in the main Dice Throw event, 620 tons of explosive were detonated in the Jornada del Muerto, the valley immediately west of the Tularosa Basin. The research described in this paper centers about the study of the seismic surface waves excited within the Tularosa and Jornada del Muerto basins by these three high explosive detonations.

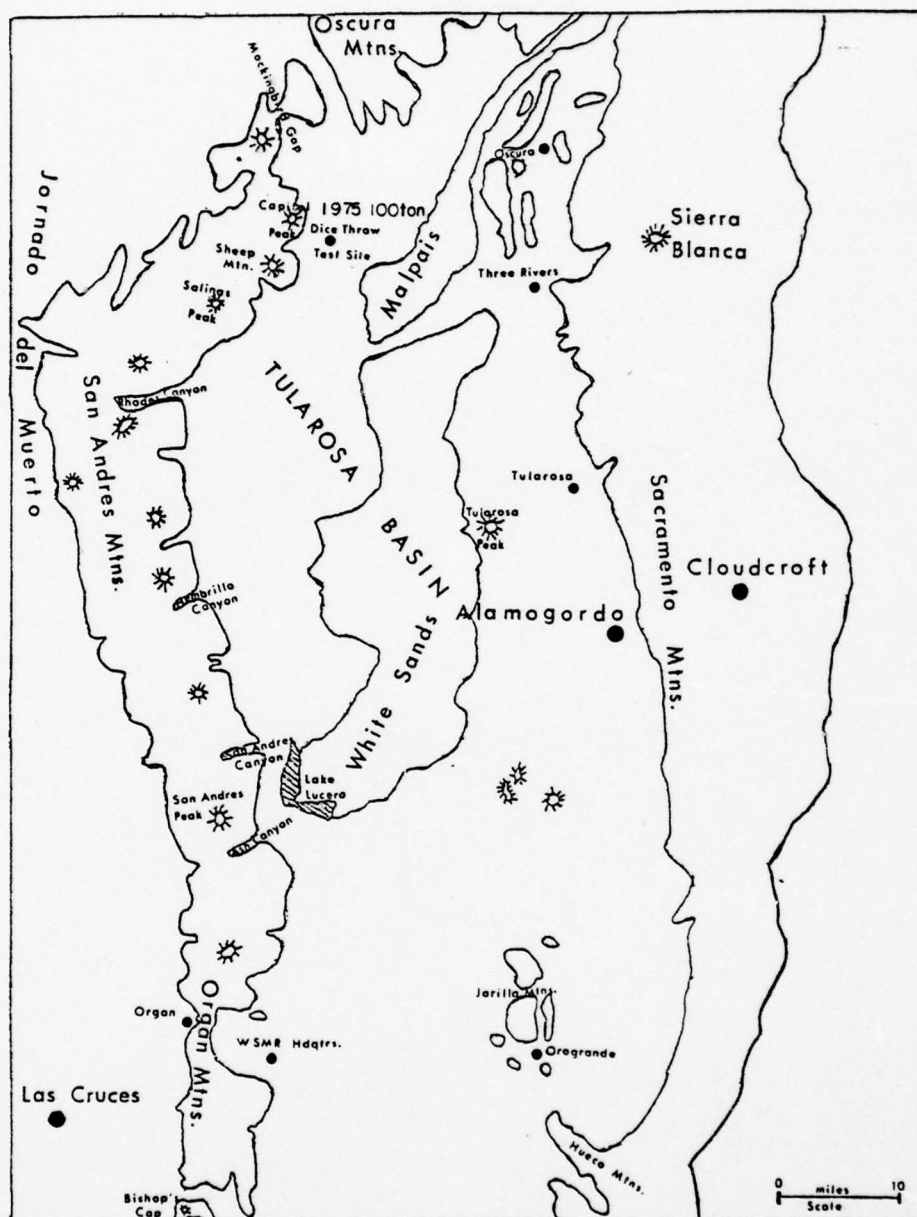


Figure 1. Index map of Tularosa Basin area (modified from Kottowski and others, 1956)

Geology and Structure

The Tularosa Basin is a graben. Although the relief within the basin is small, it is bounded on the east and west by mountains which are mostly tilted fault blocks rising from 3000 to 5000 feet (914 - 1524 meters) above the basin floor. Faulting has produced steep scarps on the west side of the Sacramento Mountains and on the east side of the San Andres Mountains. Strata in the San Andres Mountains dip gently to the west and to the east in the Sacramento Mountains. Permian rocks are exposed in several low hills trending north from the Jaxilla mountains, suggesting a partially buried fault block ridge, possibly formed by step faulting along the east side of the basin. The basin is bounded on the north by Chupadera Mesa, composed of nearly horizontal strata. The basin floor is underlain by unconsolidated bolson deposits which are more than 4000 feet (1219 meters) thick in the southern part.

Sedimentary rocks exposed along the mountain front range in age from Precambrian to Tertiary (?). As exposed in the San Andres Mountains, sedimentary rocks range in thickness from about 7200 feet (2194 meters) near Rhodes Canyon to about 10,000 feet (3047 meters) near Ash Canyon. Pre-Tertiary strata exposed in the San Andres Range are about 7200 feet (2194 meters) thick. Within the basin pre-Tertiary sedimentary rocks may

range from 12,700 feet (3870 meters) to 7200 feet (2194 meters) in thickness north to south.

Igneous and metamorphic rocks of Precambrian age crop out along the east flanks of the Organ and San Andres Mountains, along the west flank of the Sierra Oscura, and in a few places at the base of the Sacramento Mountains southeast of Alamogordo. The Organ Mountains and Sierra Blanca are composed mainly of batholithic rocks, flanked by volcanic rocks, both thought to be of Tertiary age. The youngest igneous rocks in the basin are found in the Malpais, an elongated north-south basalt flow of recent age extending from Carrizozo to the Three Rivers vicinity. (from Kottowski and others (1956), Herrick and Davis (1965), and Bachman, (1965).

The Jornada del Muerto is the basin immediately west of the Tularosa Basin. While the Tularosa basin is a graben valley, the Jornada is essentially a synclinal valley formed by the westward dipping sedimentary beds exposed in the San Andres Mountains. (Figure 2) North of Mockingbird Gap, however, the valley is bounded on the east by a major fault zone forming the Sierra Oscura. (Figure 3)

The Seismic Problem

The project Dice Throw 100 ton events of August and September, 1975, occurred near Capitol Peak, approximately 10 miles (16 kilometers) south of Mockingbird Gap (Figure 4). A 100 ton spherical charge of TNT tangent to the ground sur-

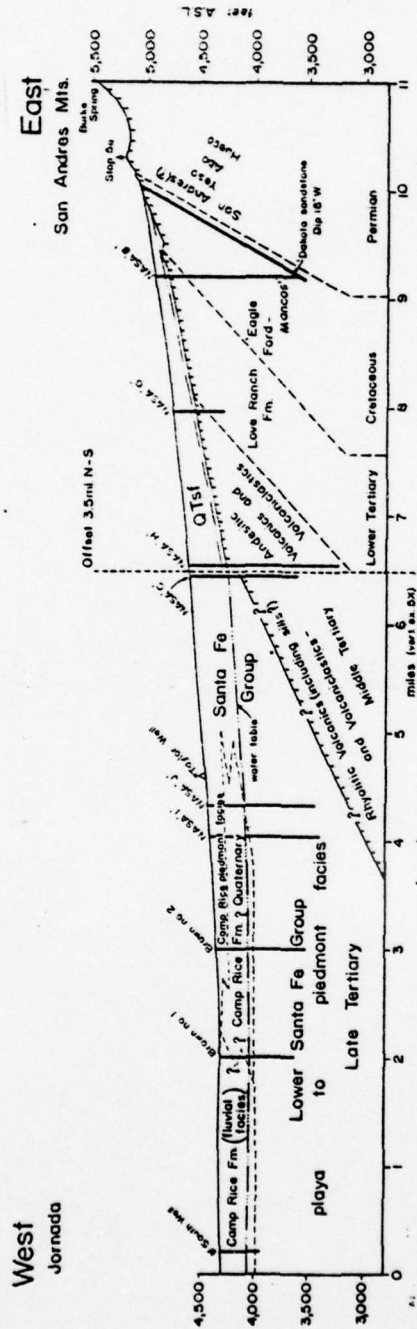


Figure 2. Cross section through the southern portion of the San Andres Mountains (from Kottlowski and Hawley, 1975)

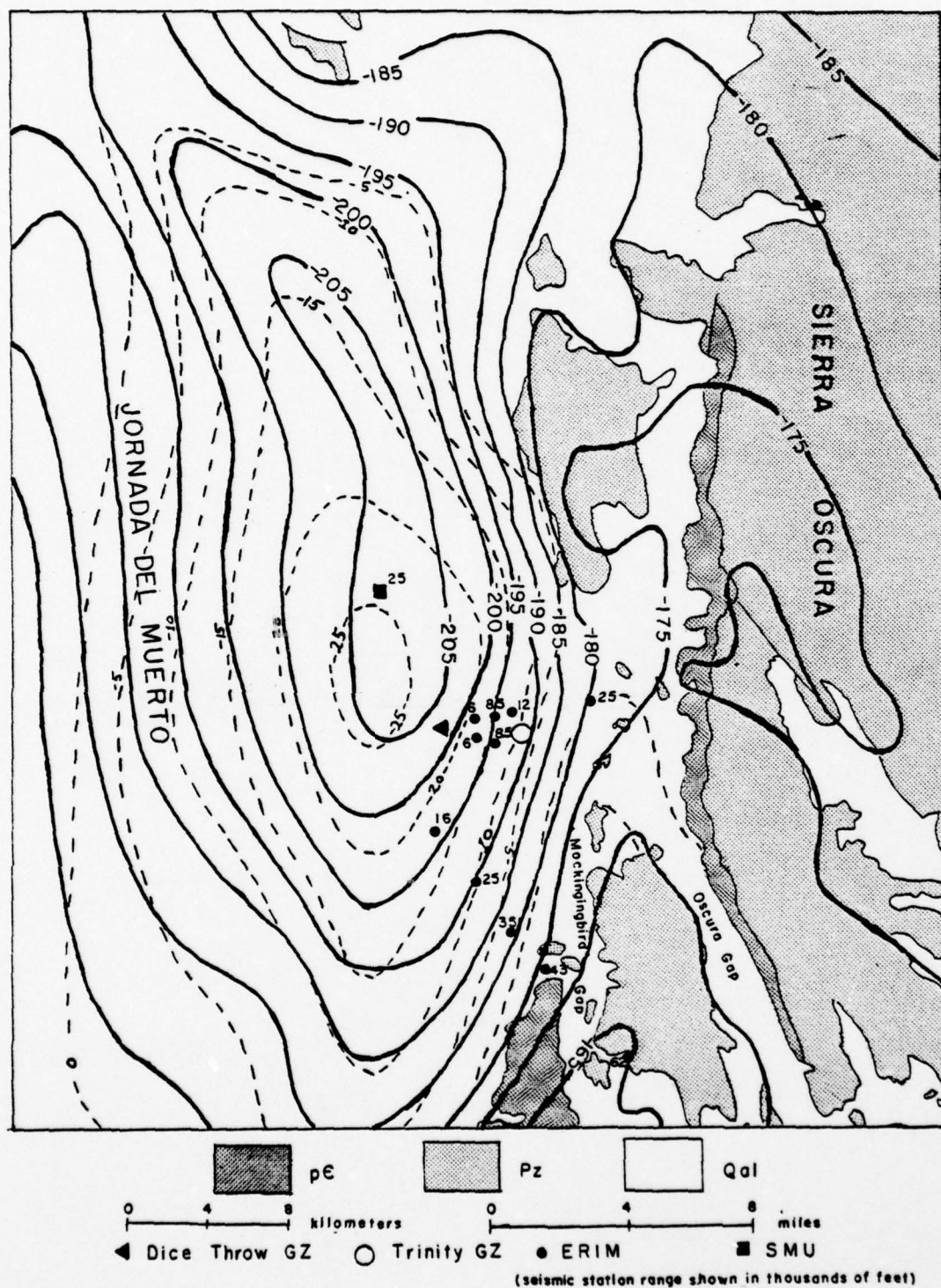


Figure 3. Test area in Jornada del Muerto. Solid contours indicate complete Bouguer anomaly; dotted lines, residual anomaly.

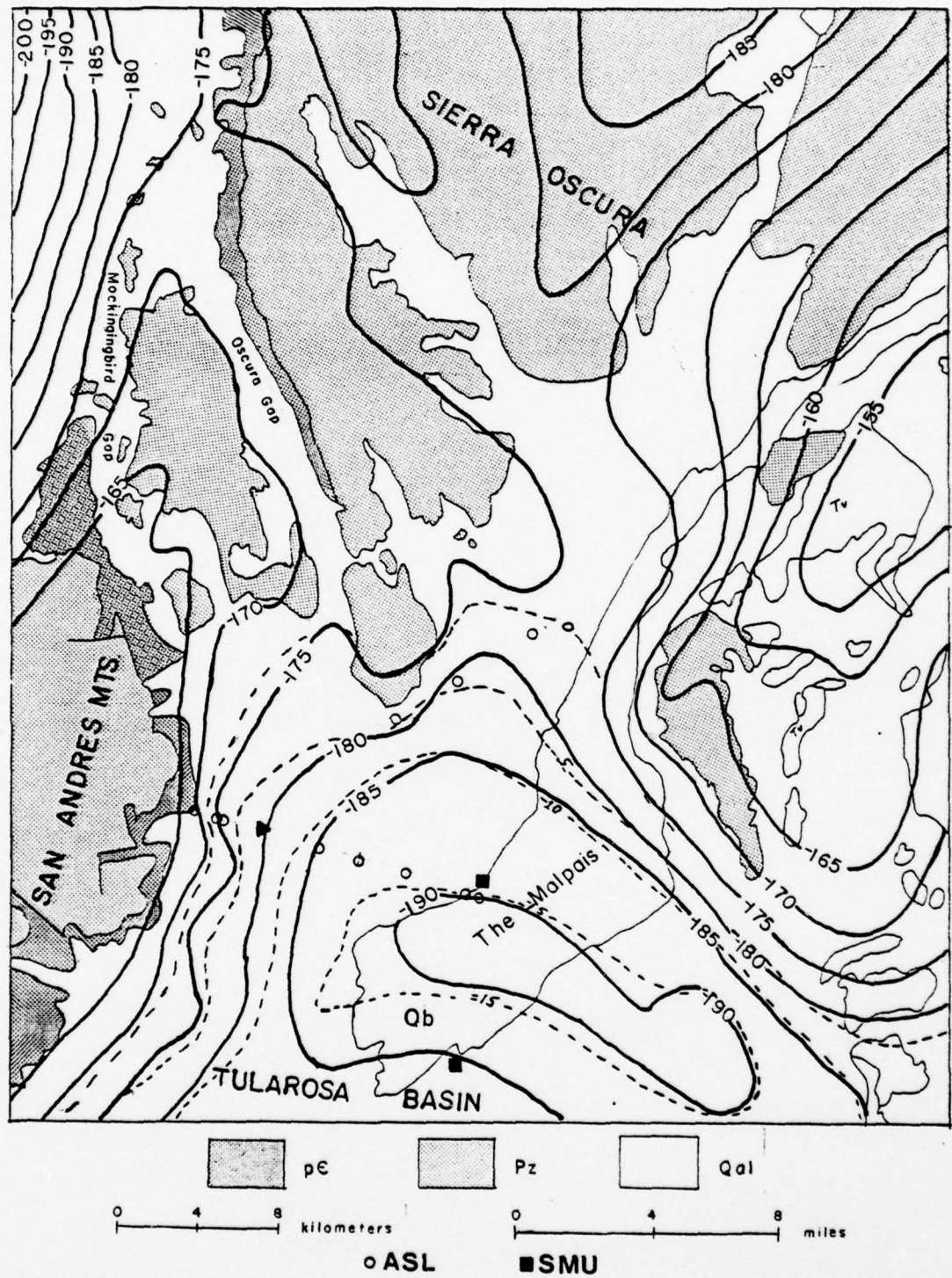


Figure 4. Test area of Tularosa Basin. Solid contours indicate complete Bouguer anomaly; dotted lines, residual anomalies.

face was detonated in pre-Dice Throw I. A spherically capped cylinder of 120 tons of ammonium nitrate - fuel oil mixture (ANFO) also placed on the surface was exploded in September, 1975, as pre-Dice Throw II.

An extensive array of seismic stations was in operation within the basin for both events. The four agencies involved in the seismic experiment were the Air Force Weapons Laboratory, the Environmental Research Institute of Michigan, the Albuquerque Seismological Laboratory, and Southern Methodist University. Distances from shot point to seismometer ranged up to 10 miles (16 kilometers) as shown in Figure 4. Preliminary examination of the seismic records revealed two well developed surface wave groups present at many stations. (Figure 5) Because of its appearance, the first surface wave arrival was initially thought to be the fundamental Rayleigh mode while the second wave group was referred to as the "X" wave.

In the main Dice Throw event of October 1976, 620 tons of ANFO were detonated on the surface of the Jornada del Muerto near Trinity site, where the test of the first atomic bomb occurred in 1945. (Figure 3.) The Environmental Research Institute of Michigan (ERIM) and Southern Methodist University (SMU) fielded an extensive seismic network for the shot as shown in Figure 3.

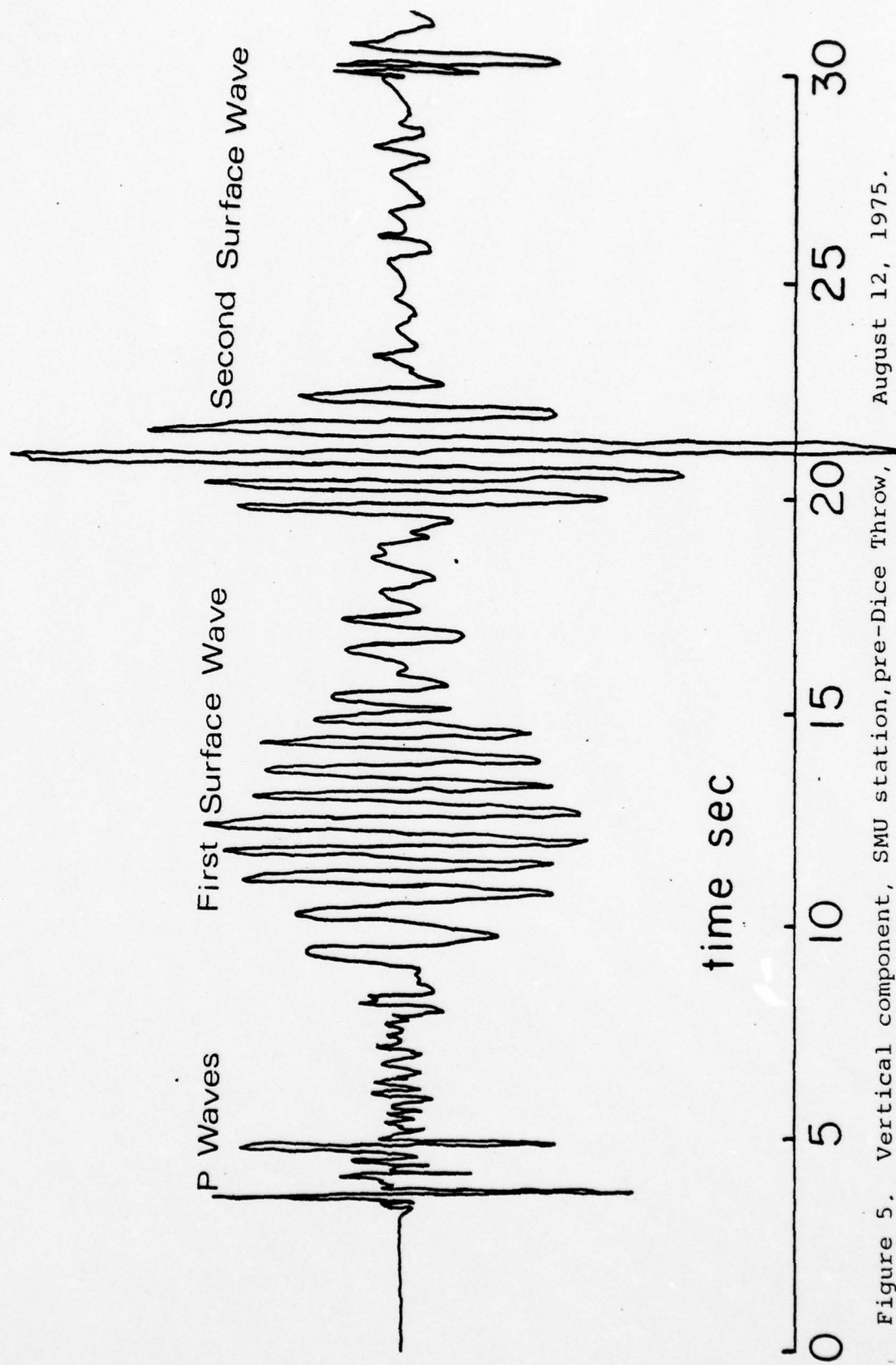


Figure 5. Vertical component, SMU station, pre-Dice Throw, August 12, 1975.

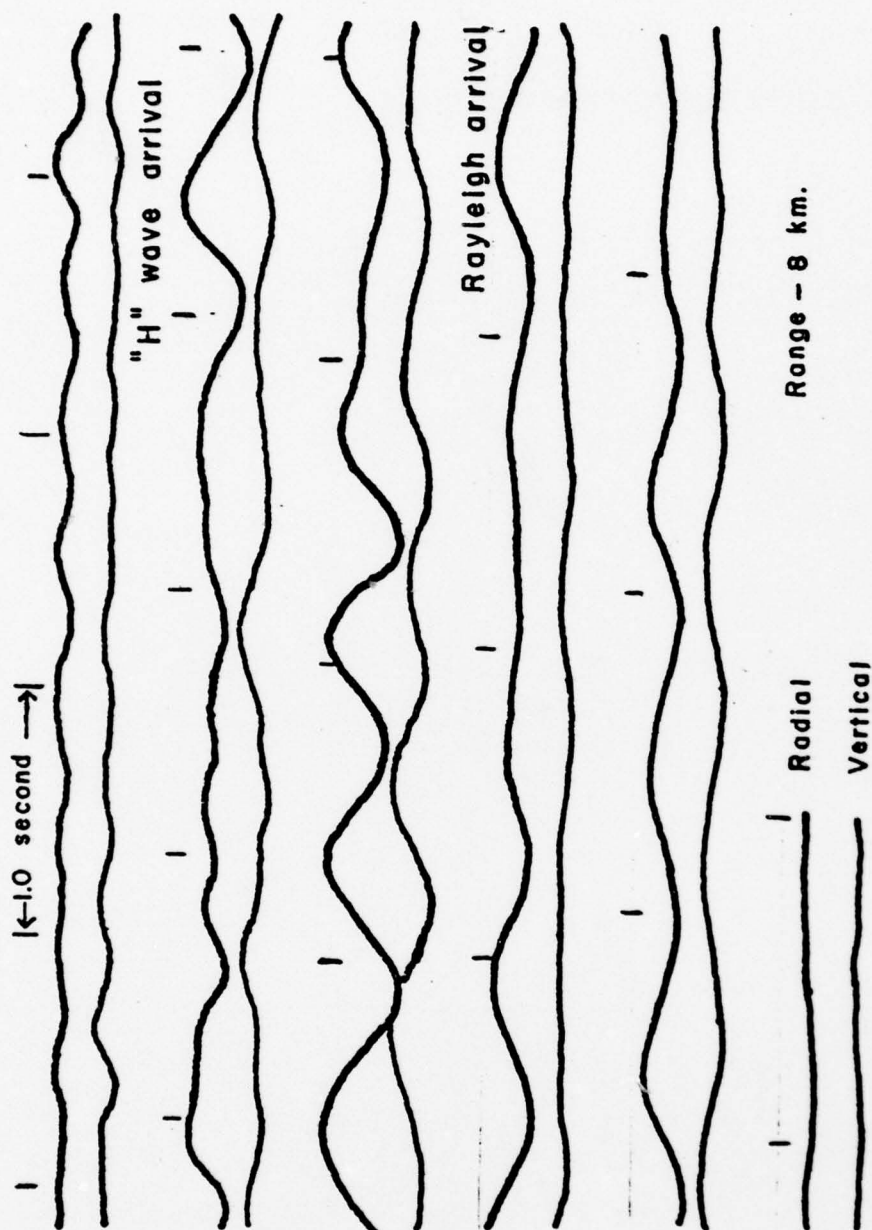
The seismic record of the October event from the SMU station at a distance of approximately 25,000 feet (7.5 kilometers) is shown in Figure 6. The record is quite similar to that recorded at the pre-Dice Throw events in the Tularosa Basin and also similar to a seismic recording of the Trinity event made by Leet (1946). (Figure 7)

Using data from seismic reflection and refraction surveys, and gravity and magnetic surveys, theoretical models which correlate well with observed wave characteristics have been developed for surface wave propagation within the Tularosa and Jornada del Muerto basins.

DICE THROW 500 TON
SMU VERTICAL 7.5 km.



Figure 6. Vertical component, SMU station,
Dice Throw, October 6, 1976.



RECORD OF EARTH MOTION, TRINITY TEST, JULY 16, 1945
(from Leet, 1946)

Figure 7. Seismogram recorded by Leet at
Trinity test, July, 1945.

THE SEISMIC REFRACTION SURVEY

In October of 1976 the Environmental Research Institute of Michigan conducted a shear wave refraction profile along a line 6000 feet (1828 meters) in length near the pre-Dice Throw test site (Figure 8). The survey line roughly coincided with a portion of a shallow reflection survey carried out earlier by Charles B. Reynolds and associates. (Figure 9) (Reynolds, 1976).

In the past, shear wave refraction profiles of over a few hundred feet in length have rarely been attempted. The hammer and plank technique has usually been employed as an SH wave source. The Environmental Research Institute of Michigan (ERIM) has developed a powerful cannon type SH wave generator which eliminates many of the problems encountered in shear wave refraction profiles. (Jackson and others, 1976) The ERIM shear wave generator is a water loaded cannon fired normal to a line of digitally recorded transverse geophones. For each recording, the cannon is fired twice. The direction of firing is reversed between shots producing SH waves of opposite polarity. P and SV waves generated are of the same polarity. When the geophone records for the two shots are plotted on the same time axis, accurate picks of the first SH breaks are made possible by the reversal of polarity as shown in Figure 10. In addition SH waves do not suffer from

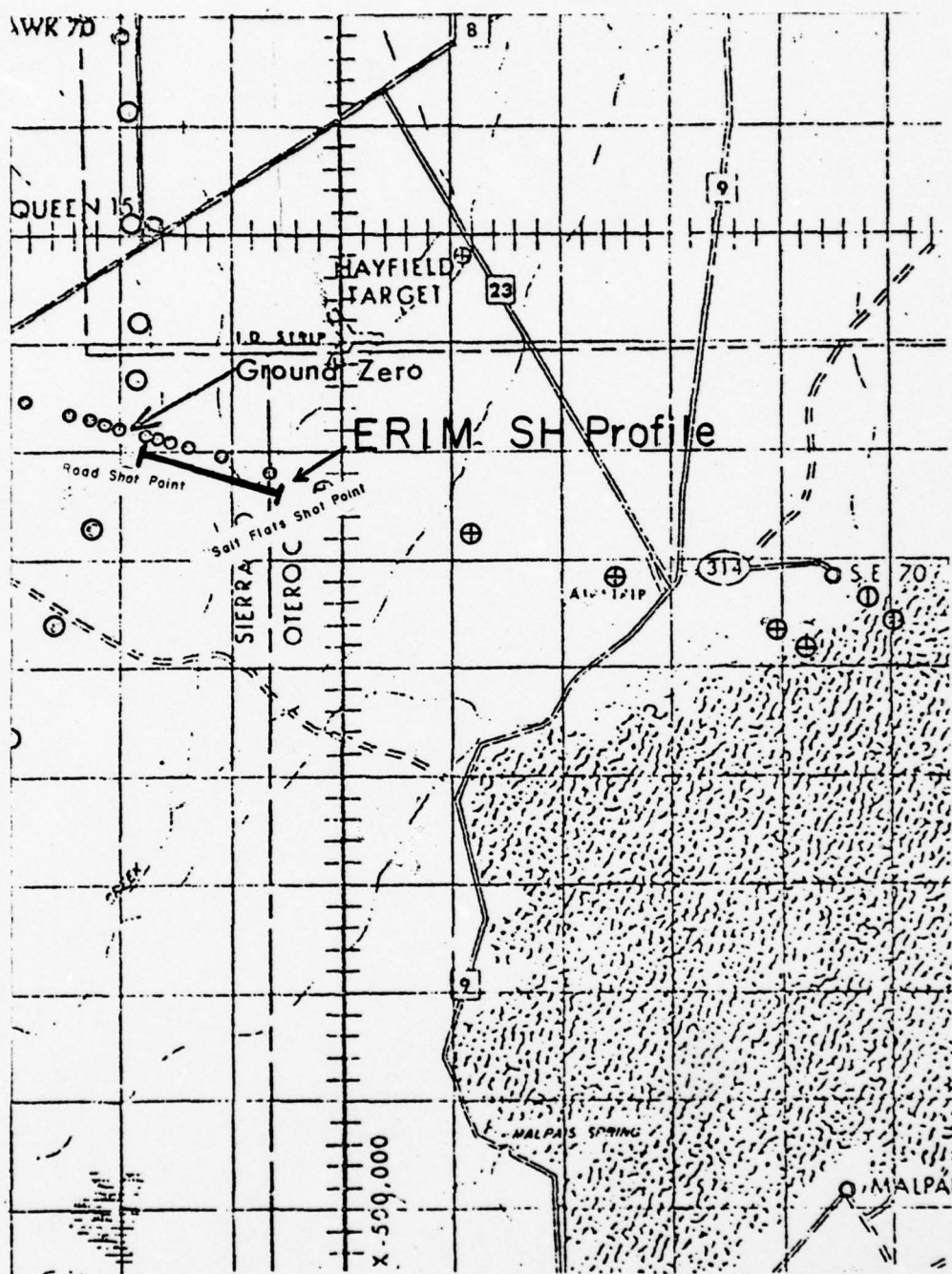


Figure 8. Location of ERM survey line.

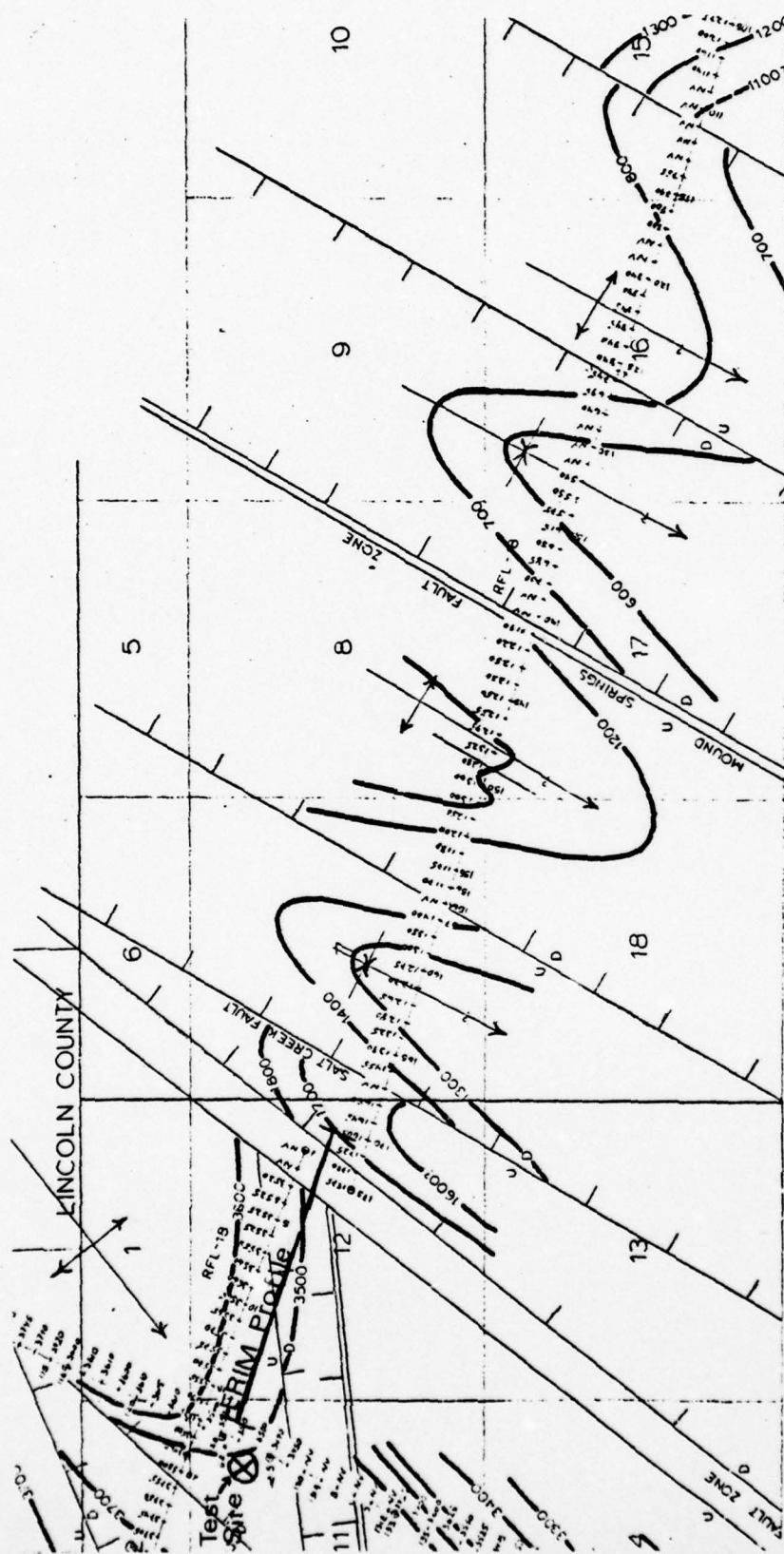


Figure 9. Location of reflection line. Contours indicate elevation in feet of base Tertiary(?). (from Reynolds, 1976)

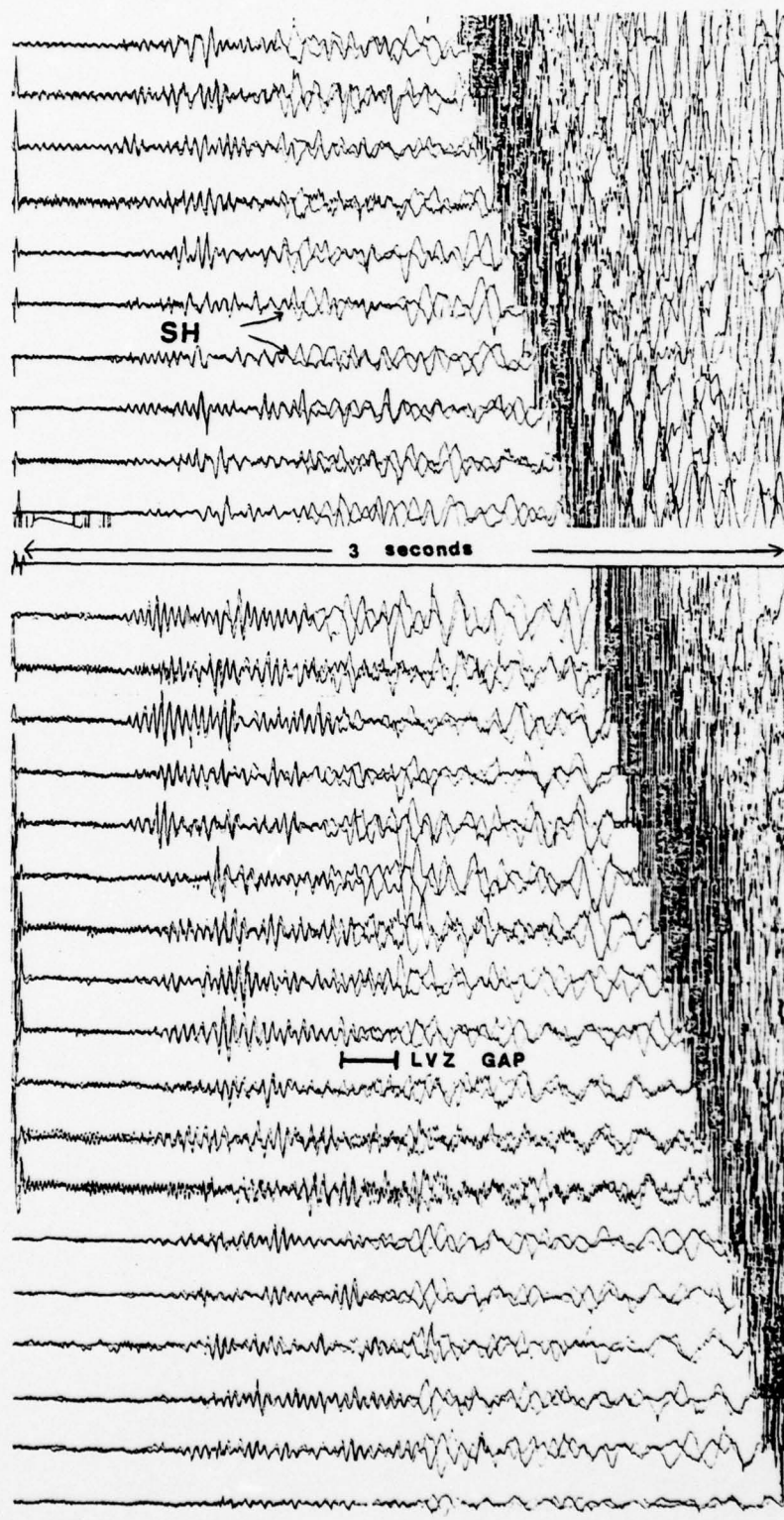


Figure 10. Section of SH record from Salt Flats shotpoint.

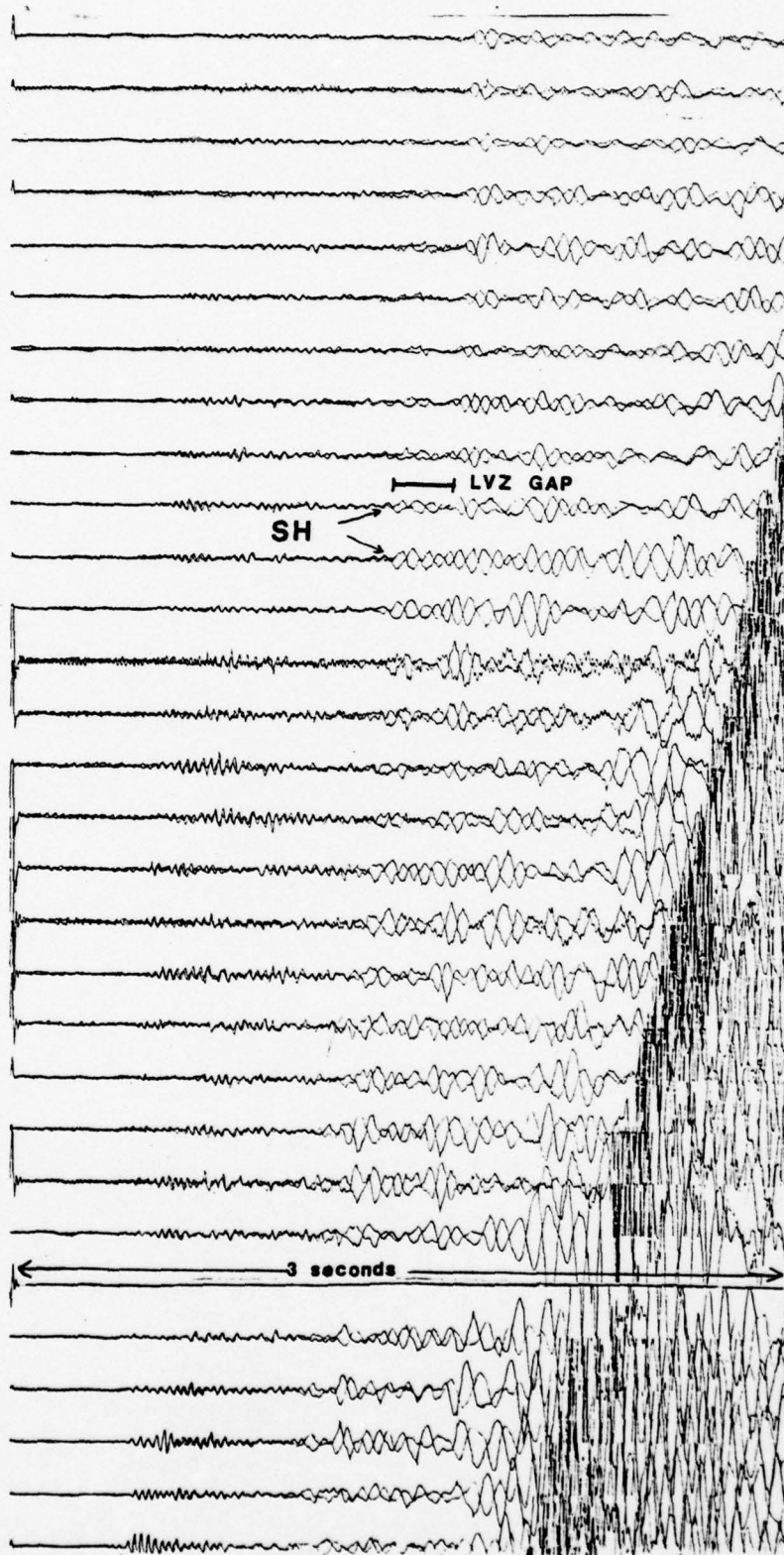


Figure 11. Section of SH record from Road shot point.

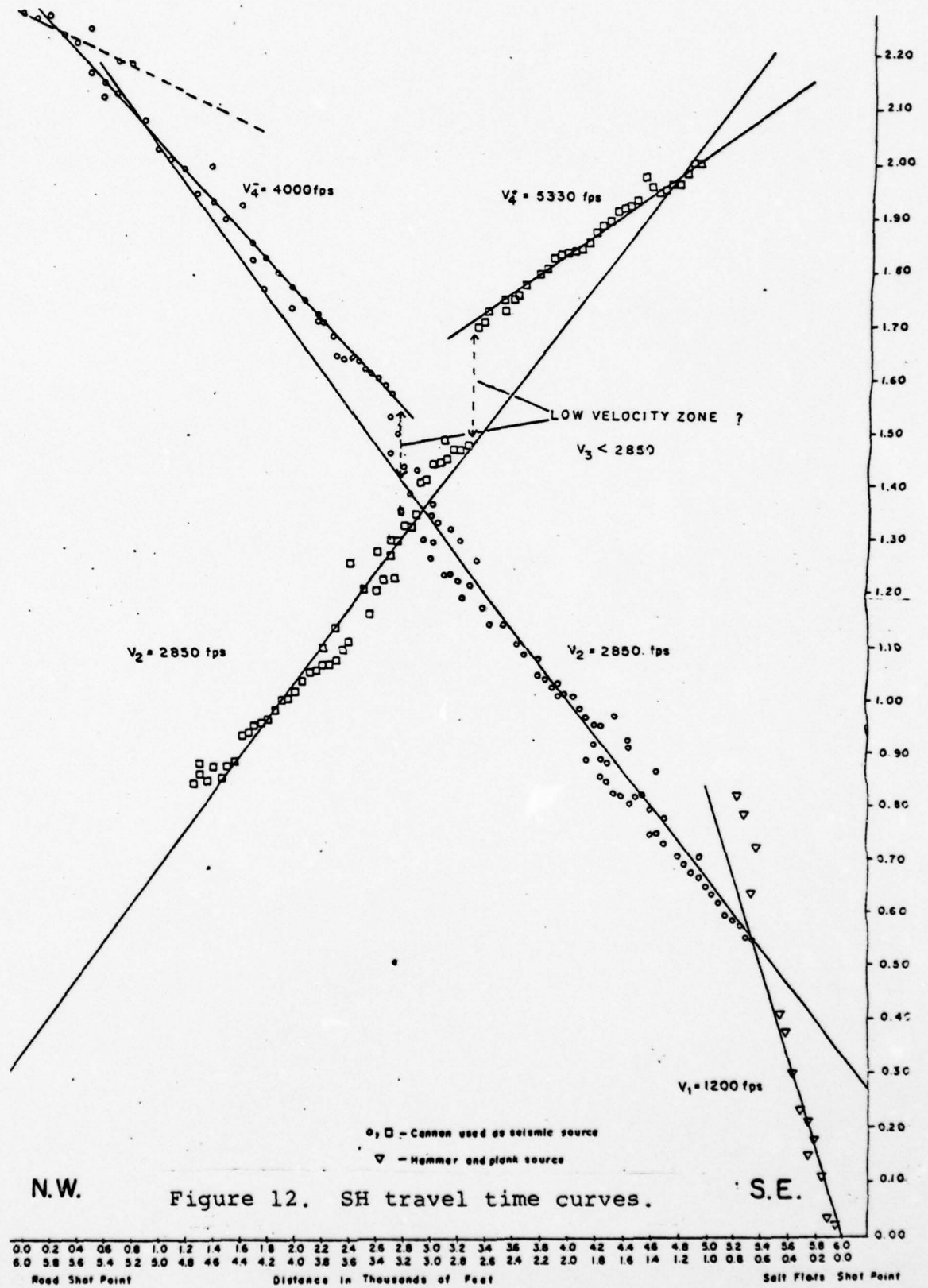


Figure 12. SH travel time curves.

P-S conversions at interfaces, as does the SV wave.

SH recordings from the ERIM survey are shown in Figures 10 and 11. A conventional P wave profile was obtained along the same line. Good arrivals were obtained out to 6000 feet (1828 meters) on the Salt Flats shot point line and to 5000 feet (1524 meters) on the reversed line.

Travel time curves from the SH line are shown in Figure 2. Three distinct branches can be seen. The slope of the third leg is dependent upon the direction of shooting indicating a dipping bed. An unusual characteristic of the SH curves is the time gap between the second and third legs. Field examples of similar appearing gaps observed in compressional wave refraction surveys have been given by Burg (1952), Press and Dobrin (1956), Domzalski (1956), and Knox (1967). These workers interpreted such gaps as indicators of low velocity zones or a layer of low velocity sandwiched between layers of higher velocity. Burg (1952) encountered a low velocity layer in the Williston Basin of North Dakota. Travel time curves from compressional wave refraction surveys there display a time gap between legs. The existence of the low velocity layer (3000 feet per second/914 meters per second) between layers of 6000 feet per second/1828 meters per second) was verified by uphole shooting. Domzalski (1956) found a shallow low velocity layer in England to be composed of sand

overlain by clay. Press and Dobrin (1956) obtained the characteristic time gap in a refraction survey in Texas in an area where the Austin Chalk is underlain by the Eagle Ford Shale of lower velocity.

Press and Ewing (1948) present a theoretical treatment of a compressional wave transmitted through a high speed surface layer overlying a thicker low speed section. Compressional waves propagated horizontally through the high speed layer are attenuated due to leakage of energy into the underlying low velocity material. The degree of attenuation increases with decreasing frequency. Thus a high speed layer overlying a slow layer acts as a high pass filter. In the field examples mentioned previously, this is evident as shown in Figure 13 from Domzalski (1956). It can be seen that the lower frequencies disappear first between 80 feet (24 meters) and 100 feet (30 meters) leaving higher frequencies which in turn die out between 160 feet (49 meters) and 200 feet (61 meters).

The characteristic frequency dependent attenuation can be seen clearly immediately before the time gap occurs on the SH records of the Salt Flats shotpoint profile in the Tularosa Basin (Figure 10). The phenomenon is less evident but still present on the reversed profile (Figure 11). A time gap is also present on the P travel time curves in Figure 14. Because of this and the similarity between the SH profile

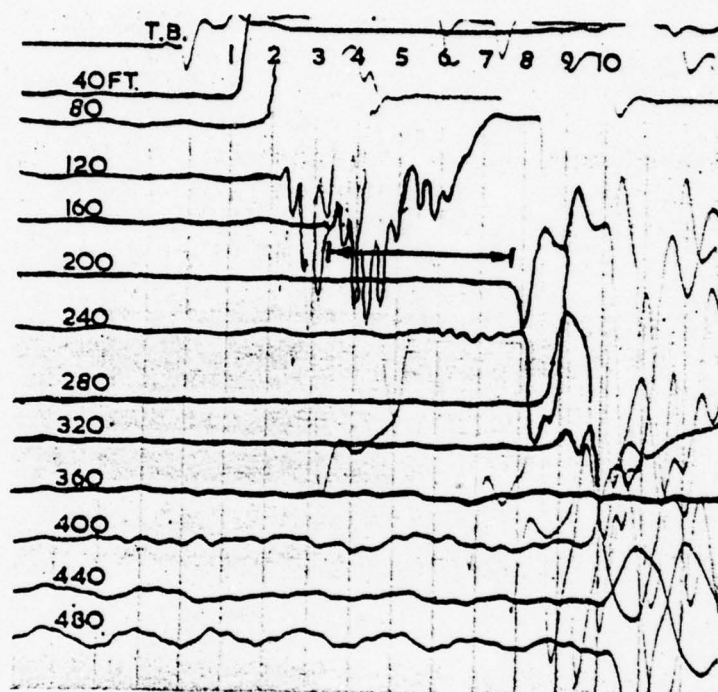


Figure 13. Field example of low velocity layer in a P wave refraction profile. (from Domzalski, 1956)

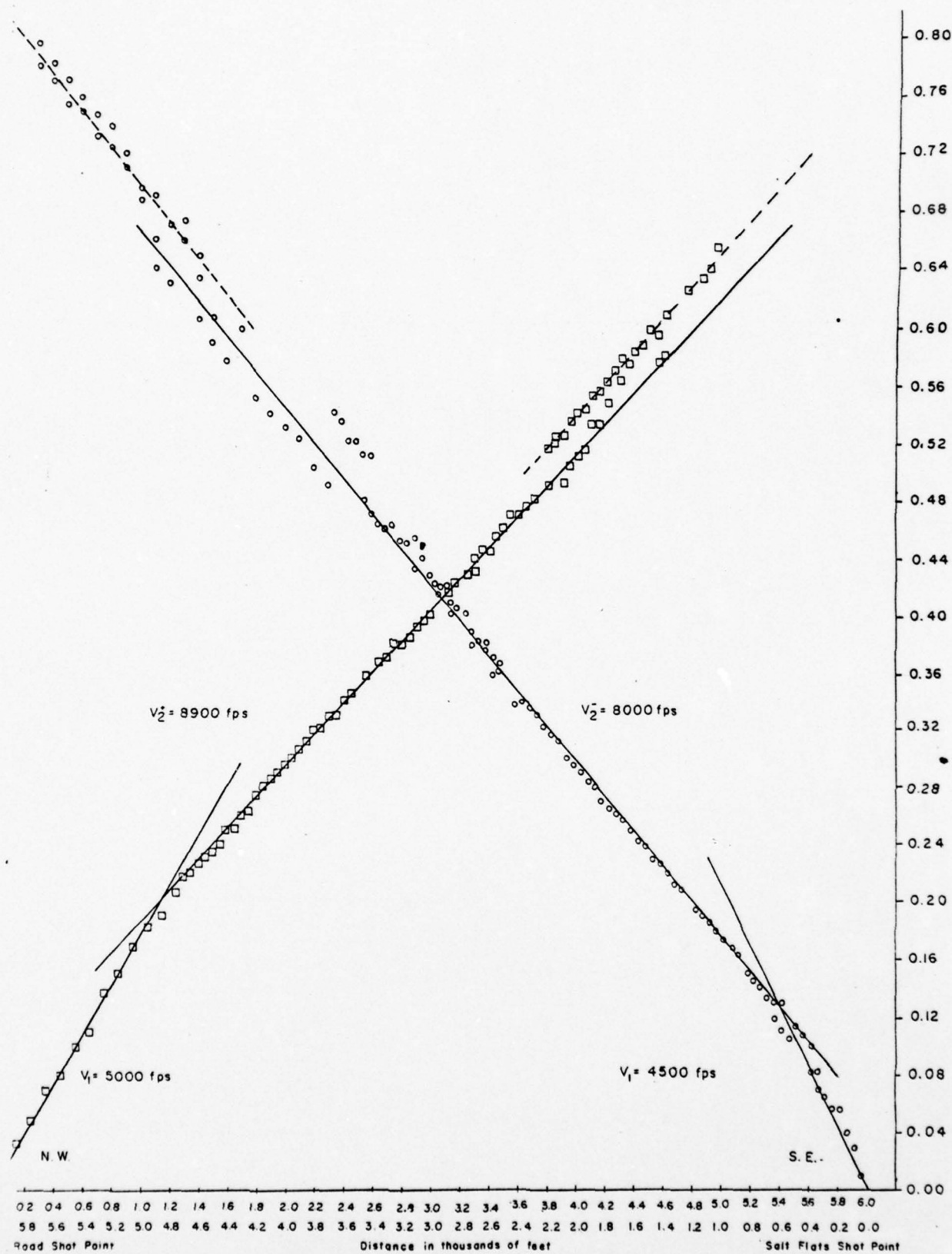


Figure 14. P wave travel time curves.

recordings and the examples presented in the literature, the time gap observed in the travel time curves is thought to be caused by a subsurface low velocity zone or velocity reversal.

The idealized shear velocity-depth structure interpreted from the SH travel time curves is shown in Figure 15. The model was obtained by use of the standard equations of Mota (1954) utilizing time intercept values for n inclined layers. To reduce overestimation of depth, a correction for the low velocity layer was made by subtracting the observed low velocity time gap from the intercept times for the third legs of the travel time curve. Thickness of the low velocity zone was estimated by assuming that the observed time delay was the two-way time needed for a refracted ray to travel through the low velocity layer. The thickness shown in Figure 15 is thought to be an upper limit. The thickness will, of course, vary with the velocity of the layer used in the above calculation.

From purely geometric considerations, a subsurface velocity reversal should not be evident from refraction data. The correction method employed for the low velocity layer is thus not valid according to ray theory. As shown in Figure 16, it is not known whether energy from the layer overlying the low velocity layer disappears at point A, B, or C. The correction is valid only if the energy disappears at point B on the travel time curve. In the examples presented by Burg

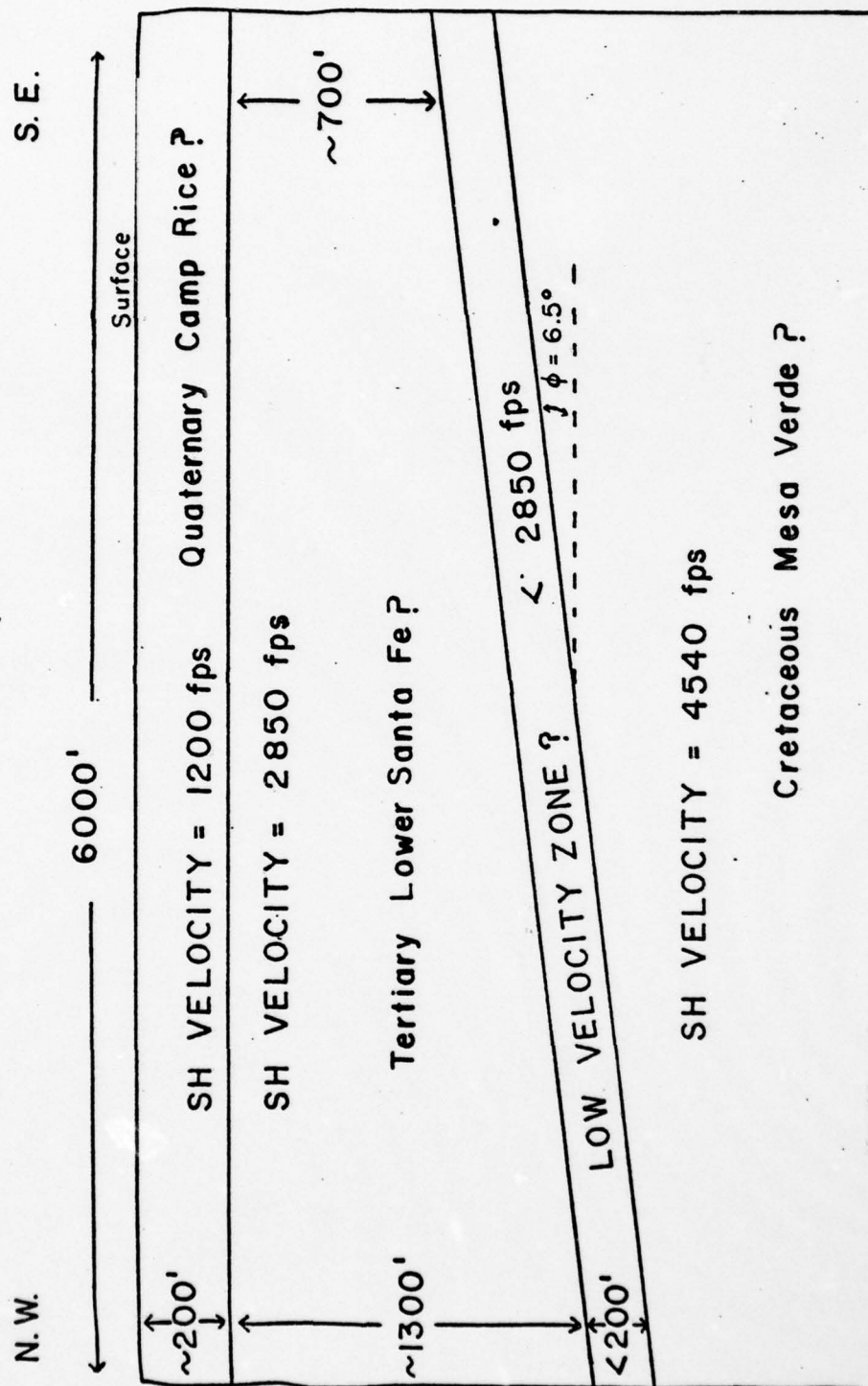


Figure 15. Idealized SH velocity-depth structure.

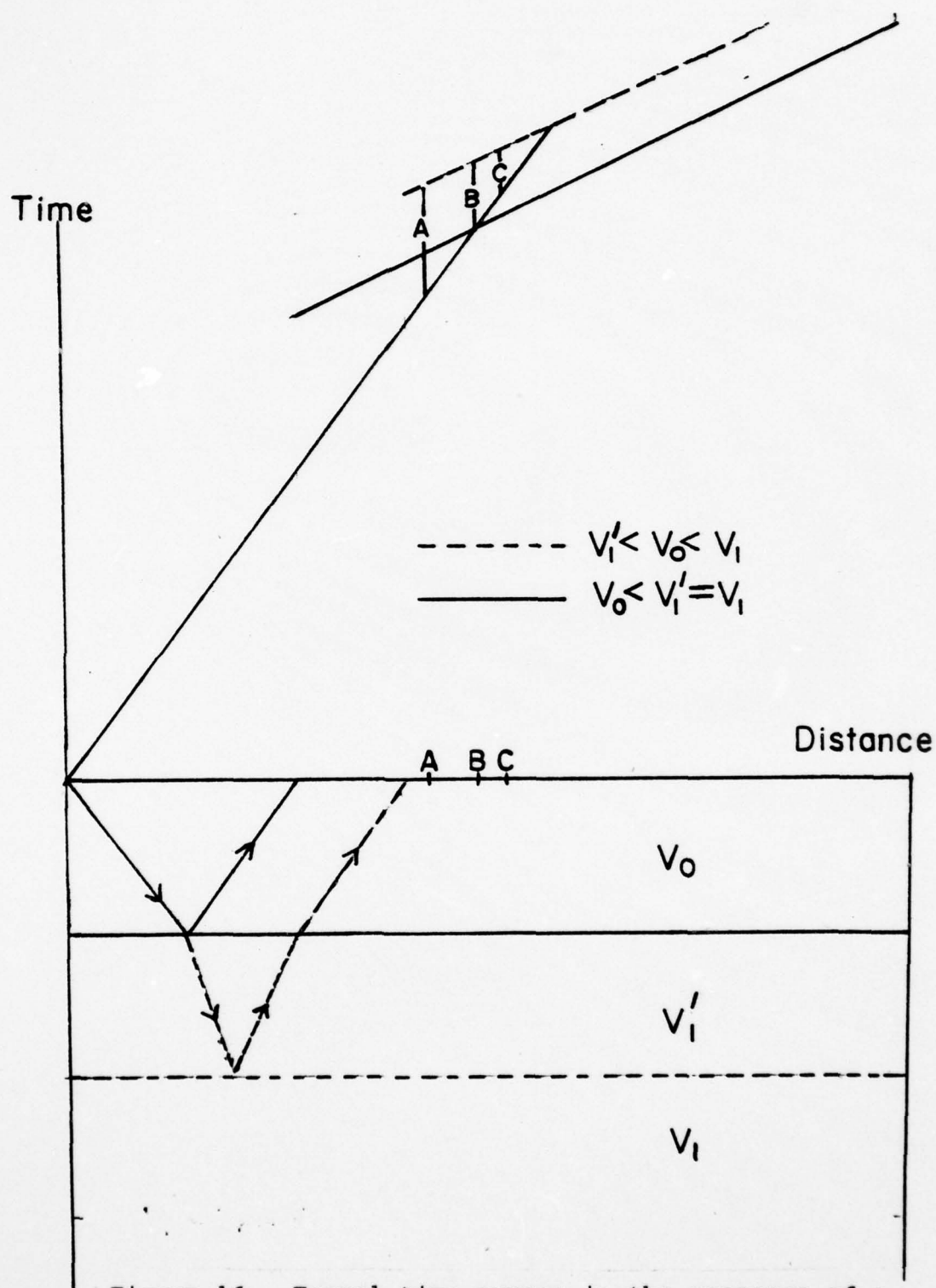


Figure 16. Travel time curves in the presence of a low velocity layer.

(1952), Domzalski (1956), Press and Dobrin (1956), and Knox (1967), there does appear to be an approximate correlation between the length of the time gap observed and the thickness of the low velocity layer as determined from bore hole data. In any case, the correction employed is in the "right direction"; that is, without it (without assuming a low velocity layer), the depth computed for the third interface would be an overestimation. What is not known is whether the correction employed is too large or too small.

The idealized P velocity-depth model derived from the travel time curves is shown in Figure 17. It is interesting to note that the P wave survey does not reveal as much of the subsurface structure as does the SH survey even though both survey lines were of the same length and identically located. On the P travel time curves, the time gap does not appear until near the end of the line. Not enough arrivals are present to define the P velocity for layer 4. These results from the P survey are not necessarily inconsistent with the SH model. Consider the simple 3 layer model shown in Figure 18. For a shear wave refraction study of this model, first arrivals from layer 3 would initially be observed at 1127 feet (343 meters) distant from the shotpoint. If a P wave refraction study were carried out of the same model, first arrivals from layer 3 would not be observed until 3750 feet (1143 meters) distant from the seismic source. In at

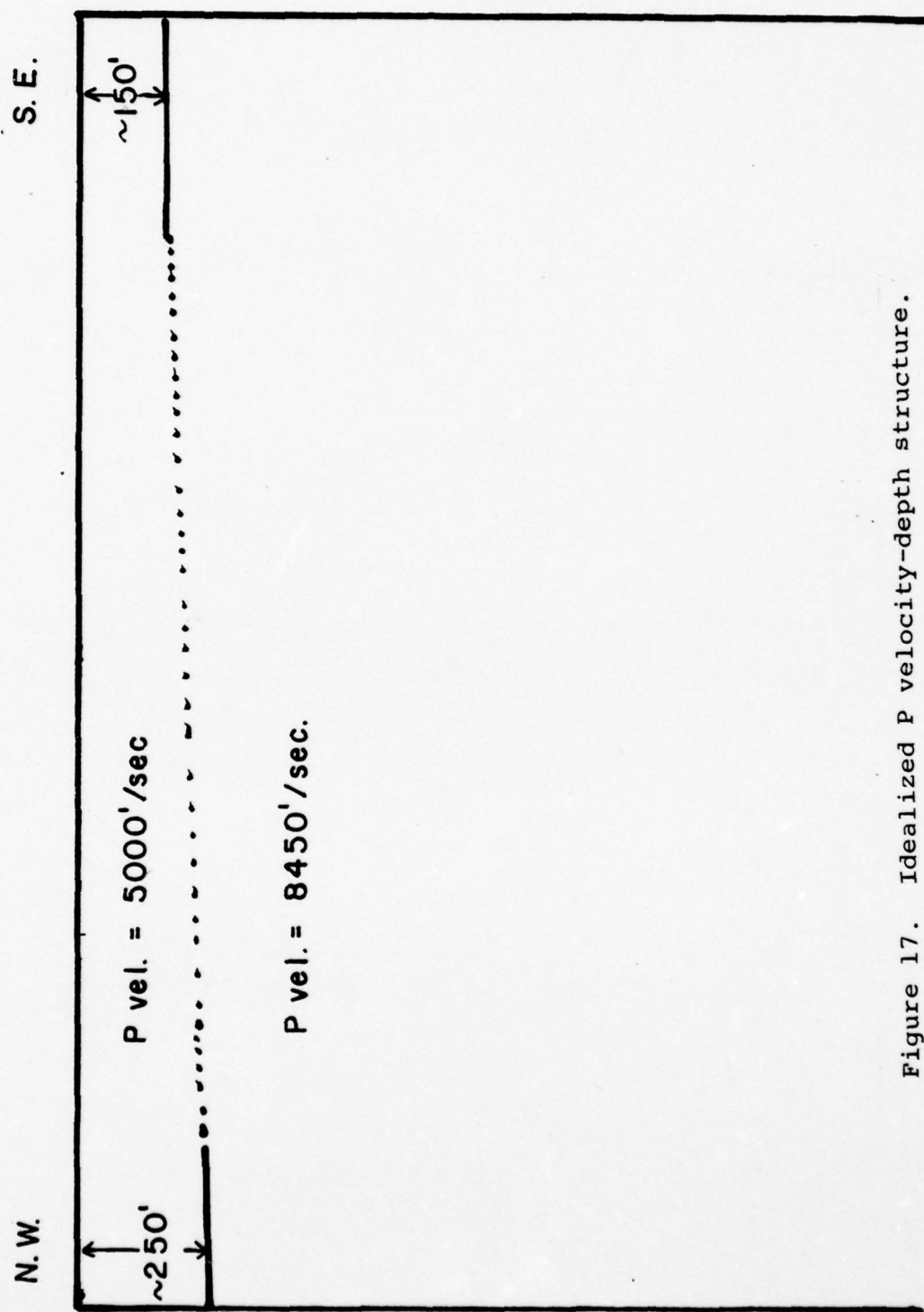


Figure 17. Idealized P velocity-depth structure.

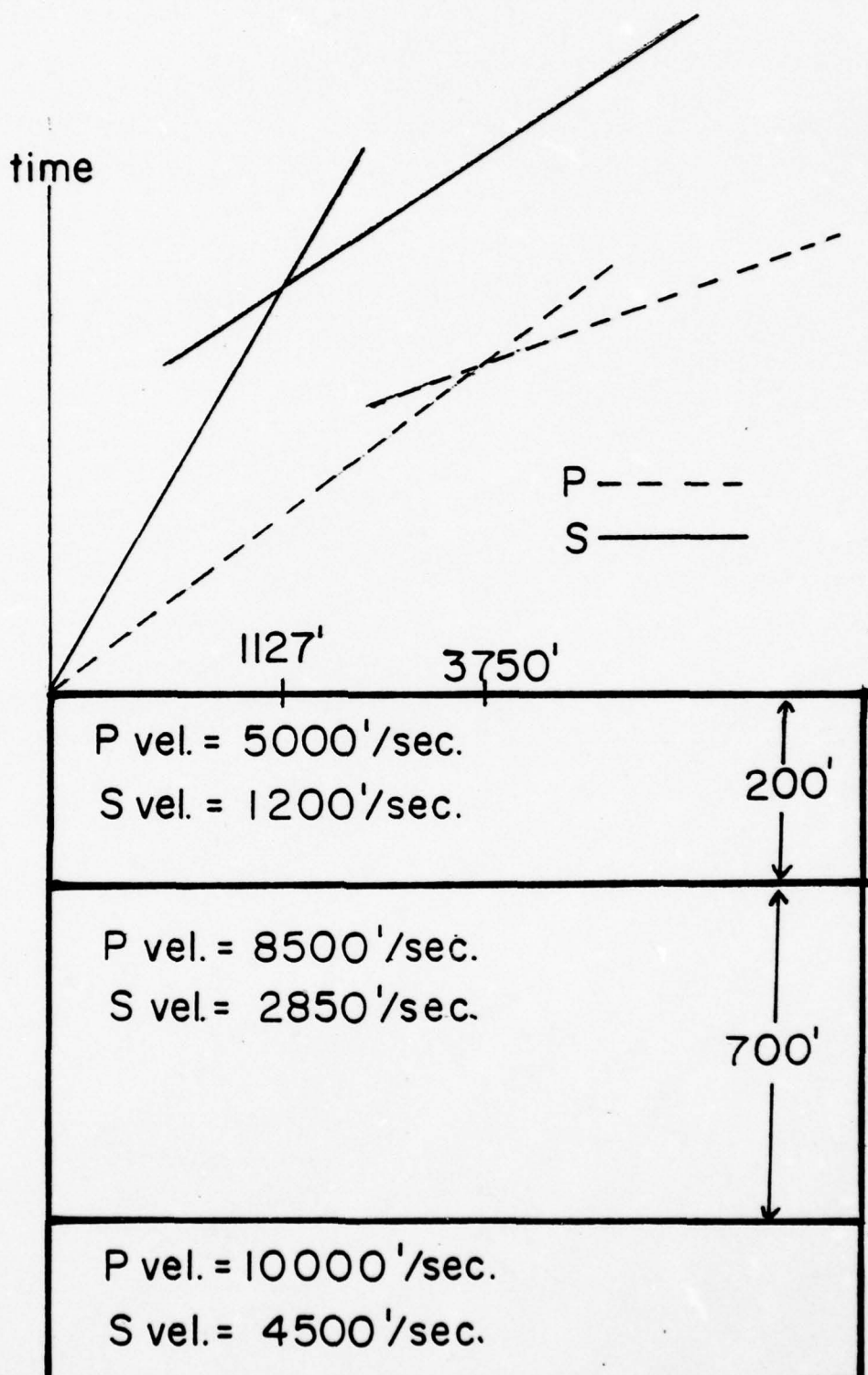


Figure 18. Comparison of P and S travel time curves for a simple layered model.

least some cases, then, a shear wave refraction profile can penetrate to a greater depth than can a P wave survey of the same length.

Jolly (1956) conducted some experiments with shear wave refraction over shale and found a significant degree of anisotropy present. The SH velocity for horizontal travel was found to be twice that of the horizontal SV velocity. For vertical travel, SH velocity was found to be approximately equal to horizontal SV velocity. The depth of weathering calculated from SH refraction data was twice that derived from P refraction data. The value computed from the P data was found to be correct from borehole data.

In the alluvial valley fill of the Tularosa Basin, the anisotropy problem should not be as severe as that experienced for shale. Jolly suggests that if simple isotropic theory is applicable, depths calculated from P refraction data should roughly correspond to depths obtained from SH data along the same survey line. The P refraction data yield 165 feet (50 meters) or 146 feet (45 meters) to the first interface for the critical distance and time intercept methods respectively. From the SH data, depths of 191 feet (58 meters) and 222 feet (68 meters) were obtained from the critical distance and time intercept methods. Some discrepancy between the SH and P measurements is likely a result of the comparatively wide geophone spacing (50 feet/15 meters);

however, the greater depths to the first interface obtained from the SH data as compared to those derived from the P wave survey probably indicate that a limited degree of anisotropy is present at least in the upper layer. Since the deeper interfaces were not well defined on the P wave profile, comparison of depths to the other layers cannot be made; however, the depths to the deeper interfaces as determined from the SH data are quite reasonable when compared with those determined from the reflection profile of Reynolds. Anisotropy, then, is not thought to be a severe problem in the bolson deposits of the Tularosa Basin.

Correlation with Reflection Data

The ERIM refraction survey line roughly coincided with a portion of a shallow reflection survey carried out by Charles B. Reynolds and associates. (Reynolds, 1976) (Figure 9). The seismic source was a weight drop. The receiving array consisted of 12 10 hz geophones spaced 12 feet apart in line. Output from the geophones was digitally recorded. The average number of weight drops per station was 3.

The portion of the reflection profile which coincided with the ERIM survey is shown in Figure 19. The general orientation of the interfaces correlates well with the model obtained from the shear wave survey. Horizon 1 of the reflection profile is thought to be correlative with the base of

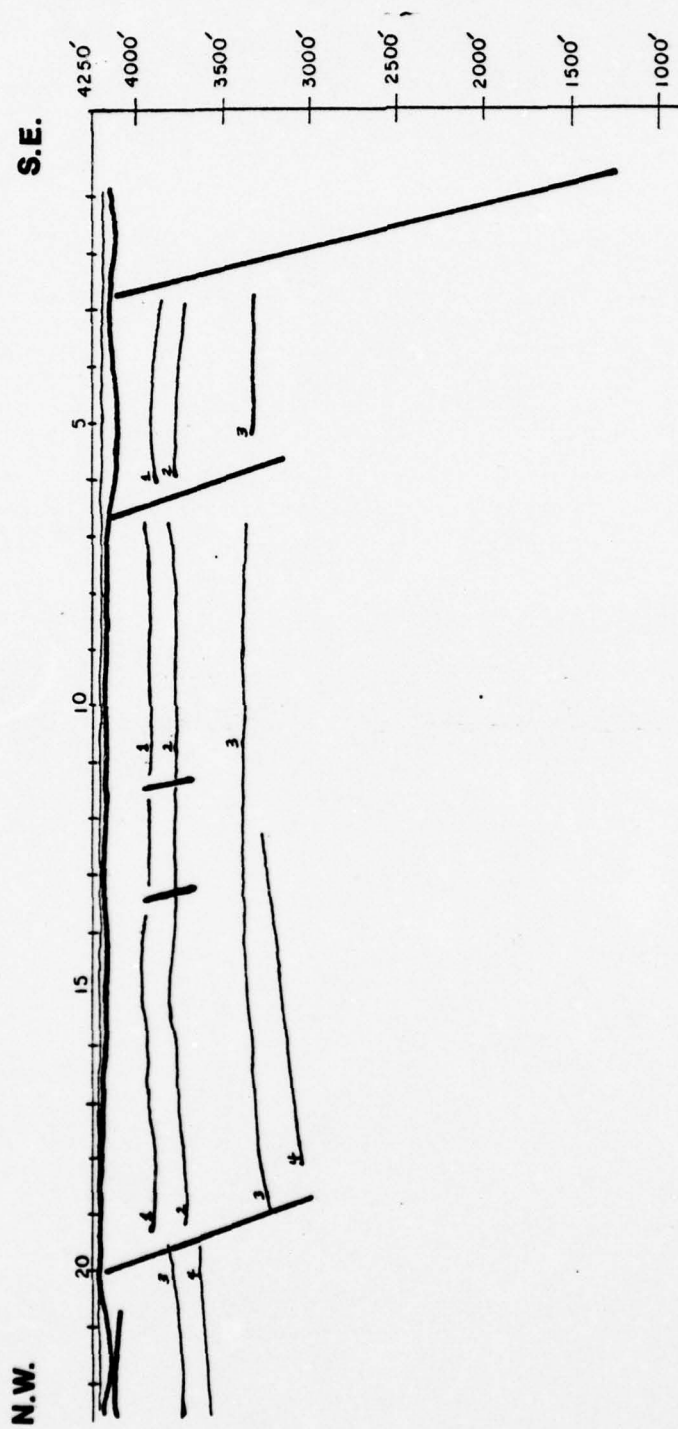


Figure 19. Cross section from reflection profile along ERIM survey line.

the first layer of the refraction profile. Horizon 3 is believed to correspond to the base of the second layer of the refraction profile while horizon 4 is thought to be the base of the low velocity zone. No distinct evidence for horizon 2 is seen on the refraction data, although the scatter present in the arrival times of the second leg of the SH travel time curve may be partially due to the presence of horizon 2, as well as to the undulating nature of the horizons and the small faults near the center of the profile.

Reflection times were converted to depths by Reynolds using the velocity function $\bar{v} = 6000$ feet per second (1828 meters per second) + 3000 feet per second (914 meters per second) $\cdot T$, where T is the two-way time. In light of the P wave velocities observed on the refraction profile, this velocity function is probably slightly fast above 200 feet (61 meters) and somewhat slow below that depth. The indicated depth to horizon 1 on the reflection profile is then a little too deep while the thickness between horizon 1 and horizon 3 is too small. Depth to horizon 1 averages about 200 feet (61 meters) as interpreted by Reynolds from the reflection data. The distance between horizon 1 and horizon 3 from the reflection data averages about 500 feet (152 meters). The thickness of the layer between horizon 3 and horizon 4 of the reflection profile is about 200 feet (61 meters) under the northwest end of the refraction line. This

layer, thought to be the low velocity layer, appears to wedge out on the reflection profile near the opposite end of the refraction profile.

The overall correspondence between the SH refraction model and the subsurface model obtained from the reflection survey is quite good. The thickness of 1300 feet (396 meters) under the northwest end of the survey for layer 2 is probably too large; however, the thickness of 700 feet (213 meters) determined for the second layer at the southeast end of the profile is quite reasonable since the thickness indicated by the reflection profile (500 feet, 152 meters) is probably 15-20 per cent too small because of the velocity function.

Stratigraphic Interpretation

The stratigraphy of the Cenozoic bolson deposits within the Tularosa Basin is little known. Few deep boreholes (>400 feet, 122 meters) exist, especially on the west side of the basin, and there are none within 15 miles (24 kilometers) of the pre-Dice Throw test site.

The stratigraphic section observed in the San Andres Mountains has been extensively described by Kottowski and others (1956), Kottowski (1975), and Kottowski and Hawley (1975). Diagramatic sections of the pre-Cenozoic strata through the length of the San Andres range, presented by

Kottlowski (1975), are shown in Figures 20 and 21. A cross section through the southern part of the range, drawn by Kottlowski and Hawley (1975), is shown in Figure 2.

McLean (1970) discussed the hydrologic properties of the bolson fill of the Tularosa Basin. He indicated that basin filling had begun by early Miocene time. Streams flowing into the center of the basin deposited coarse sediments in fans near the mountain front and fine grained alluvium farther out into the basin. Uplift may have continued into the Pleistocene. Lacustrine deposits are dominant in the center of the basin. During the Wisconsin glaciation, Lake Otero, the predecessor of Lake Lucero, covered 700 square miles (1812 square kilometers) in the Tularosa Basin.

The Cenozoic deposits of the basins of the Rio Grande valley in New Mexico are composed predominantly of the calcareous sands and sandstones of the Santa Fe Group. Kottlowski and others (1956) state that sedimentary rocks resembling the Santa Fe Group occur in the Tularosa Valley where they are predominantly clays with large amounts of gypsum.

Reynolds (1976) interpreted horizon 3 in the area of the ERIM refraction profile as the base of Tertiary (top of bedrock) deposits and suggested that in this area, horizon 3 might be an angular unconformity. Horizon 1 was thought to be the base of Quaternary deposits.

Data from the ERIM shear wave profile support the strati-

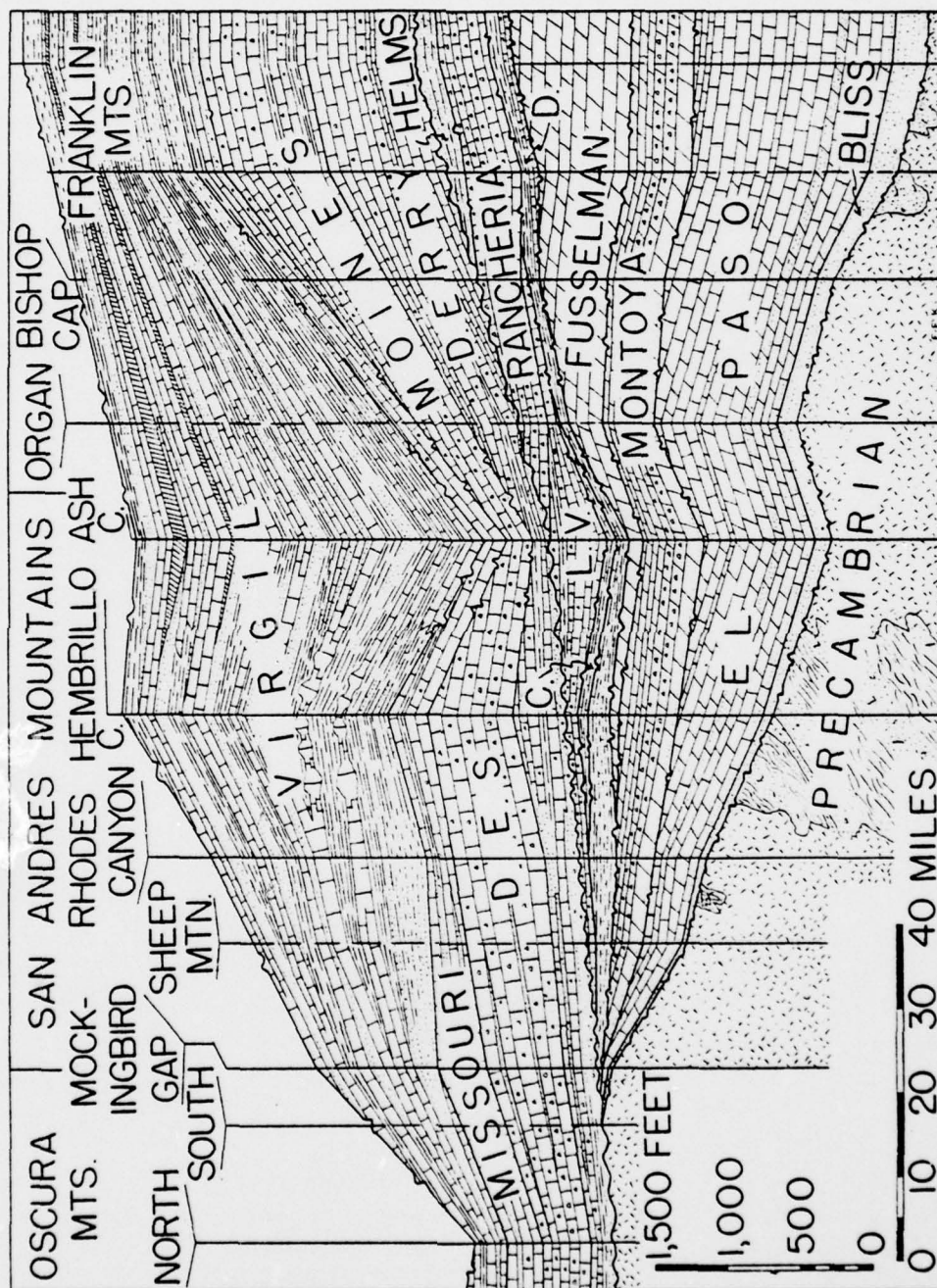


Figure 20. Lower section of pre-Tertiary strata in San Andres Mountains. (from Kottlowski, 1975)

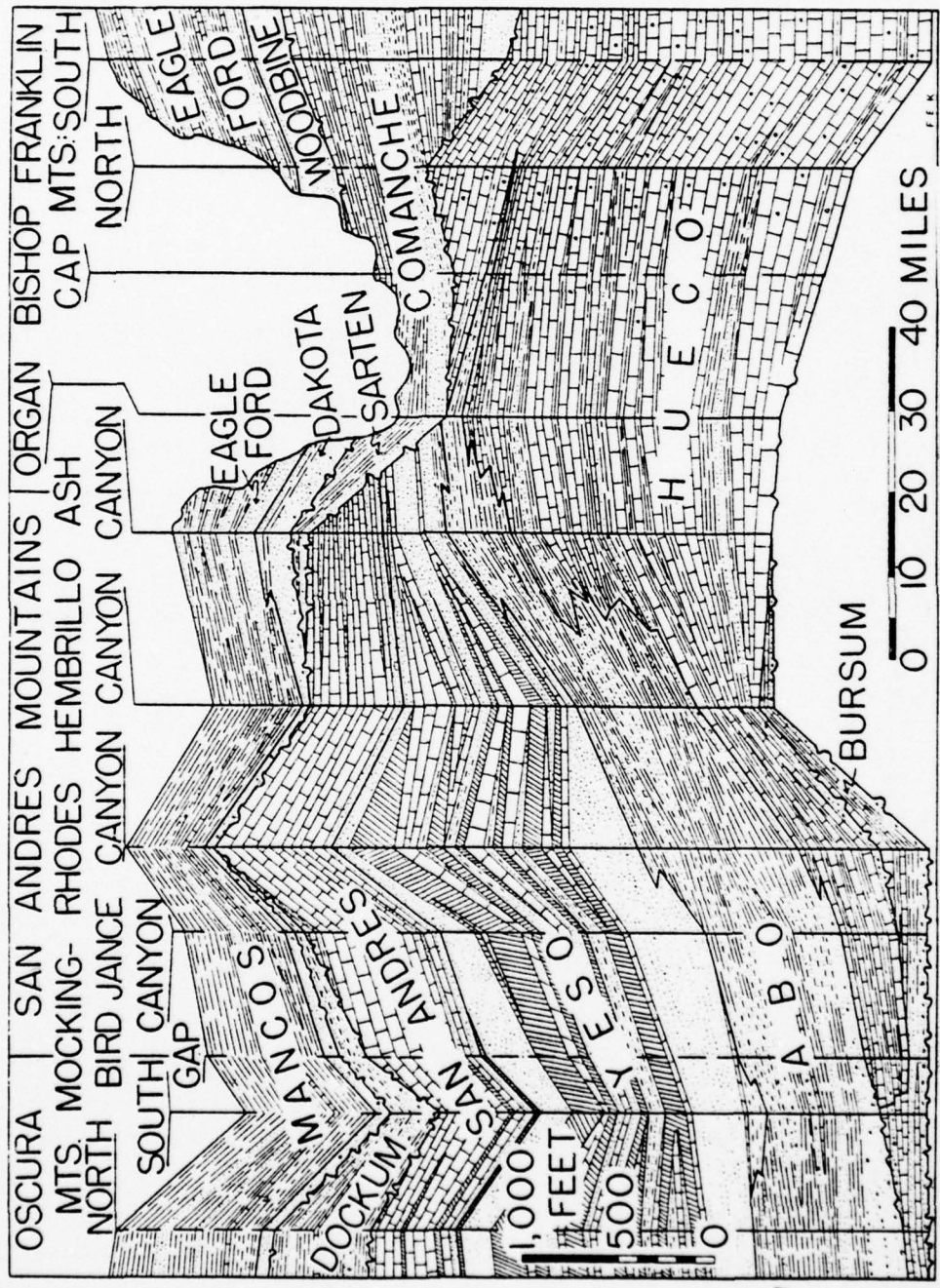


Figure 21. Upper section of pre-Tertiary strata in San Andres Mountains. (from Kottlowski, 1975)

graphic interpretation presented by Reynolds. The three distinct velocities suggest three distinct lithologies. The upper two layers of the shear wave profile are likely correlative with the stratigraphic units of the Cenozoic deposits of the adjacent Jornada del Muerto as seen in the cross section (Figure 2.) presented by Kottlowski and Hawley (1975). The 1200 feet per second (366 meter per second) layer likely represents the Tularosa equivalent of the Camp Rice formation of Quaternary age. The 2850 feet per second (868 meters per second) layer is identified as the Tularosa equivalent of the lower Santa Fe Group.

The dip of the lowest layer seen by the shear wave refraction profile is likely related to the tectonic activity which resulted in the formation of the San Andres Mountains and the Tularosa Basin. According to Seager (1975), extensive faulting and basin formation in the Rio Grande rift area began in Late Oligocene - Early Miocene time. The 4500 feet per second (1371 meter per second) layer then must be older than Miocene.

Several possibilities exist for the correlative stratigraphic unit of the lowest layer seen on the SH refraction profile. In the cross section of a portion of the Jornada del Muerto in Figure 2, a volcanic section is seen underlying the lower Santa Fe Group; however, an aeromagnetic study of the Tularosa Basin by Bath (1977) does not suggest that

any buried volcanics are present near the pre-Dice Throw test site.

The Love Ranch formation of Eocene (?) age seen in Figure 2 is a possibility. The Love Ranch unit, as described by Kottlowski and others (1956), is composed of intercalated cobble and boulder conglomerates and reddish siltstone. Although the Love Ranch formation is not seen in the northern San Andres Mountains, similar rocks are present near Carrizozo and Three Rivers and at Cerro Colorado in the northern portion of the Jornada del Muerto. At the type locality in the southern San Andres Mountains, Love Ranch, the formation is over 2000 feet (609 meters) in thickness. (Kottlowski and others, 1956).

Other possible candidates for the stratigraphic equivalent of the deepest layer observed from the refraction data are two Late Cretaceous units, the Eagle Ford - Mancos formation and the Mesa Verde formation. Northwest, west, and east of the San Andres Mountains, a black carbonaceous shale is called the Mancos Shale. No outcrops occur within the northern and central portions of the San Andres range. In the southern portion of the mountains near Love Ranch, shaly beds outcrop which are correlative with the Mancos Shale but are of a facies similar to the Eagle Ford Shale and are referred to as the Eagle Ford Shale. The Mesa Verde Group overlies the Mancos Shale. It is composed of conglomerate, sandstone,

siltstone, shale and local coal beds. The thickness of the Mesa Verde formation is as much as 1000 feet (305 meters) within the basin. Although it is not observed in the San Andres Mountains, it is penetrated by wells in the Jornada del Muerto and near Three Rivers and Carrizozo. (Kottlowski and others, 1956; McClean, 1970)

Without borehole data it is not possible to positively assign a particular stratigraphic identification to the deepest layer detected by the refraction survey. Because of the scarcity of in situ shear wave velocity measurements available, it is also difficult to determine the lithology of the layer; however, Jolly (1956) found a horizontal SH velocity of 4850 feet per second (1478 meters per second) for unweathered shale. The velocity of 4540 feet per second (1371 meters per second) observed is then certainly consistent with an interpretation of the lowest layer as a shale unit. The Mancos and Mesa Verde formations both contain large amounts of shale. Because of this and because the Mesa Verde formation is the youngest consolidated unit found in wells in the basin, it is thought to be the most likely candidate for the stratigraphic unit correlative with the deepest layer observed by the refraction survey. The Love Ranch formation is not reported in wells within the basin (McLean, 1970) and is therefore not likely to be as widely distributed as either the Mancos or Mesa Verde formations.

SH velocity determined by Jolly (1956) for the weathered layer in the shale was 1600 feet per second (488 meters per second). This suggests that the low velocity layer observed on the refraction profile might be an ancient weathered zone of the Mancos or the Mesa Verde formation. A simple change in lithology such as clay overlying sand, as described by Domzalski (1956), could, of course, also produce a low velocity layer.

GRAVITY AND MAGNETIC DATA

Previous Work and Available Data

Gravity and magnetic surveys of portions of the Tularosa and Jornada del Muerto Basins made during 1975 together with the results of earlier surveys have given an insight as to the general structural character of the Tularosa Basin and the northern section of the Jornada del Muerto. Bath and others (1977) discussed results of combined analysis of gravity and magnetic data in the Tularosa Basin and proposed that in general, the western half of the valley contains the greatest thickness of valley fill and is structurally quite simple when compared to the eastern portion of the valley. Bath (1977) presented aeromagnetic maps and interpretations of several magnetic anomalies within the Tularosa Valley. McLean (1970) used gravity data along with some seismic and well control to produce a contour map of the elevation of consolidated (pre-Tertiary) rock within the basin. Sanford (1968) reported the results of a gravity survey in the Rio Grande Valley near Socorro, New Mexico, to the northwest of the Jornada del Muerto. Healey (1976b) assembled a complete Bouguer

gravity anomaly map of the Tularosa Basin and the northern portion of the Jornada del Muerto. He obtained a residual gravity map for the area along with an interpreted cross section through a portion of the basin near the pre-Dice Throw test site.

Gravity

Complete Bouguer anomaly maps for the pre-Dice Throw and Dice Throw test areas are shown in Figures 4 and 3. These are portions of a complete Bouguer anomaly map assembled by Healey (1976b) from various data sources. Residual anomalies are also shown on the maps. Healey obtained the residual anomalies by fitting a third order polynomial to the gravity data and subtracting the polynomial values from the complete Bouguer anomalies. (Note: the residual anomalies were obtained from an earlier complete Bouguer map (Healey 1976a) which did not include additional survey points in the Jornada del Muerto used to compile the present map. The earlier map does however correspond well with the present map. Therefore, residual anomalies obtained from the earlier map are thought to be quite adequate for the rough interpretations to be discussed in this paper.)

The two-dimensional interpretation near the pre-Dice Throw test site as presented by Healey (1976a) is shown in Figure 2. The location of the line and the data points is

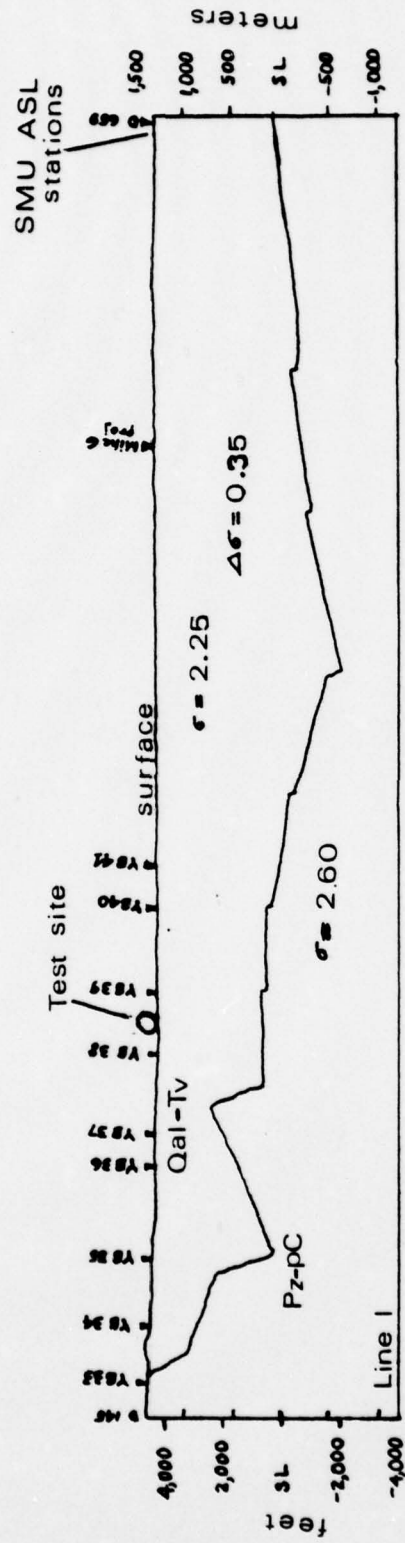


Figure 22. Cross section interpreted from gravity data in the Tularosa Basin. (from Healey, 1976a)

shown in Figure 23.

McLean (1970) obtained a map of the elevation of the top of consolidated rock (pre-Tertiary) from gravity data using well and seismic control where available. McLean's interpretation of the northern portion of the Tularosa Basin is shown in Figure 24.

Comparing the two interpretations at the pre-Dice Throw test site, we find that Healey predicts a depth to bedrock of about 3000 feet (914 meters). McLean's elevation of consolidated rock map indicates a depth to bedrock below the pre-Dice Throw test site of about 1200 feet (366 meters).

The reflection and refraction data discussed previously indicate the presence of what apparently is consolidated rock (Mancos? or Mesa Verde?) on the basis of velocity at a depth of 1000 to 1300 feet (305 to 396 meters).

As seen in Figure 22, Healey assumed a density of 2.25 for Quaternary and Tertiary rocks and a density of 2.60 for all Paleozoic - Pre-Cambrian rocks yielding a density contrast of 0.35. This density contrast does not take into account the presence of a Mesozoic section beneath the surface of the Tularosa Basin near the pre-Dice Throw test site. Although erosion has removed the Mesozoic section from the peaks of the northern portion of the San Andres range, most of the section likely remains intact below the bolson deposits of the basin because it is

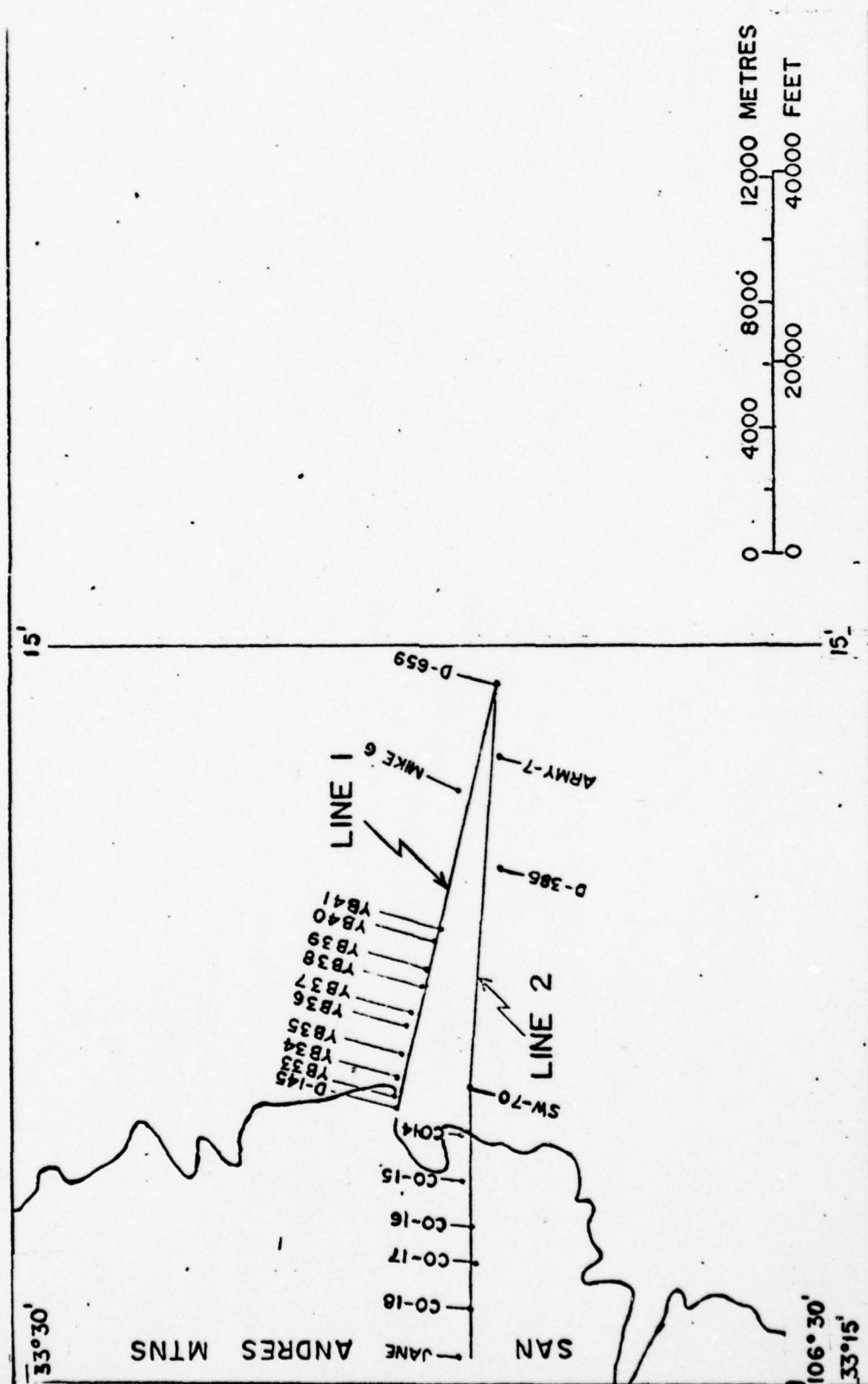


Figure 23. Location of cross section and gravity survey points. (from Healey, 1976a)

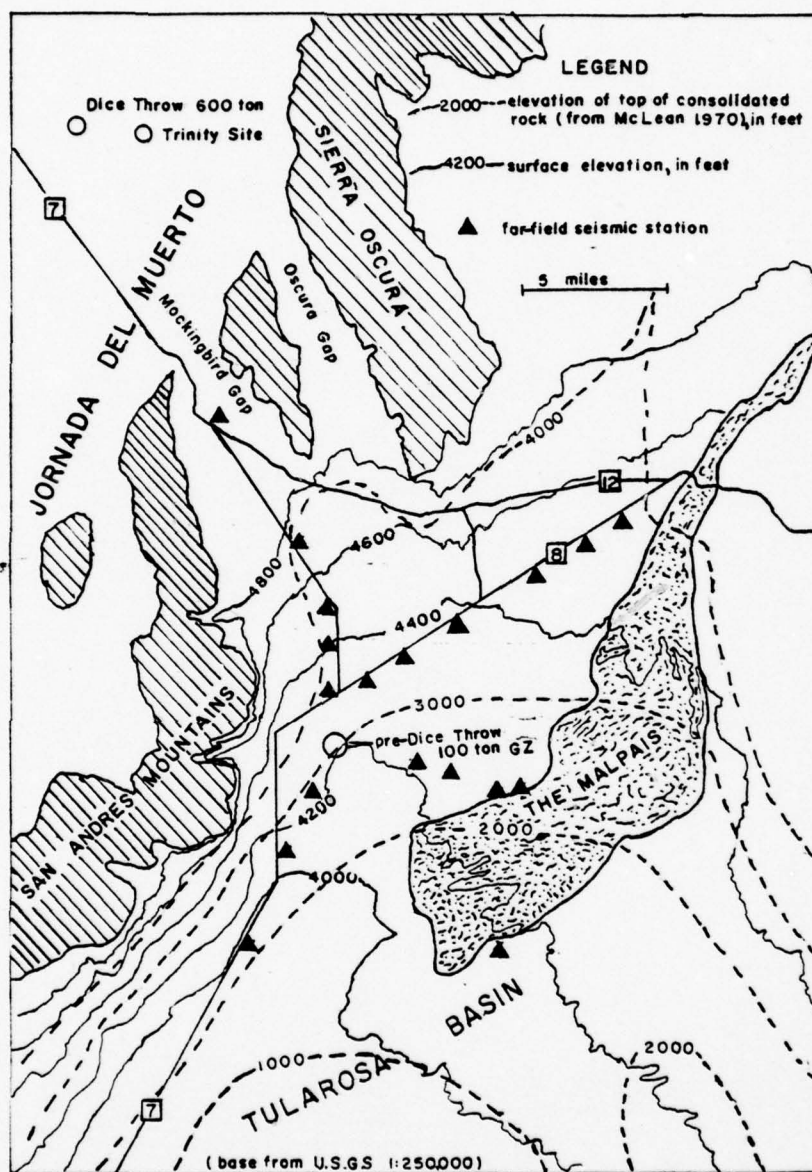
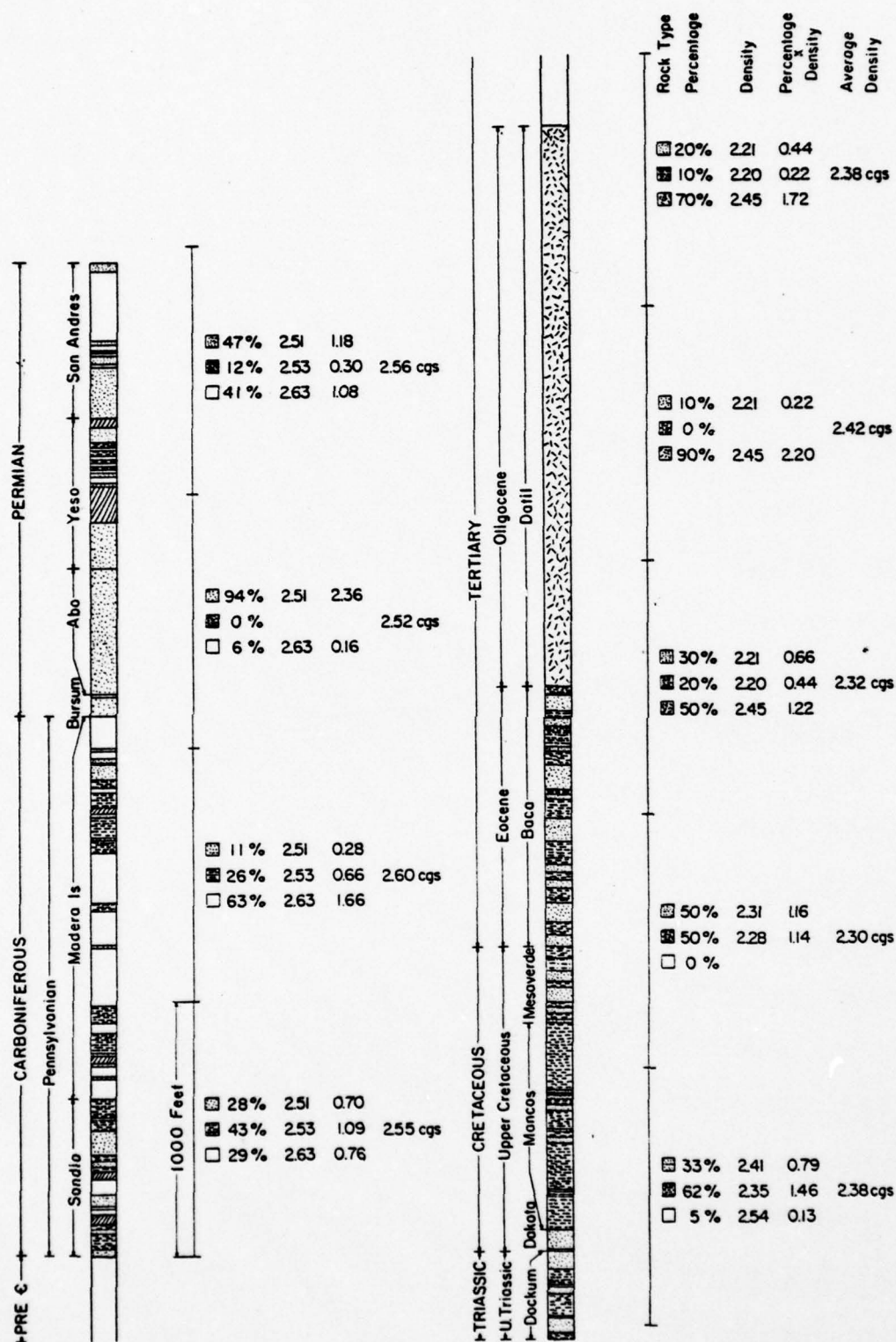


Figure 24. Elevation of top of consolidated rock in the Tularosa Basin.

found in wells within the basin.

Sanford (1968) presented an interpretation of a gravity survey in the Rio Grande Valley near Socorro, New Mexico, about 50 miles (80.5 kilometers) distant from the pre-Dice Throw test area. He assumed that the stratigraphic section shown in Figure 25 was present under the valley fill of the Santa Fe Group. Below the Datil and Baca formations, which are probably not present, the section is roughly similar to that which is thought to be present below the basin fill of the Tularosa Basin. As shown in Figure 25, Sanford divided the section into layers of thickness 1000 feet and calculated an average density for the layers based on the percentage of rock type in each layer. The densities were obtained from field measurements and published data. In addition to the densities shown on the geologic column, Sanford found the average density of the Santa Fe Group comprising the alluvial valley fill to be 2.2.

A comparison of the measured densities given by Sanford and the densities assumed by Healey for interpretational purposes reveals that the depth to bedrock found by Healey is much too large if bedrock is taken to mean pre-Tertiary. From Sanford's geologic column it can be seen that the 1500 feet (457 meters) of ~~Mesozoic~~ section immediately below the Tertiary have an average density of about 2.35. The Paleozoic section of about 4000 feet (1219 meters) thickness has an average density



of about 2.56. If we assume that Sanford's densities are approximately correct, the difference between the actual densities and those assumed by Healey places the valley fill - bedrock interface proposed by Healey somewhere near the top of the Paleozoic section or base of Mesozoic rather than at the base of Santa Fe (?) fill. If the 1500 feet (457 meters) of Mesozoic section assumed by Sanford are present here, then the cross section interpreted by Healey is roughly in agreement with the results of the seismic surveys and with the bedrock map of McLean.

The gravity data compiled by Healey (1976a,b) for the Dice Throw test area in the Jornada del Muerto are shown in Figure 3. The Dice Throw test site appears to lie near the center of an elongate north-south depression paralleling the mountain front of the Sierra Oscura. The deepest portion of the depression has a residual gravity anomaly of over 25 milligals. At the Dice Throw test site, the residual Bouguer anomaly is about 21 milligals compared with an average residual anomaly of about 10 milligals at the site of the refraction survey near the pre-Dice Throw test site.

It is reasonable to assume that the majority of the difference in the residual gravity anomalies between the pre-Dice Throw and Dice Throw test sites is due to a greater thickness of the Santa Fe Group (?) in the Jornada del Muerto test area. Assuming the Santa Fe density given by Sanford

(1968) and using an infinite slab approximation, 11 milligals is equal to approximately 1800 feet (550 meters) of the Santa Fe formation. Using the thickness of the Santa Fe (?) obtained from seismic data at the pre-Dice Throw test site as a control, we expect a total thickness of the Santa Fe Group (?) of about 2800 - 3000 feet (853 - 915 meters) near the Dice Throw test site. This correlates well with a depth to base of Tertiary (?) obtained by reflection survey of 2500 - 2600 feet (762 - 792 meters) immediately west of the Dice Throw test site. (Reynolds, 1976) (Figure 26)

Magnetics

Bath (1977) has presented an interpretation of an aeromagnetic survey of the Tularosa Basin flown by Project Magnet of the United States Naval Oceanographic Office. The ~~residual magnetic~~ map of the northern half of the Tularosa Basin is shown in Figure 27. According to Bath, the residual anomalies obtained by subtracting the International Geomagnetic Reference Field (IGRF) are too negative to be credible in some areas in the western portion of the map. To obtain a more realistic residual map, he fitted a planar surface to the data by least squares adjustment and subtracted the surface from the IGRF residuals. The zero datum was in effect increased by 190 gammas. The resulting map is shown in Figure 28.

According to Bath, the extensive areas of negative anom-

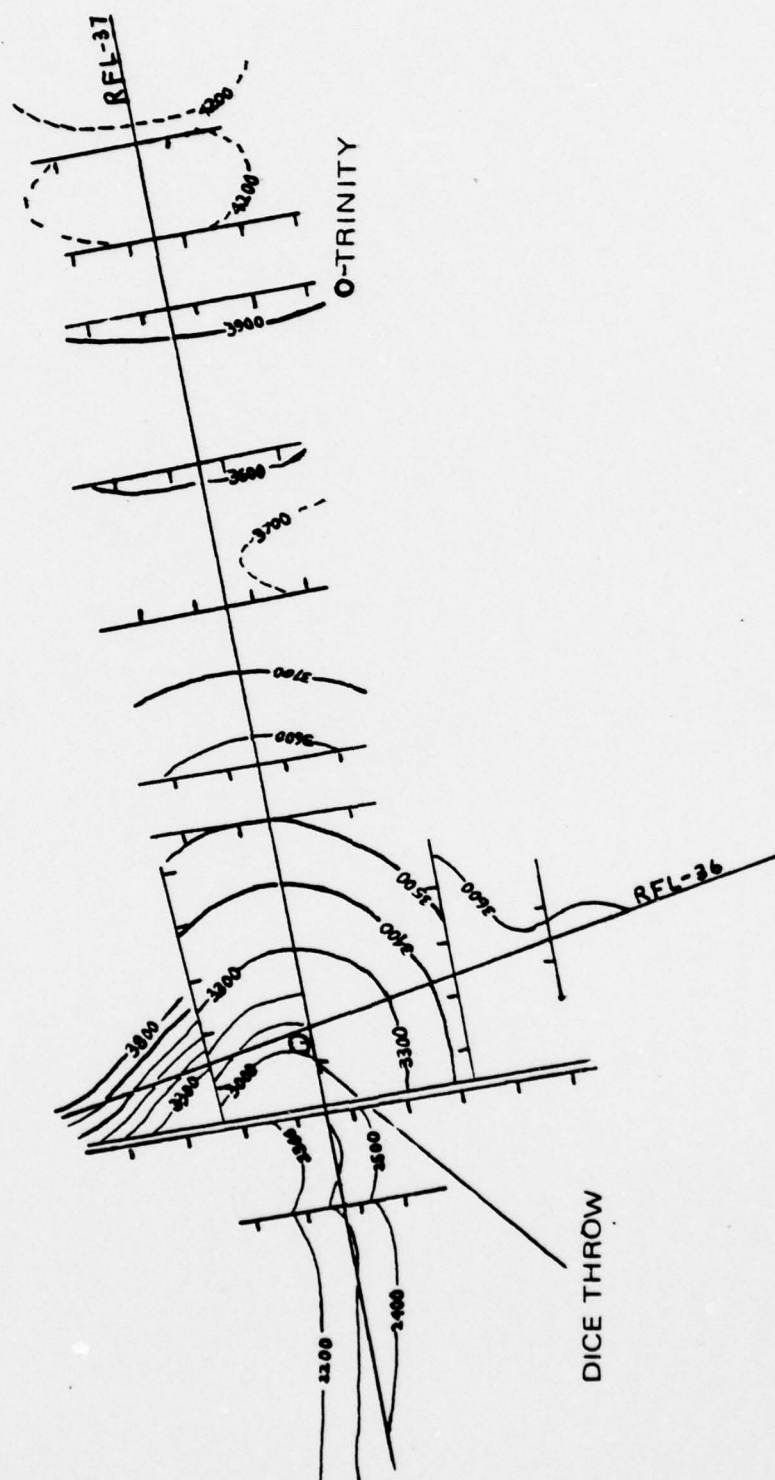


Figure 26. Elevation in feet of base of Tertiary (?) in Dice Throw test area. (from Reynolds, 1976)

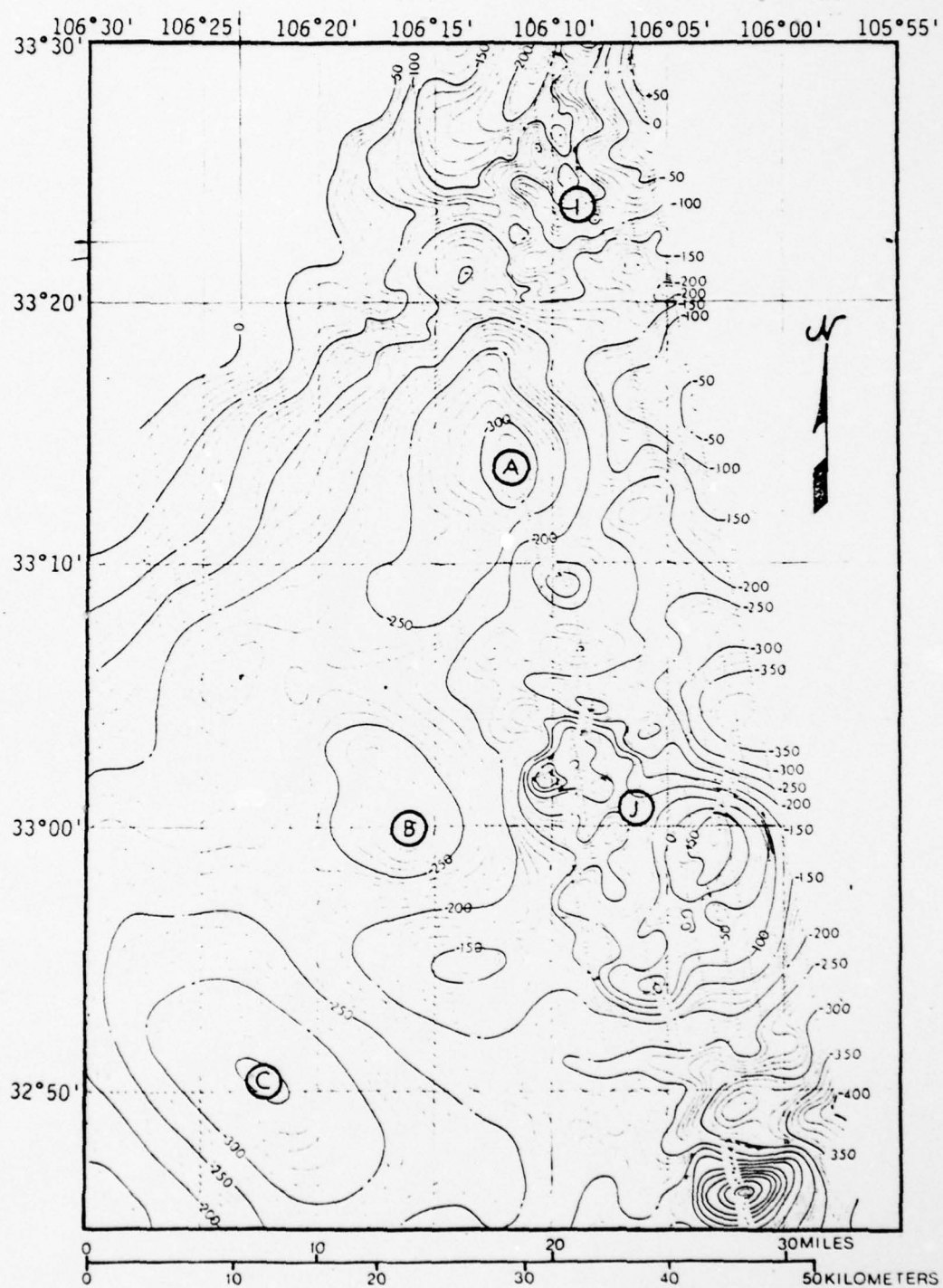


Figure 27. IGRF map of northern portion of Tularosa Basin. (from Bath, 1977)

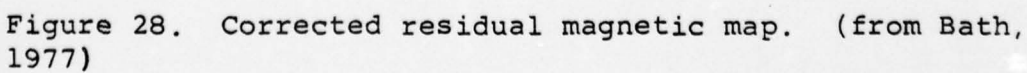


Figure 28. Corrected residual magnetic map. (from Bath, 1977)

ally evident in Figure 28 are the result of an increase in thickness of non-magnetic alluvium and older sediments overlying magnetized Precambrian rock. The minima at A, B, and C are thought to indicate areas of thicker sediments.

Bath states that the prominent positive anomalies can be explained by a decrease in thickness of non-magnetic sediments overlying either Precambrian rock or large masses of igneous rock. In the northwestern corner of the map, a northward increase in magnetic intensity is caused by an increase in elevation of the top of buried magnetic rock. Because of the low anomaly gradient, Bath identifies the magnetic rock as Precambrian rather than a younger igneous intrusion. An increase in elevation of the top of Precambrian rock is compatible with the gravity map of Healey and the gravity interpretation given by McLean.

The positive anomaly at J is thought by Bath to represent a Late Cretaceous or Cenozoic intrusive. An irregular anomaly pattern is found over the Malpais. Although it is strongly magnetized, its average thickness of 65 feet (20 meters) is too thin to produce a prominent anomaly at the elevation at which the survey was flown. (5700 feet, 1737 meters)

SURFACE WAVE PROPAGATION IN THE TULAROSA BASIN

Description of Seismic Array

An extensive seismic network was in operation within the Tularosa Basin for both of the pre-Dice Throw explosions. As shown in Figure 4 , four agencies, the Air Force Weapons Laboratory, the Environmental Research Institute of Michigan, the Albuquerque Seismological Laboratory, and Southern Methodist University participated in the seismic experiment. This section will be concerned primarily with a discussion of the seismic waves recorded by the stations fielded by the Albuquerque Seismological Laboratory (ASL) and Southern Methodist University (SMU).

Six of the seven seismic stations operated by ASL employed the model AS-2 field system developed at ASL. These consist of three model S-13 Geotech seismometers recording the radial, transverse, and vertical components in analog form on magnetic tape. The seventh system was an L-7 velocity seismograph. (Hoffman and Harding, 1977)

The SMU field systems also employed the Geotech S-13 seismometer recorded in analog form on magnetic tape. For

the August, 1975, event the SMU station recorded two vertical components a short distance apart. One radial component in addition to the two verticals was in operation at the SMU station for the September, 1975, detonation.

The AS-2 and the SMU systems both have a velocity response curve essentially flat between 1-30 hertz. The L-7 system response is flat to velocity between 0.1-30 hertz.

The Observed Surface Waves

Many of the seismic records of the August, 1975, pre-Dice Throw detonation are unusual in that two well developed groups of surface waves are present. The record from the SMU station on the north side of the Malpais is shown in Figure 5 and is typical. The phenomenon was most evident on records from the ASL and SMU stations, all of which were positioned on an east-west line through the shot point as shown in Figures 4 and 29. The ASL records of the August blast are shown in Figures 30 -36.

The configuration of the SMU and ASL seismic array was modified for the September, 1975, explosion. The position of the ASL stations is shown in Figure 37. The SMU station was moved to the south edge of the Malpais as shown in Figure 4. Records from the ASL stations are shown in Figures 38 -44.

The seismic record from the SMU station at a range of approximately 33,000 feet (10,000 meters) distant from the

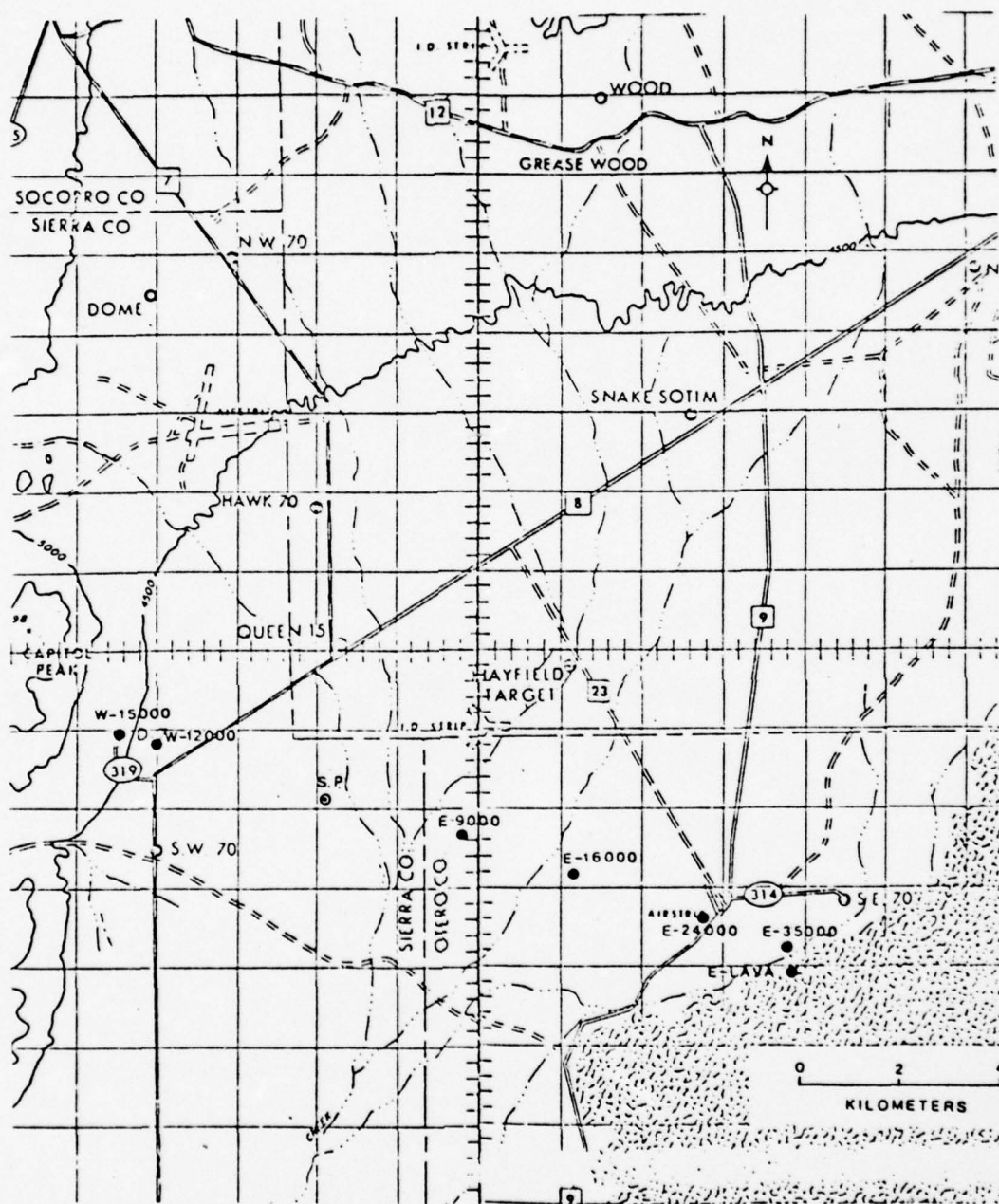


Figure 29. ASL station locations for August, 1975, pre-Dice Throw event. (from Hoffman and Harding, 1977)

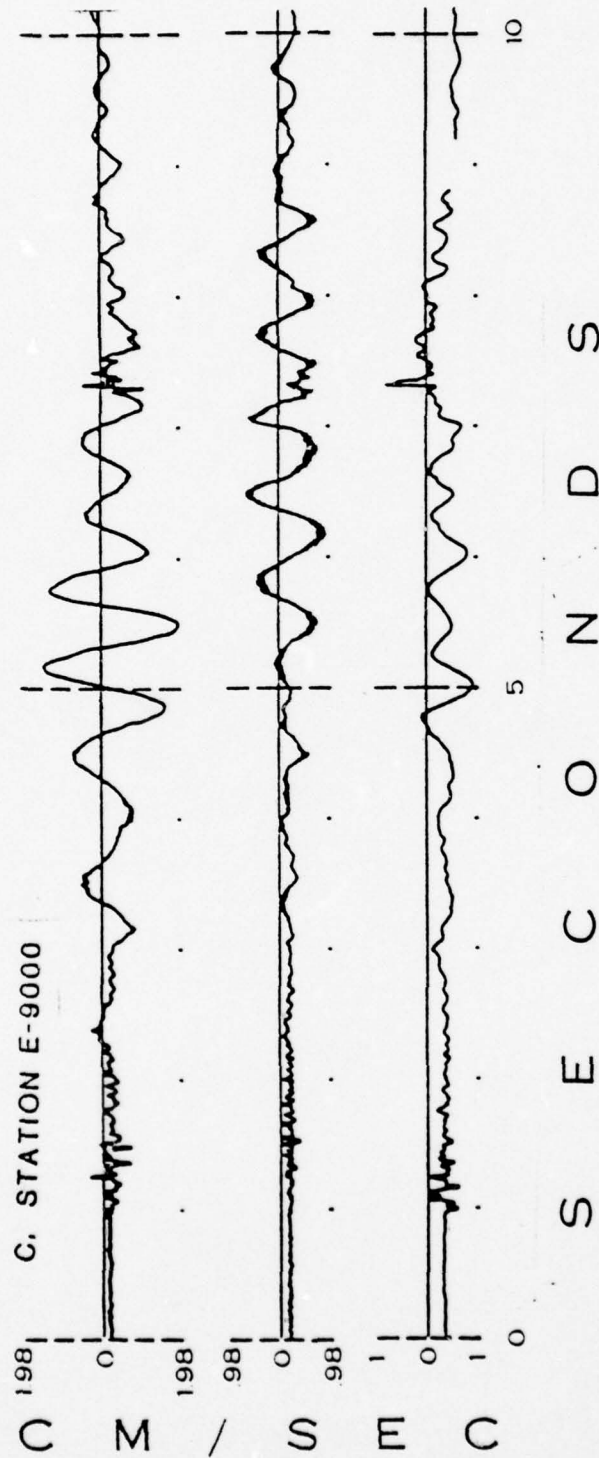


Figure 30. Recording from L-7 system at station E-9000, August, 1975, event. (from Hoffman and Harding, 1977)

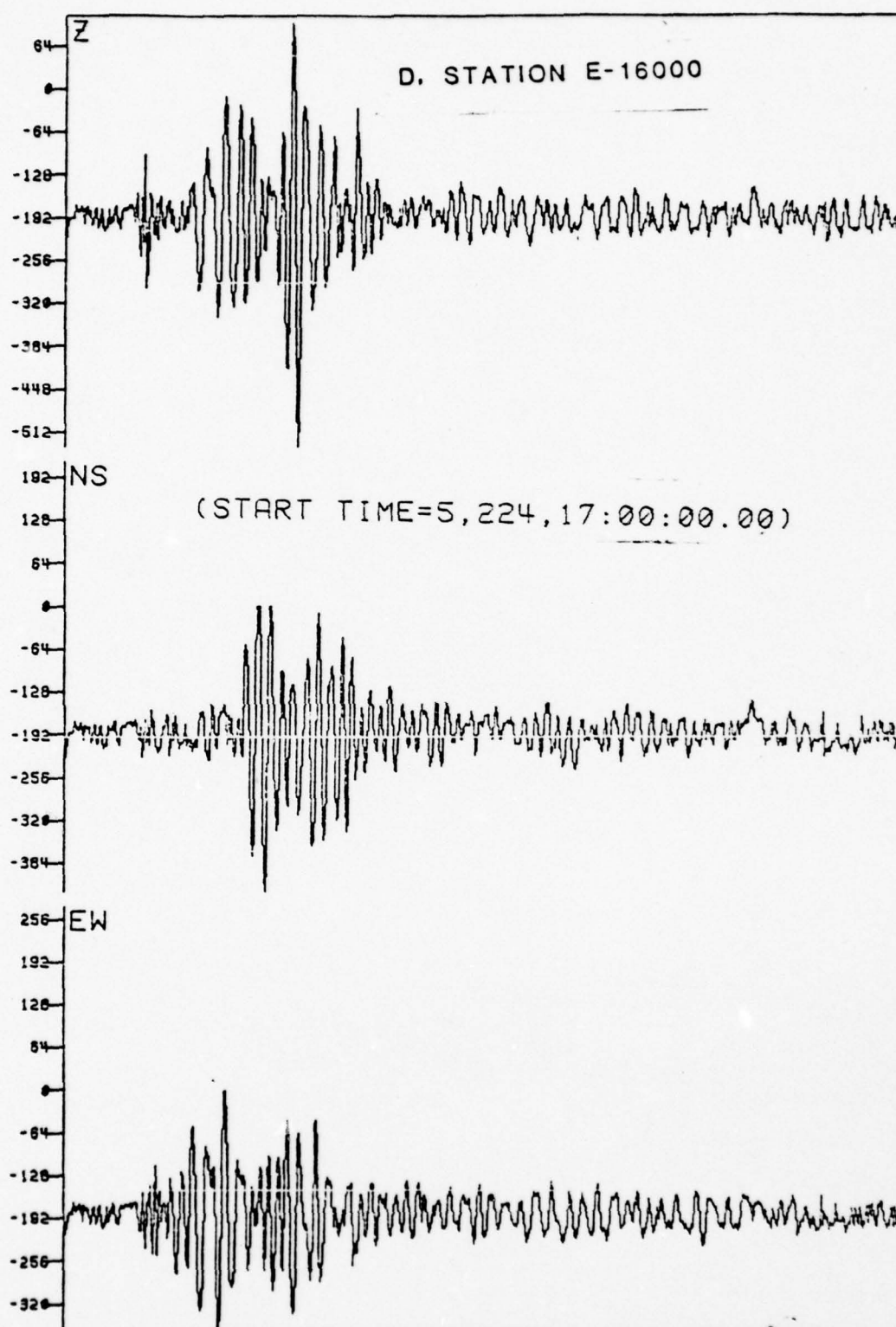


Figure 31. Recording from station E-16000. August, 1975, event. (from Hoffman and Harding, 1977)

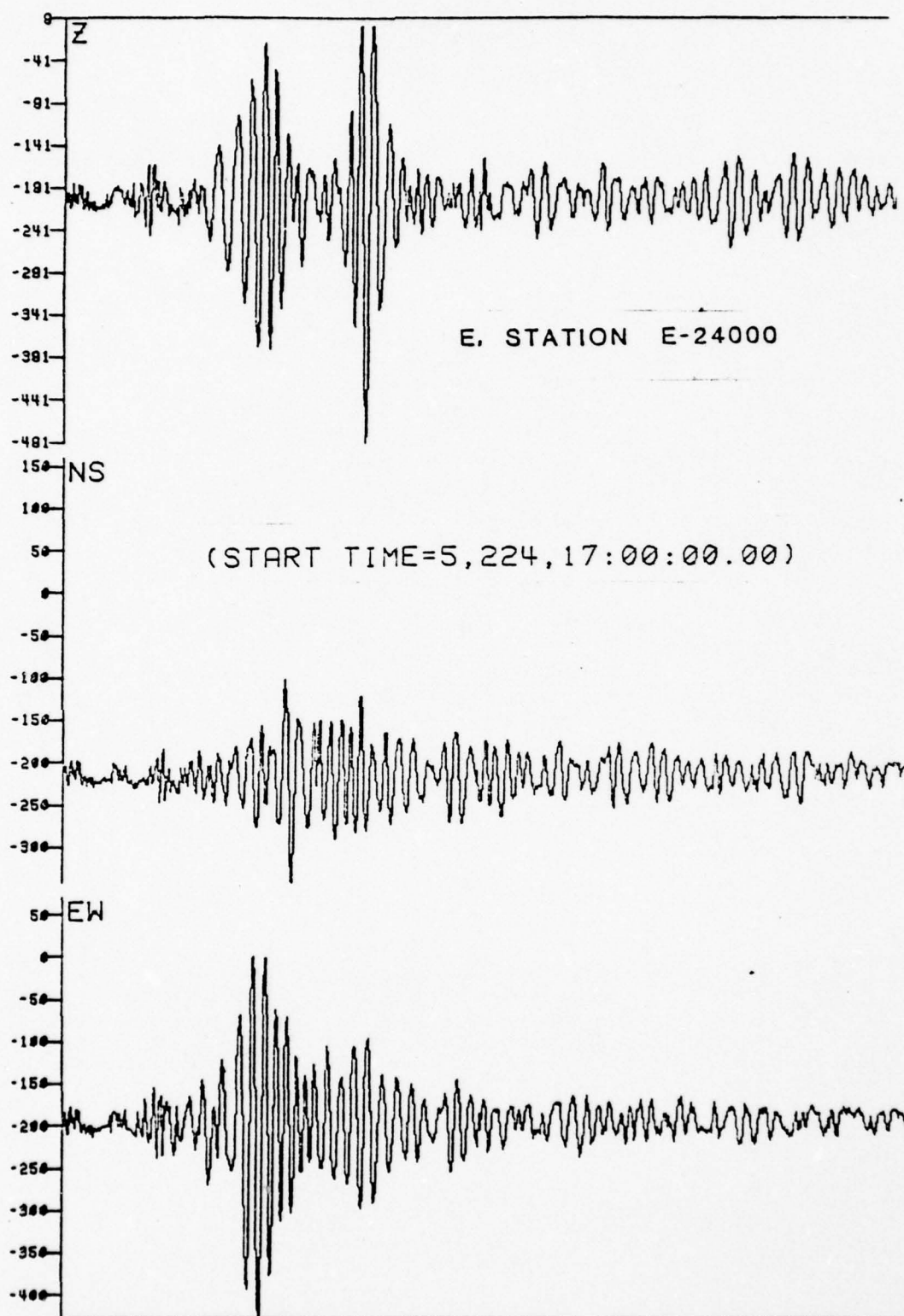


Figure 32. Recording from station E-24000. August, 1975, event. (from Hoffman and Harding, 1977)

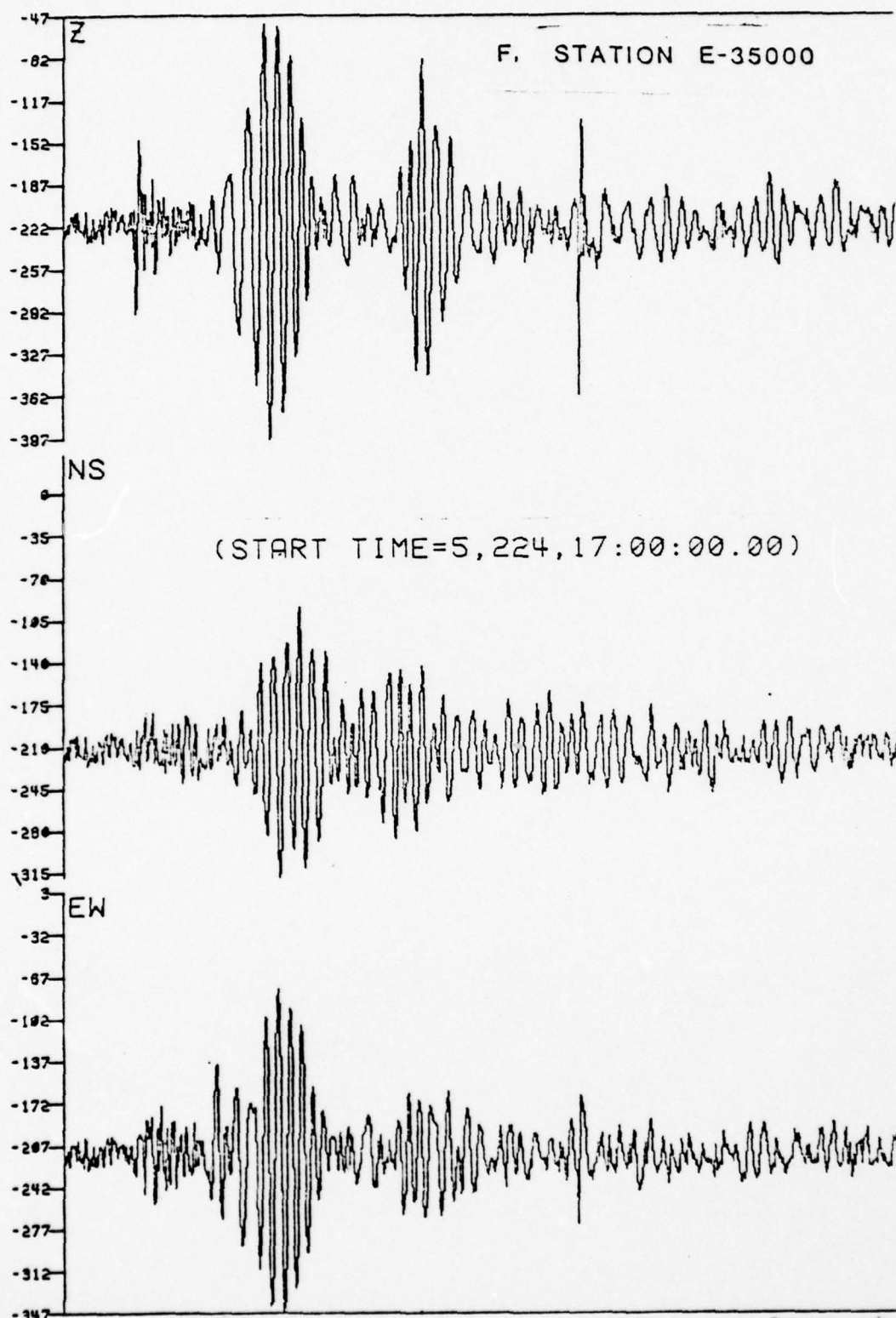


Figure 33. Recording from station E-35000. August, 1975, event. (from Hoffman and Harding, 1977).

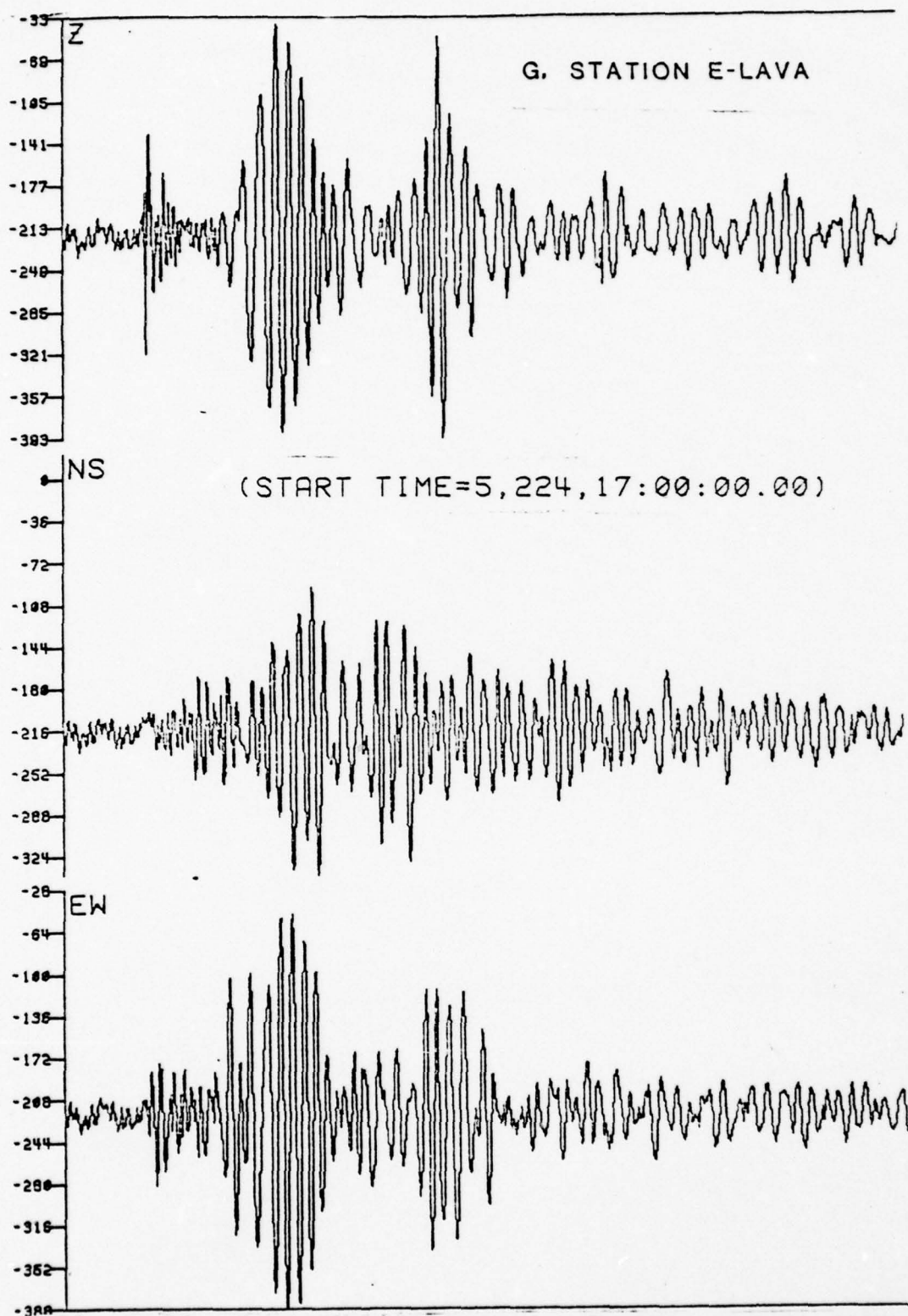


Figure 34. Recording from station E-LAVA. August, 1975, event. (from Hoffman and Harding, 1977)

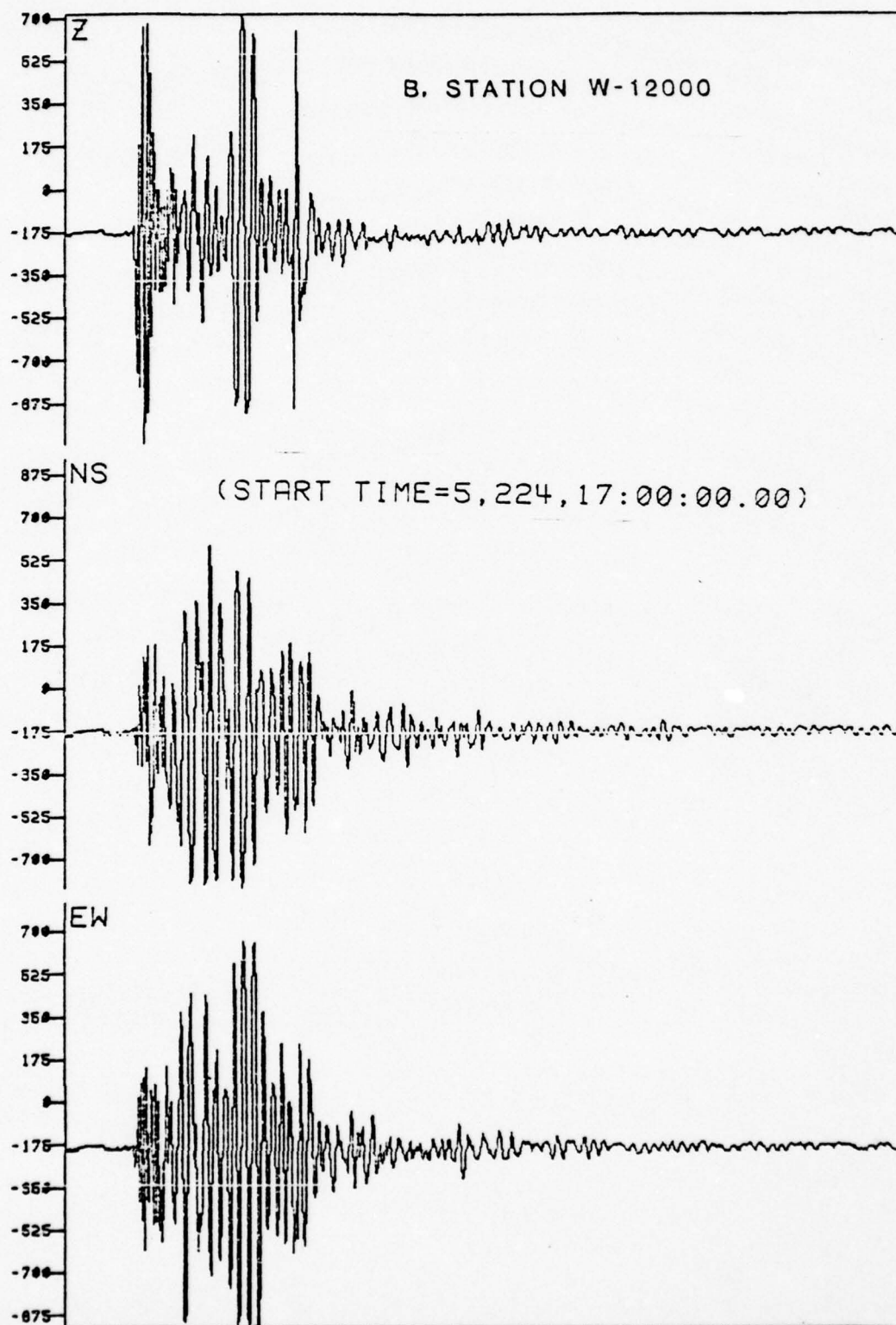


Figure 35. Recording from station W-12000. August, 1975, event. (from Hoffman and Harding, 1977)

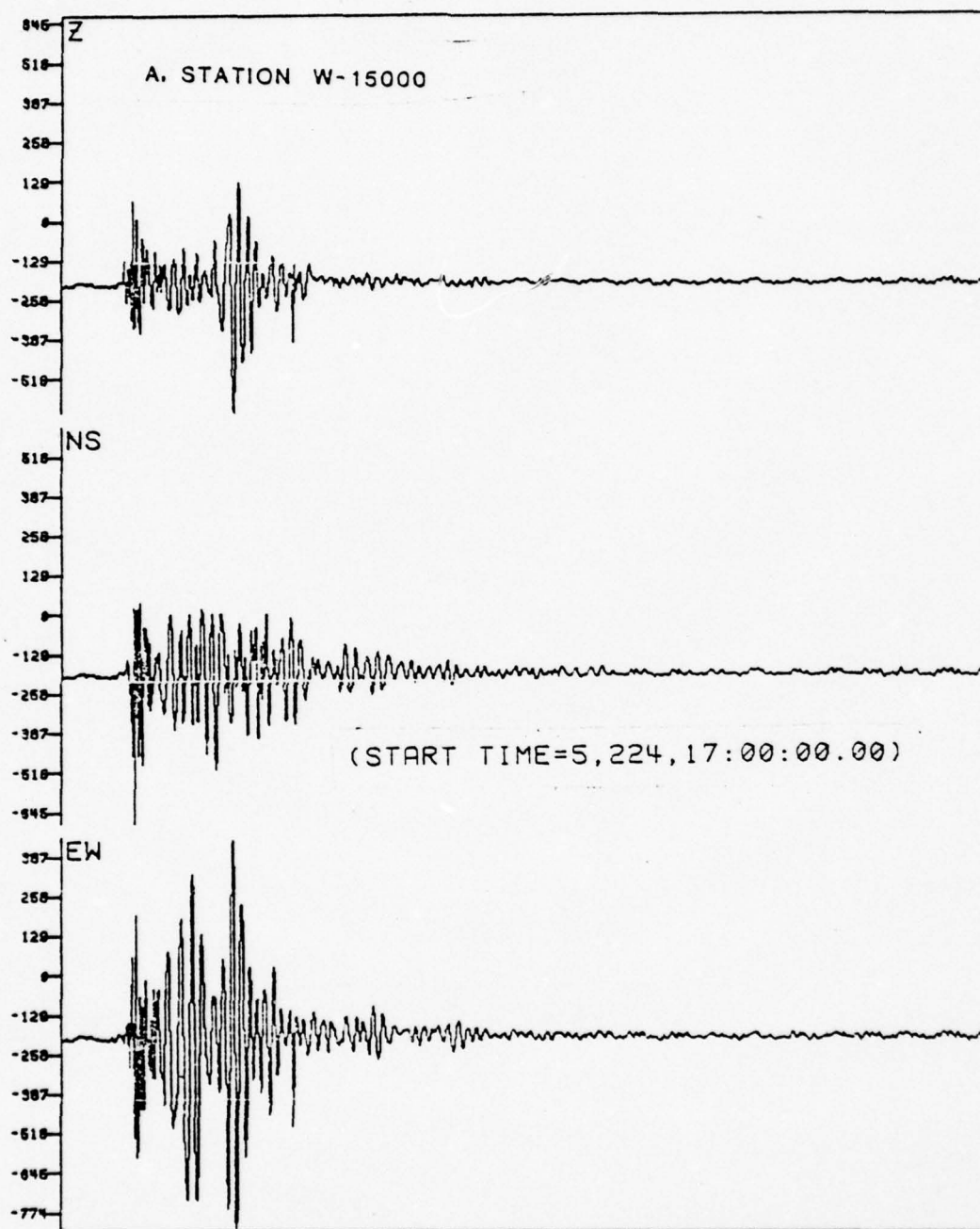


Figure 36. Recording from station W-15000. August, 1975, event. (from Hoffman and Harding, 1977)

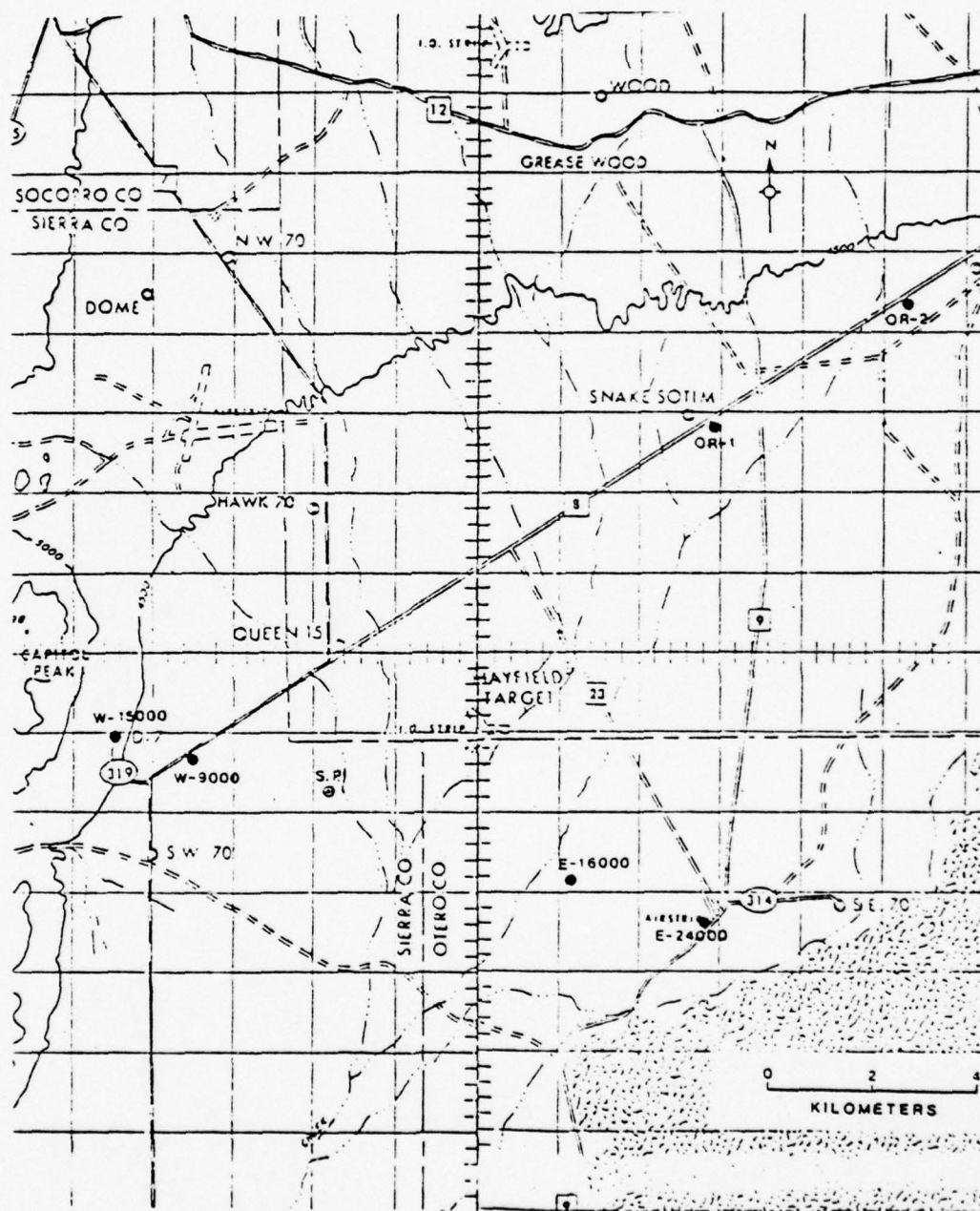


Figure 37. ASL station locations for August, 1975, event.
(from Hoffman and Harding, 1977)

C. STATION E-16000

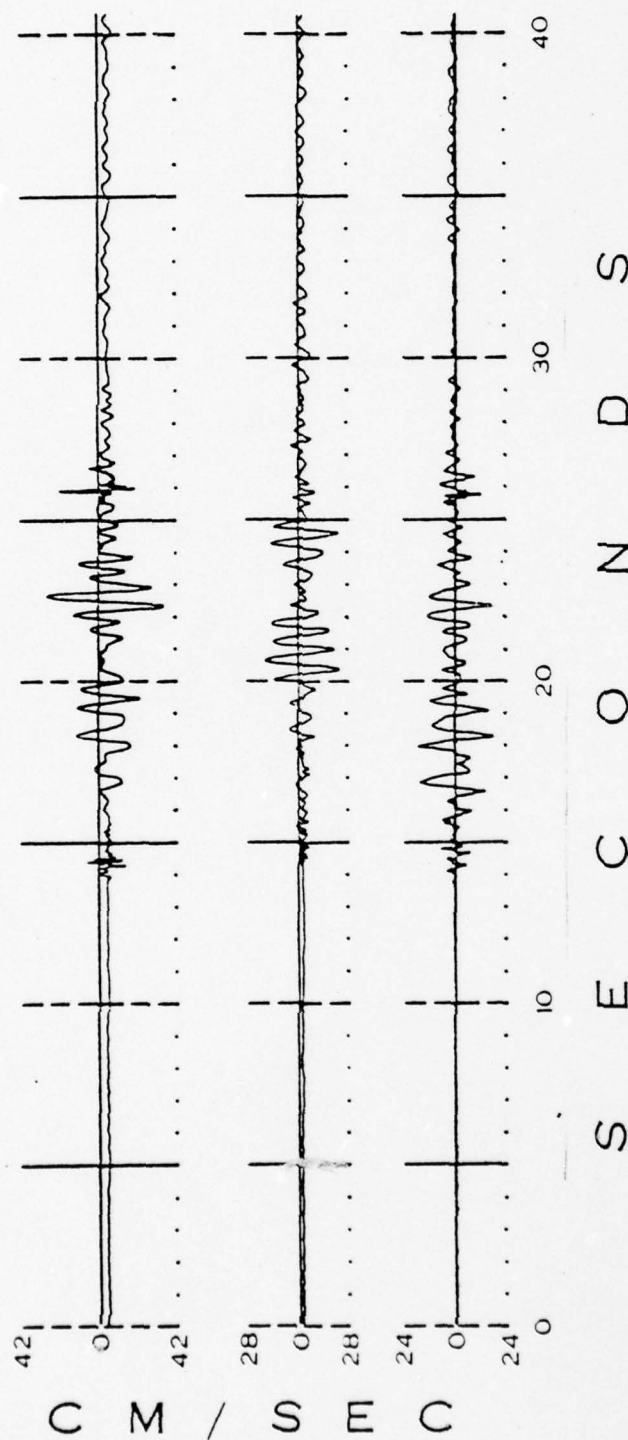


Figure 38. L-7 system recording from station E-16000. September, 1975, event. (from Hoffman and Harding, 1977)

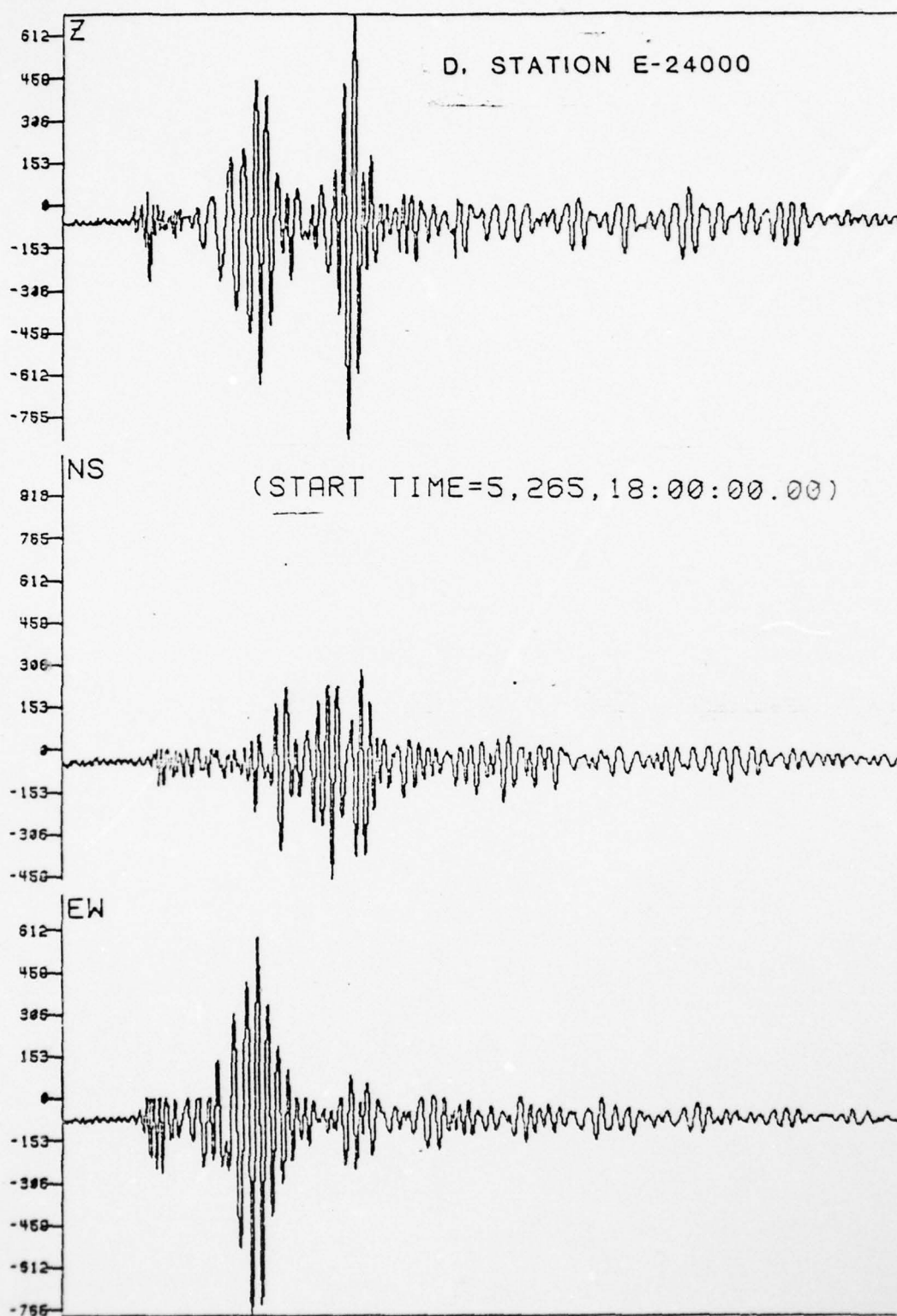


Figure 39. Recording from station E-24000. September, 1975, event. (from Hoffman and Harding, 1977)

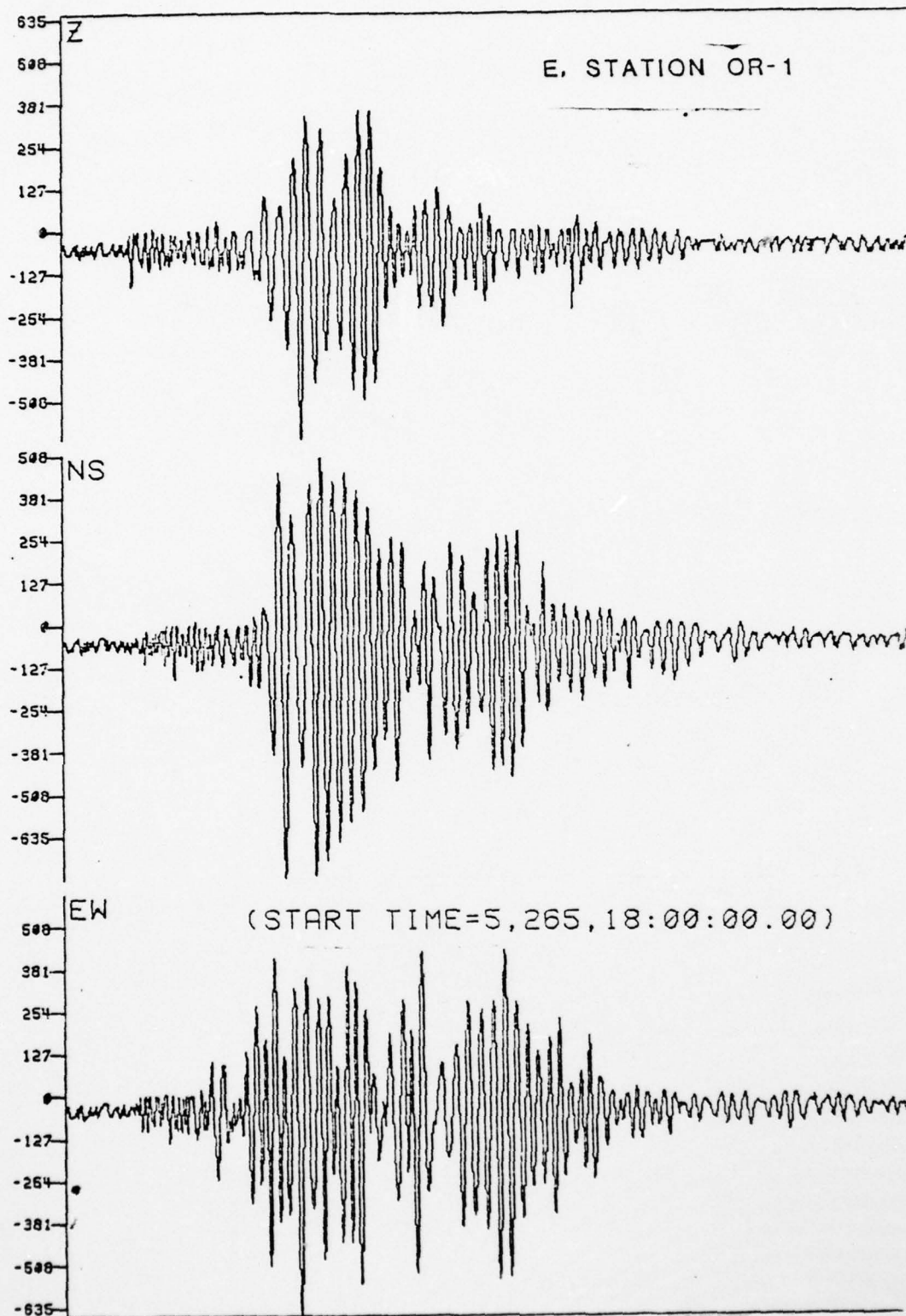


Figure 40. Recording from station OR-1. September, 1975, event. (from Hoffman and Harding, 1977)

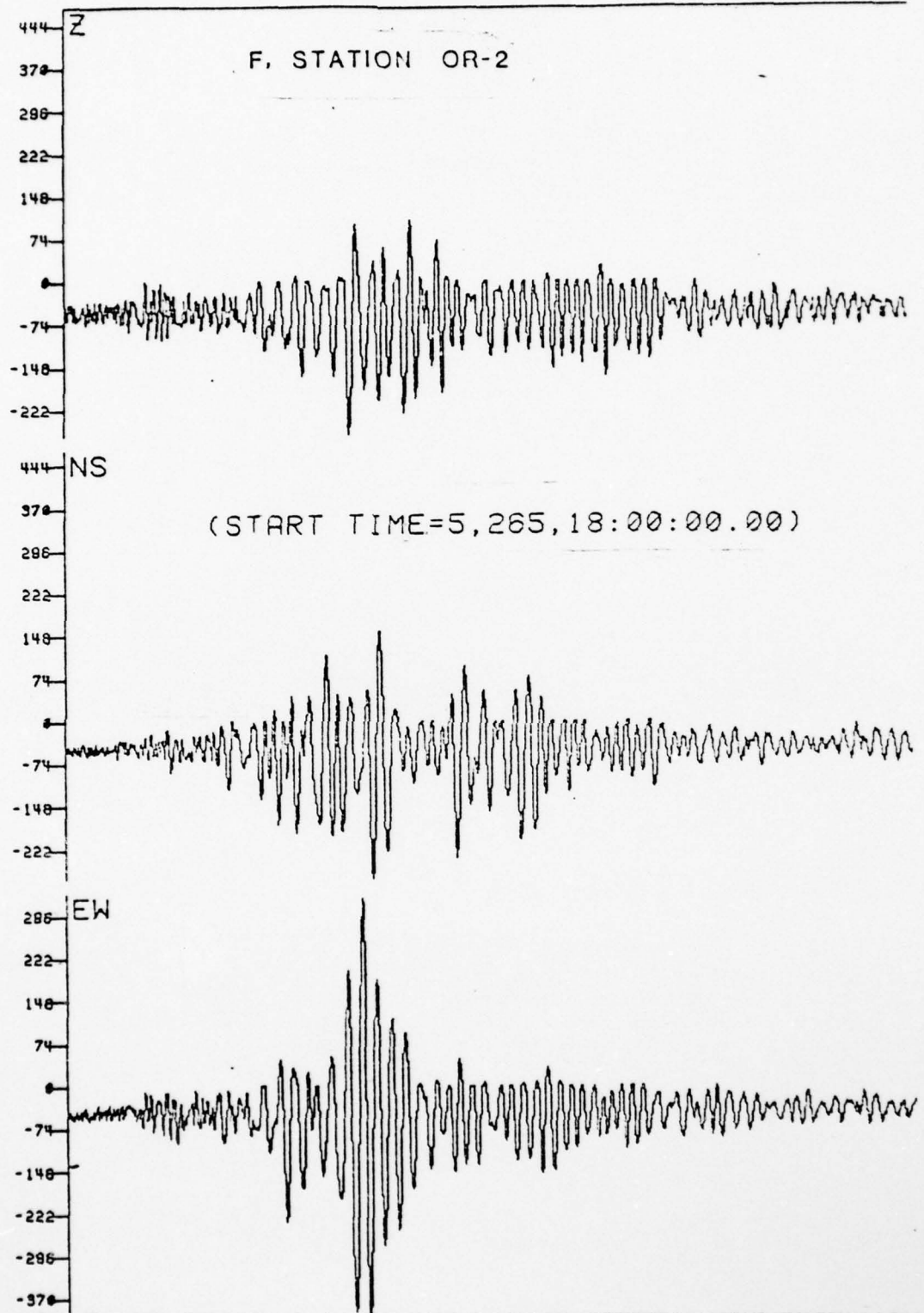


Figure 41. Recording from station OR-2. September, 1975, event. (from Hoffman and Harding, 1977)

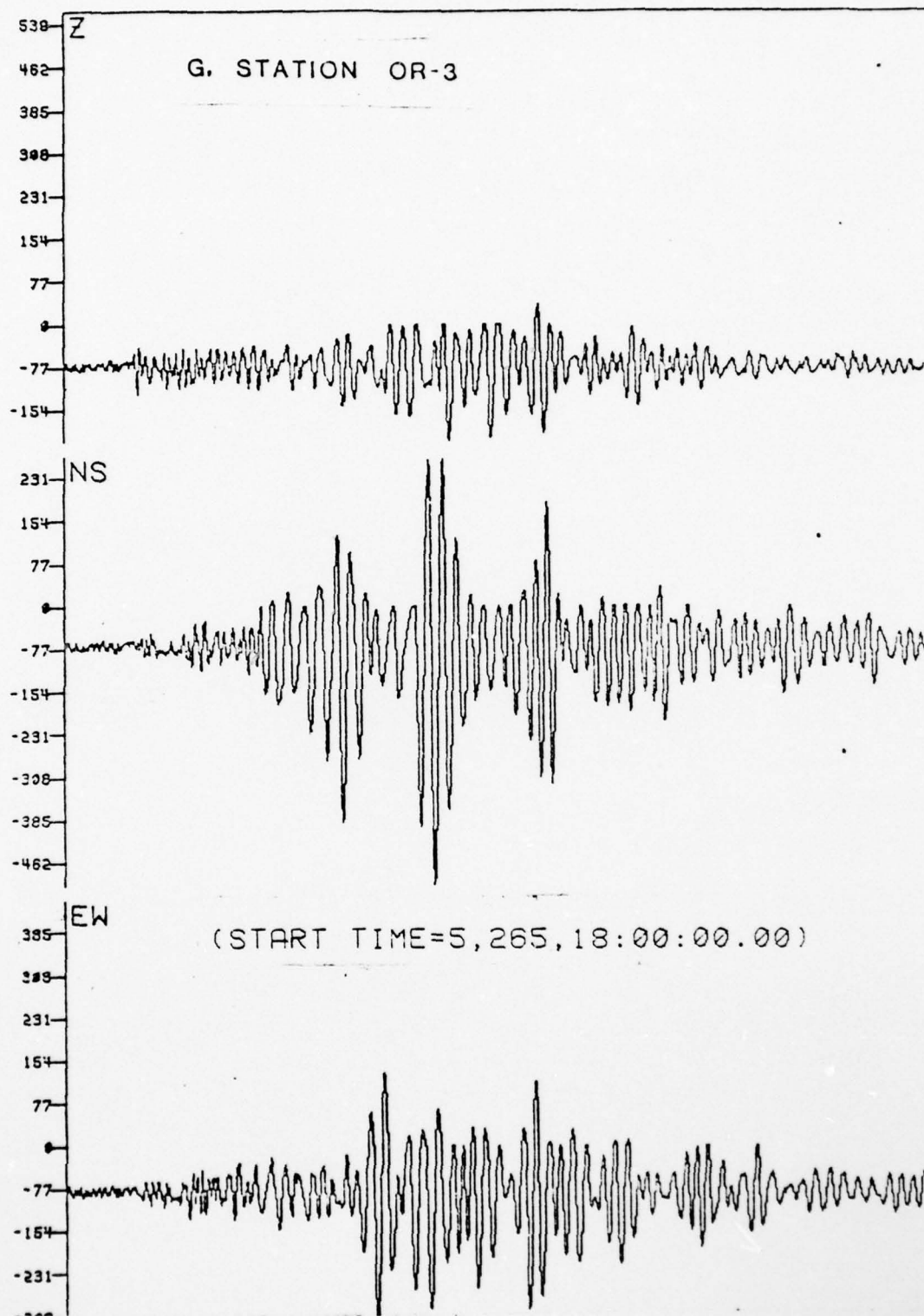


Figure 42. Recording from station OR-3. September, 1975, event. (from Hoffman and Harding, 1977)

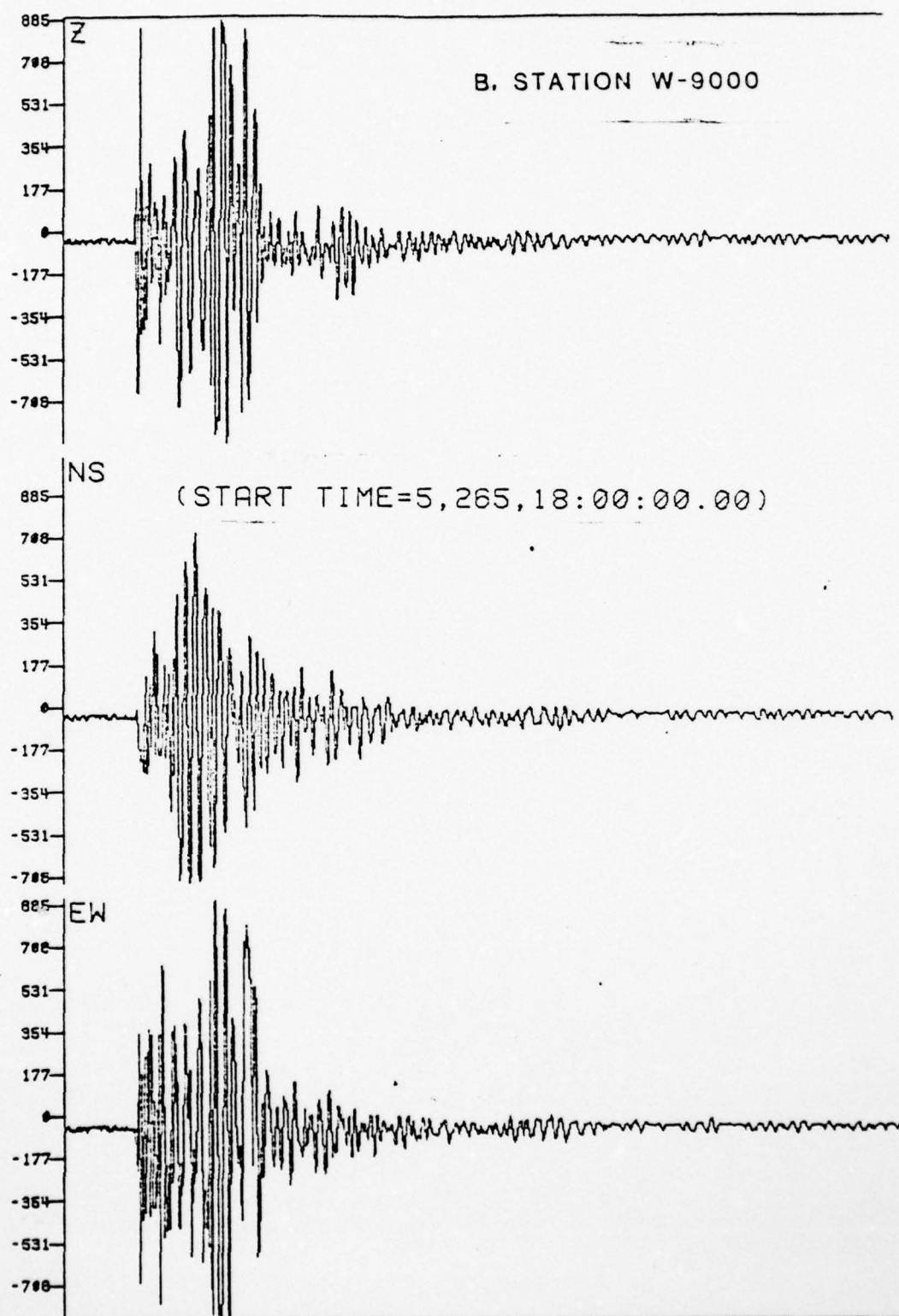


Figure 43. Recording from station W-9000. September, 1975, event. (from Hoffman and Harding, 1977)

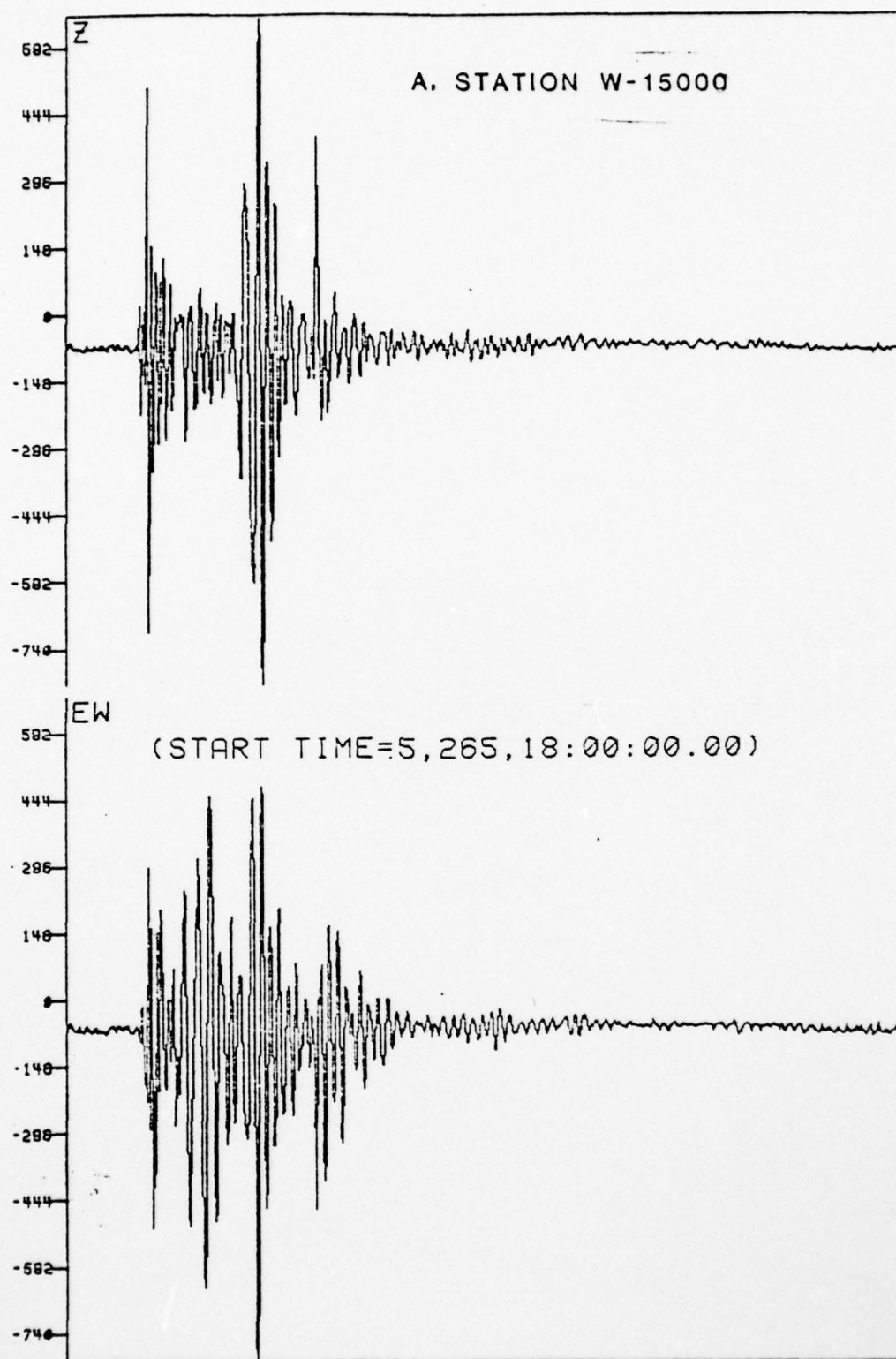


Figure 44. Recording from station W-15000. September, 1975, event. (from Hoffman and Harding, 1977)

August, 1975, explosion clearly shows two well developed surface wave groups. The first surface wave arrival is normally dispersed and has an apparent average group velocity of about 2600 feet per second (.8 kilometer per second). The second arrival is slightly inversely dispersed, has an apparent group velocity of about 1600 feet per second (.5 kilometer per second) and is about one-half of the duration of the first group. Fourier spectral content of the two wave groups is quite similar (Figure 46), suggesting that the second wave might be a reflection of the first or perhaps a multiple impulse phenomenon caused by the nature of the explosion; however, records from the ASL stations along the east-west line through the shotpoint reveal true moveout of the two phases as distance from the shotpoint increases, implying that the two phases possess two distinct group velocities. (Figures 30 -36) In addition, the two phases pull apart with increasing distance to the west of the shotpoint as well as to the east, ruling out a reflection from the nearby mountain front. The two phases are present on the radial and vertical components. Motion on the transverse components is generally of lesser amplitude and appears for the most part to be unrelated to motion in the vertical and radial planes.

The ASL stations reoccupied for the second shot recorded seismograms almost identical to those obtained from the August detonation, indicating that the change in explosive and charge

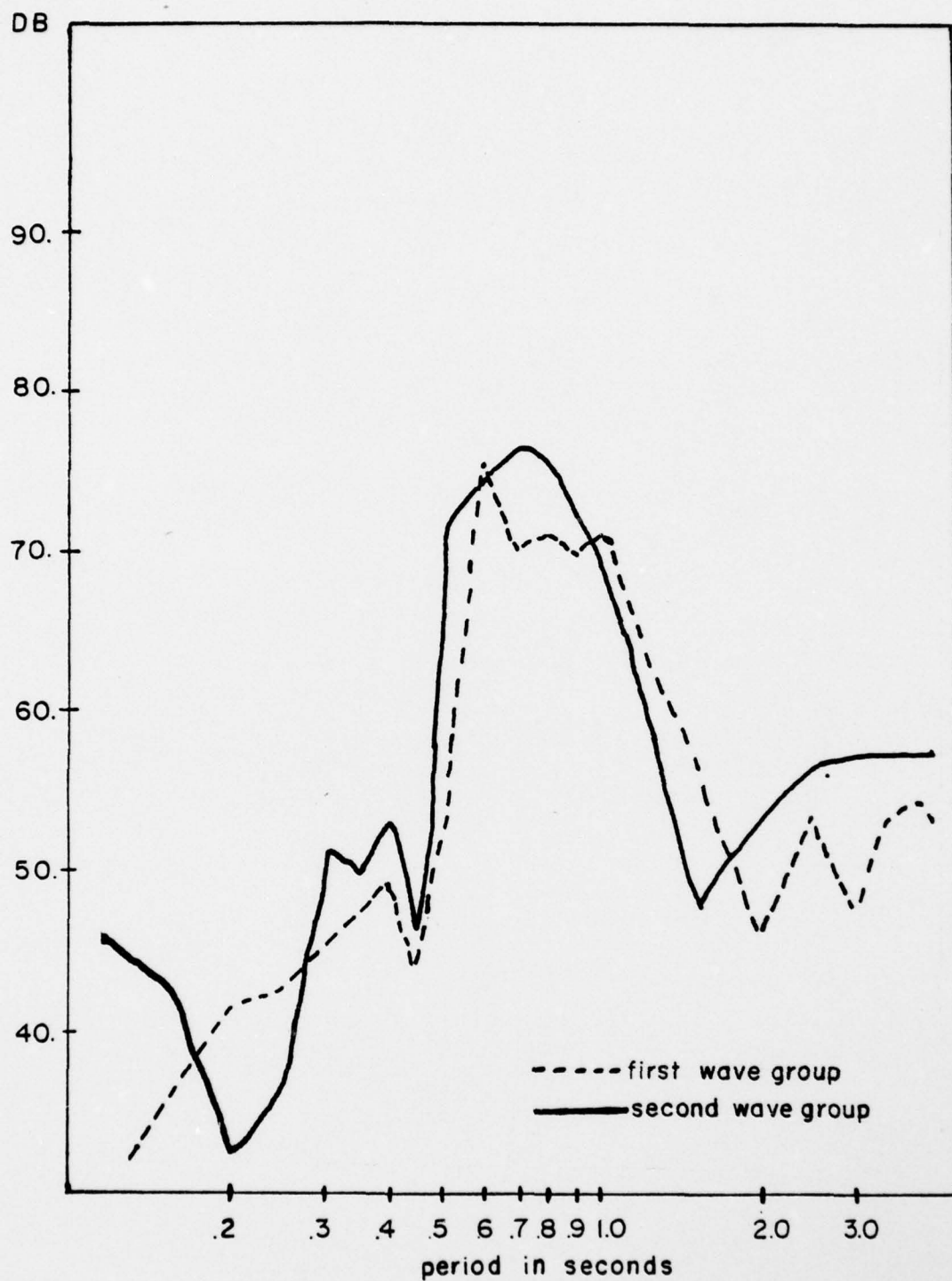


Figure 46. Comparison of spectra of first and second surface wave groups received at SMU station. August, 1975, event.

configuration and slight shift in location of ground zero (~800 feet, 244 meters) between tests had little effect on the seismic source function.

The records from ASL stations OR-1, OR-2, and OR-3 in operation for the second Tularosa Basin shot reveal quite complex surface wave groups in contrast to the two well defined groups observed on records from the east-west line through the shotpoint. On the record from the SMU station south of the Malpais shown in Figure 45 , a wave group with two beats with roughly the same apparent group velocity as the first surface wave arrival evident on records of the first shot is present. No distinct wave group resembling the second wave group observed at the August shot is seen at the proper time on the SMU record.

Explanation of Surface Waves Observed East of the Shotpoint

A number of field studies of surface wave propagation in unconsolidated media have been performed in the past. Levshin (1962) has summarized the results of such investigations up to 1962. According to Levshin, the wave having the lowest group and phase velocity usually corresponds to the fundamental mode Rayleigh wave. The waves arriving before the fundamental mode have been variously interpreted as " M_2 (Sezawa waves), coupled and hydrodynamic waves, and C waves (of the second kind)." Most of these studies, including that of Levshin,

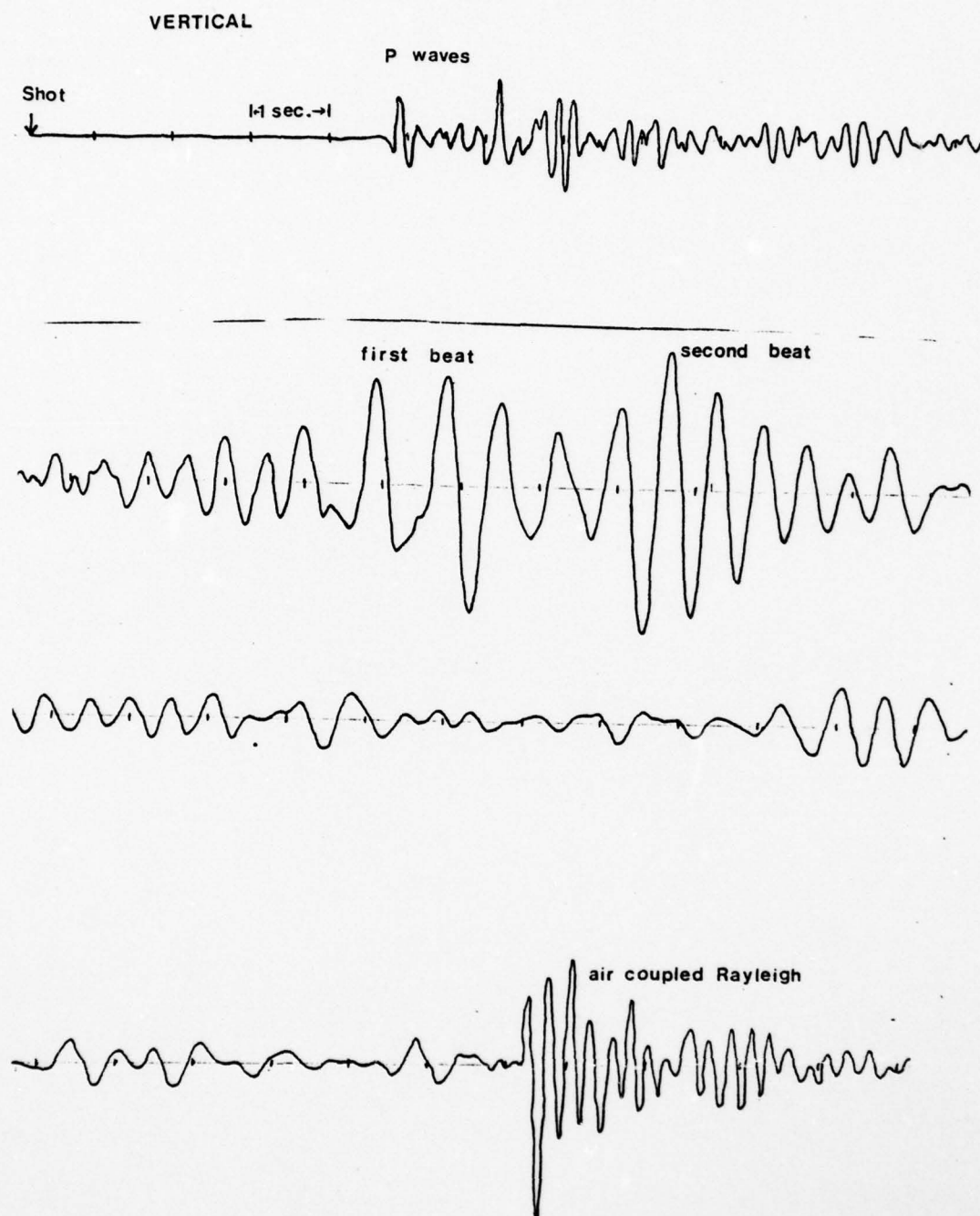


Figure 45. Recording from SMU station south of the Malpais. September, 1975, event.

have dealt with the problem on a small scale, with the observed waves in the frequency range 20-50 Hertz being excited by hammer and plank or small explosions. A notable exception is the seismogram recorded by Leet (1946) at the test of the first atomic bomb, the Trinity event, which occurred in the Jornada del Muerto near the site of the October, 1976, Dice Throw 500 ton explosion. Leet observed two phases on the radial and vertical components. He referred to the first arrival as the "hydrodynamic" wave because of its prograde particle motion. The second arrival was identified as the fundamental mode Rayleigh wave. Levshin observed several groups of Rayleigh type waves. He identified the slowest arrivals as the fundamental mode; the faster waves were thought to be higher modes of the Rayleigh wave. (Figure 7)

From initial appearances, the first surface wave arrival especially as seen on the SMU record in Figure 5 seems to be a classical example of a fundamental mode Rayleigh wave propagating upon the surface of a layered medium. In contrast, the second arrival is inversely dispersed and almost pulselike. The identification of the first surface wave arrival as the fundamental mode Rayleigh wave is not, however, consistent with the characteristic particle motion of the two wave groups. Figures 47 -62 show particle motion plots from the AS-2 stations on the east-west line through the shotpoints. The diagrams were obtained by computer plotting of digital

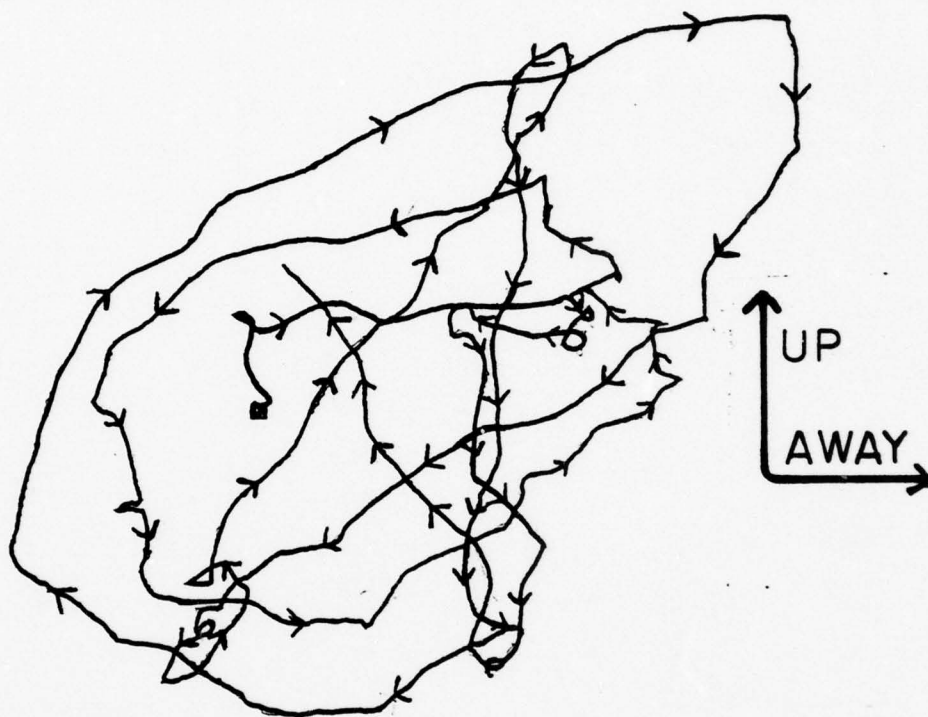


Figure 47. Particle motion of first surface wave group.
E-16000. August, 1975.

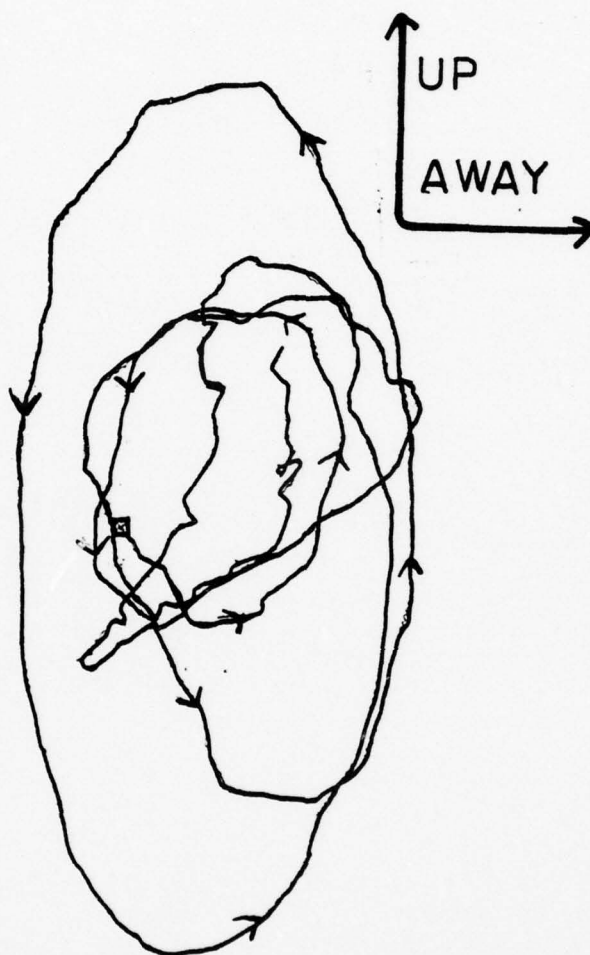


Figure 48. Particle motion of second surface wave group.
E-16000. August, 1975.

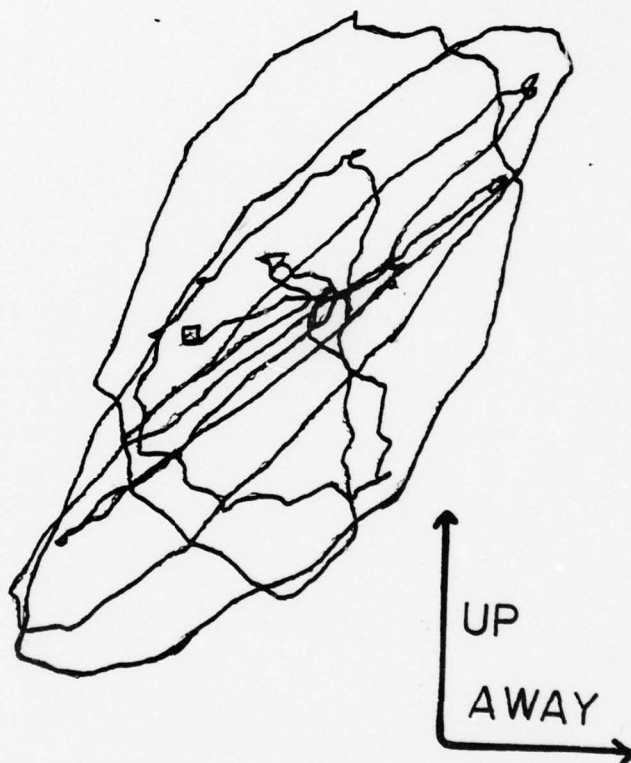


Figure 49. Particle motion of first surface wave group.
E-35000. August, 1975.

AD-A054 161

SOUTHERN METHODIST UNIV DALLAS TEX DALLAS GEOPHYSICAL LAB F/G 8/11
GEOPHYSICAL MODEL STUDIES OF THE TULAROSA BASIN, NEW MEXICO.(U)
DEC 77 R E REINKE, E HERRIN

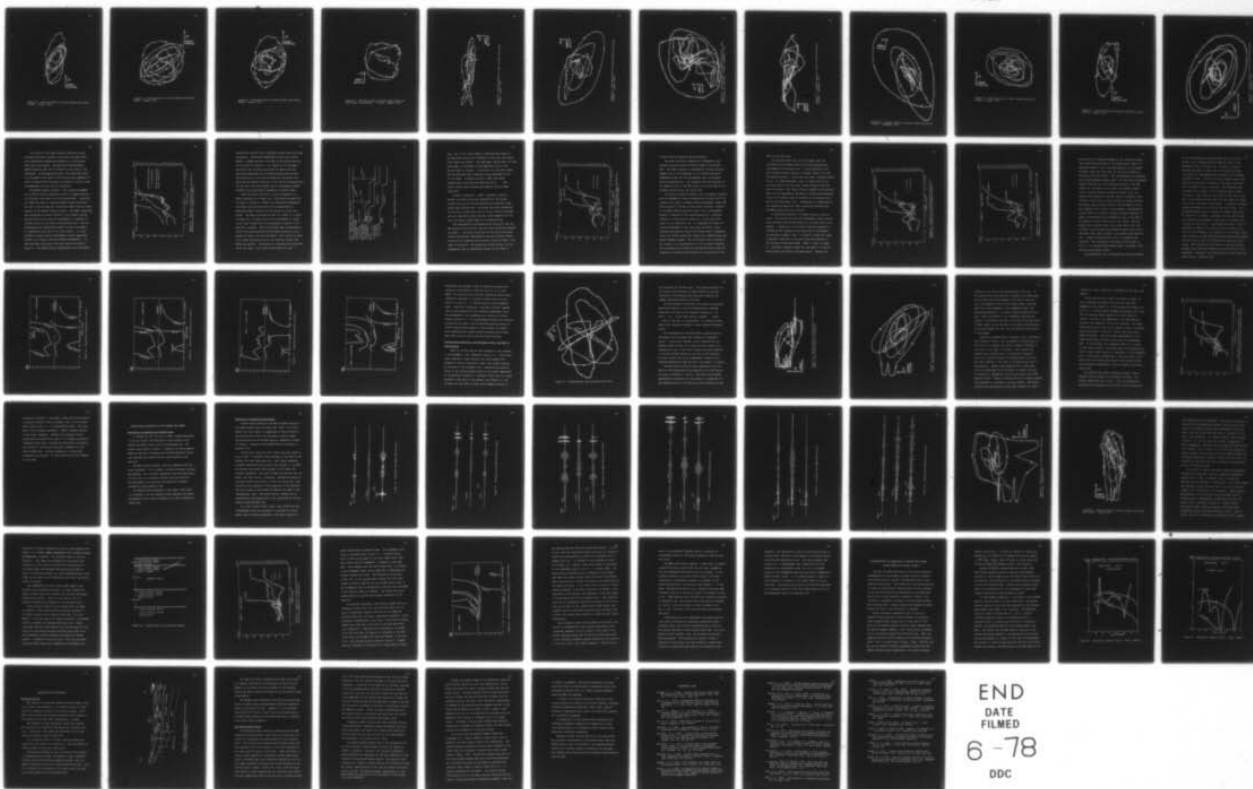
AFOSR-76-2890

UNCLASSIFIED

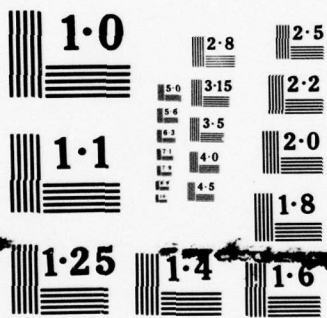
AFOSR-TR-78-0779

NL

2 OF 2
ADA
054161



END
DATE
FILMED
6-78
DDC



NATIONAL BUREAU OF STANDARDS



Figure 50. Particle motion of second surface wave group.
E-35000. August, 1975.

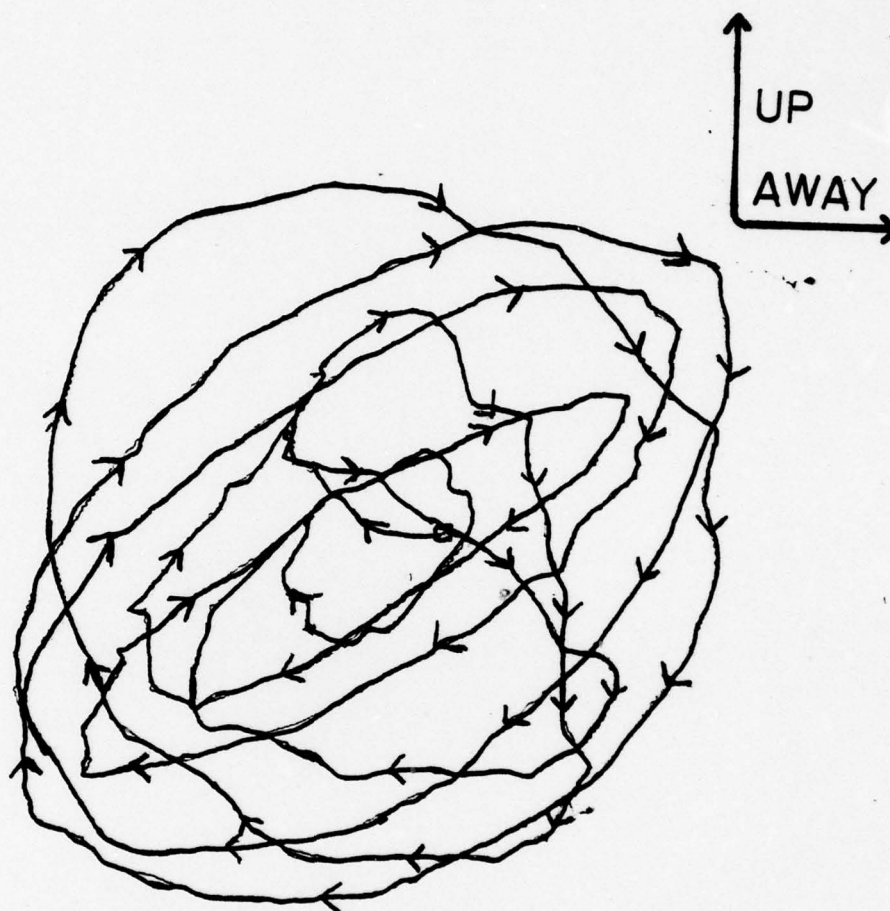


Figure 51. Particle motion of first surface wave group.
E-LAVA. August, 1975.

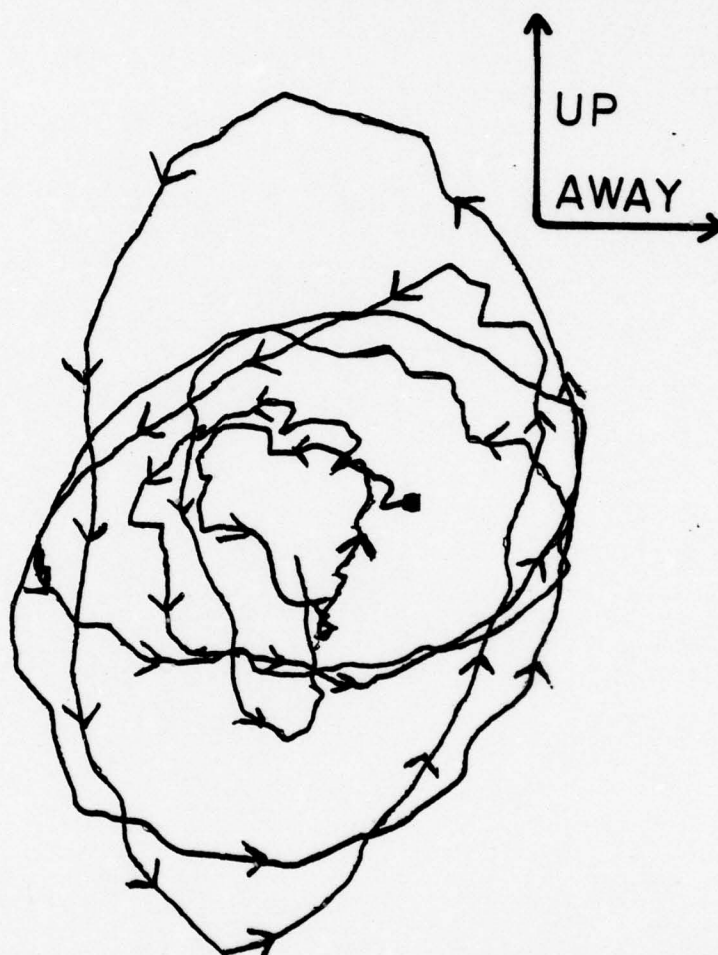


Figure 52. Particle motion of second surface wave group.
E-LAVA. August, 1975.

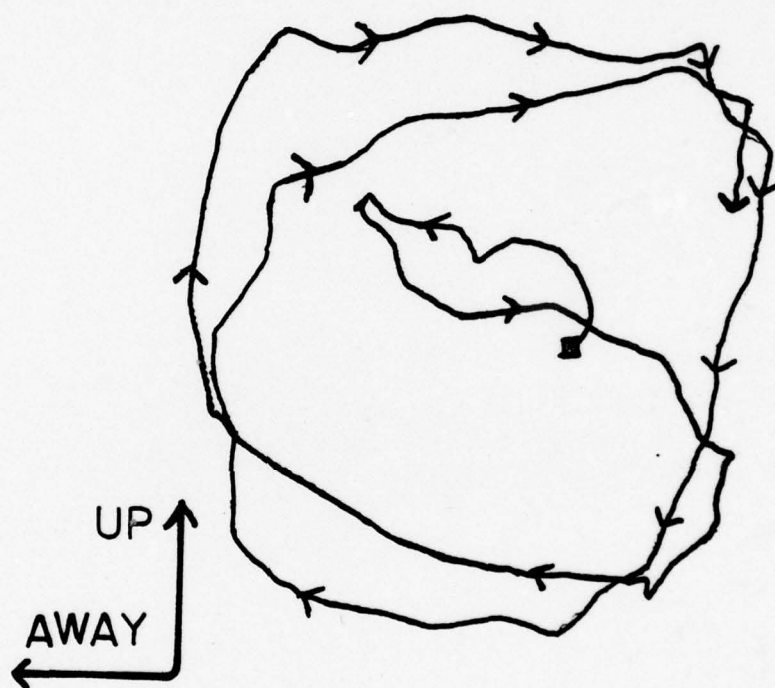


Figure 53. Particle motion of surface wave group (two wave groups not distinct). W-12000. August, 1975.

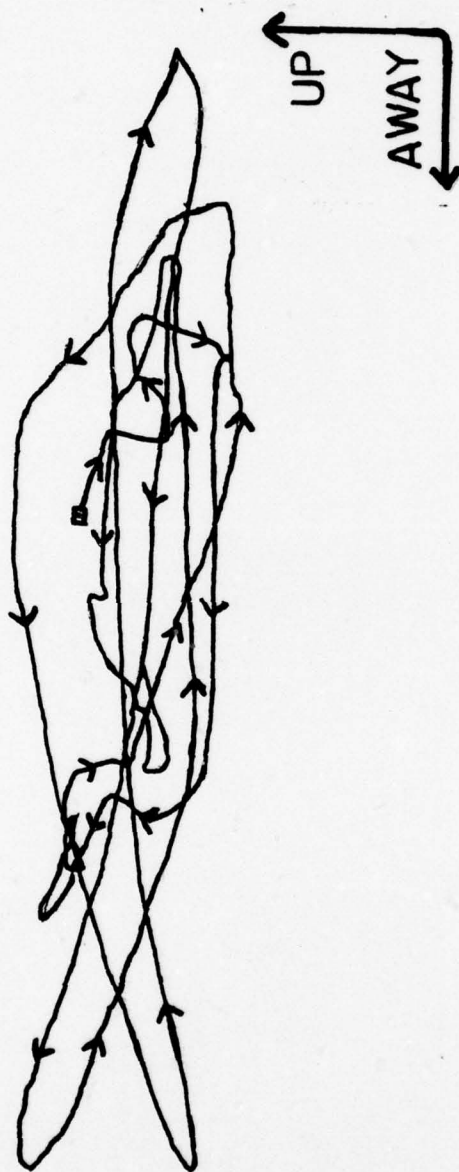


Figure 54. Particle motion of first surface wave group.
W-15000. August, 1975.

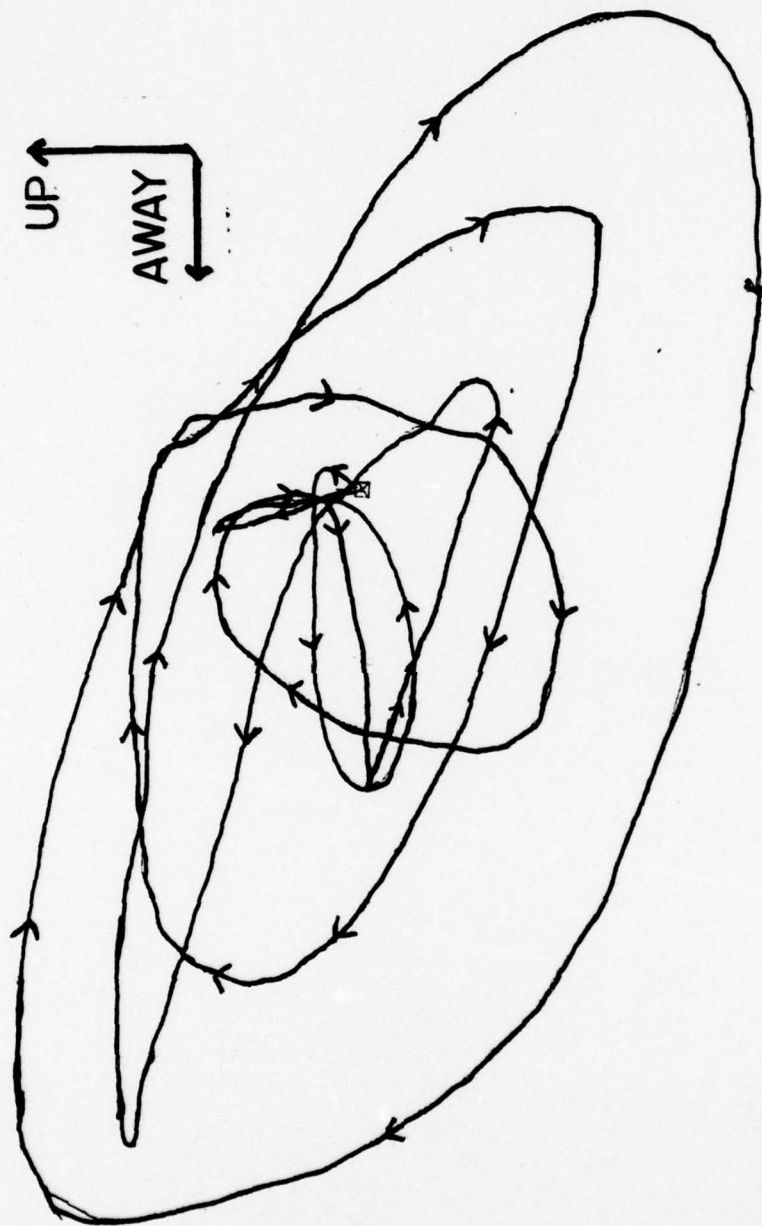


Figure 55. Particle motion of second surface wave group.
W-15000. August, 1975.

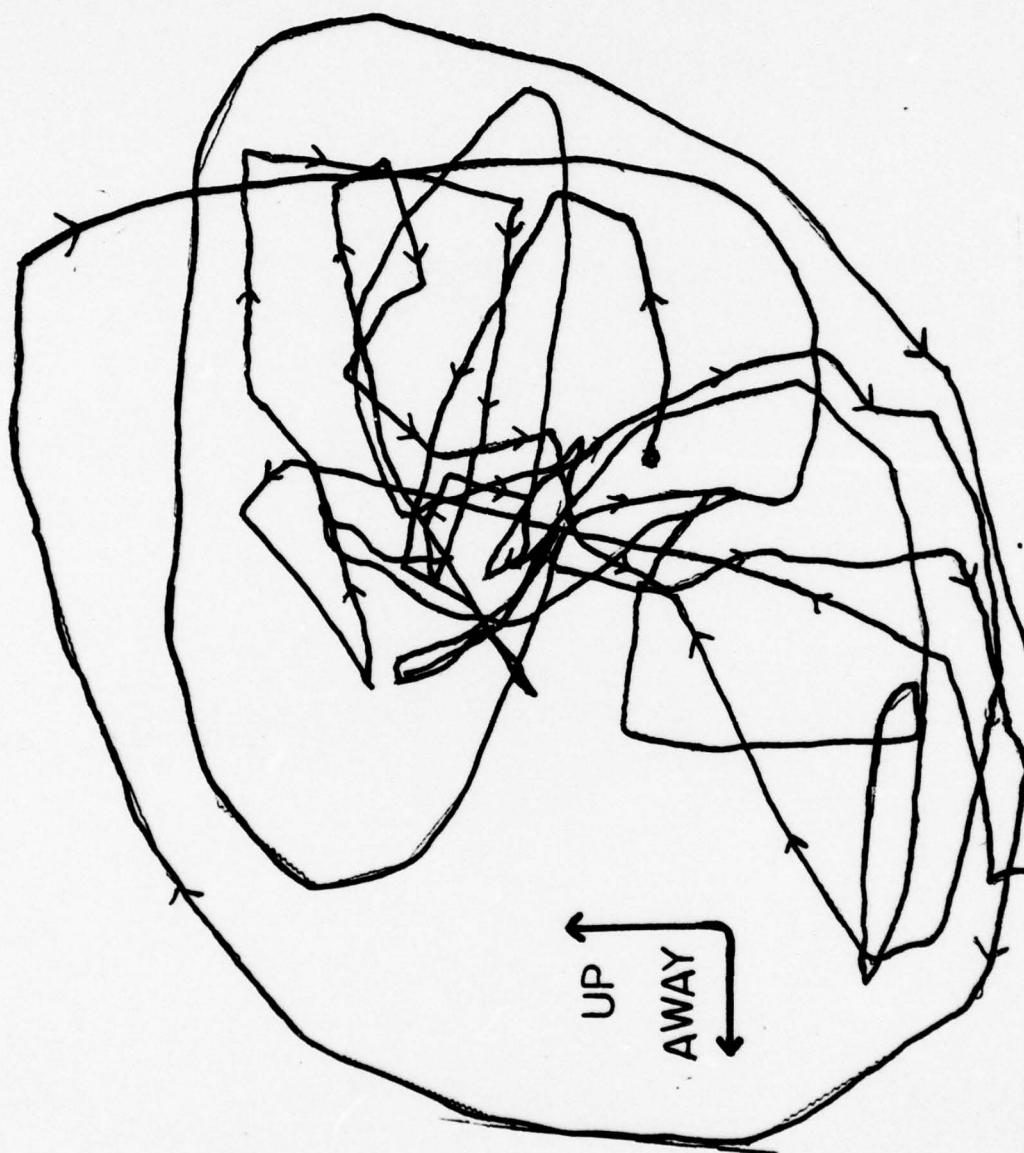


Figure 56. Particle motion of surface wave group. (two wave groups not distinct). W-9000. September, 1975.

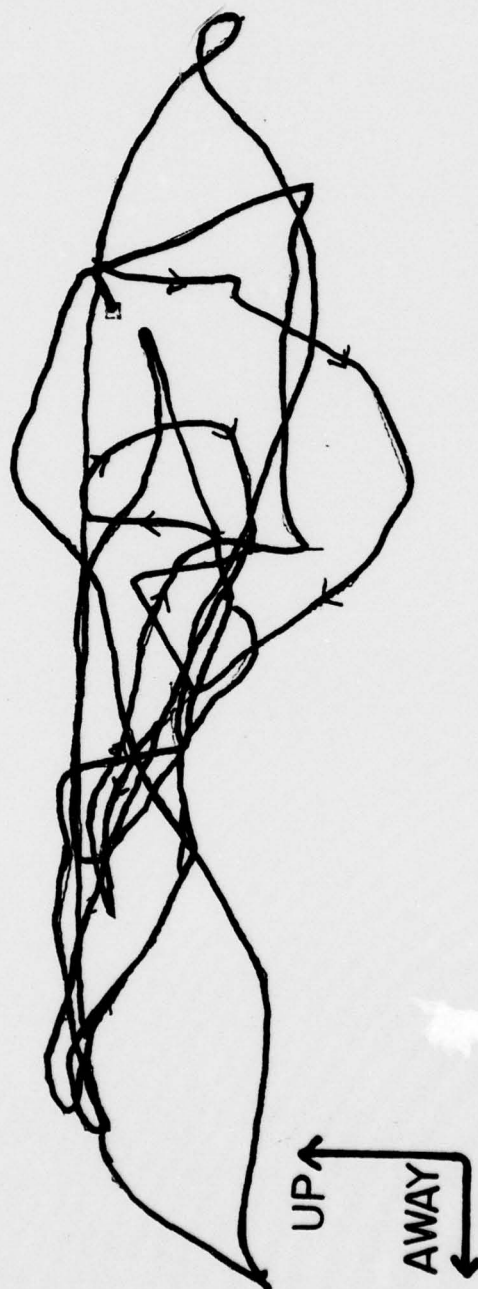


Figure 57. Particle motion of first surface wave group.
W-15000. September, 1975.

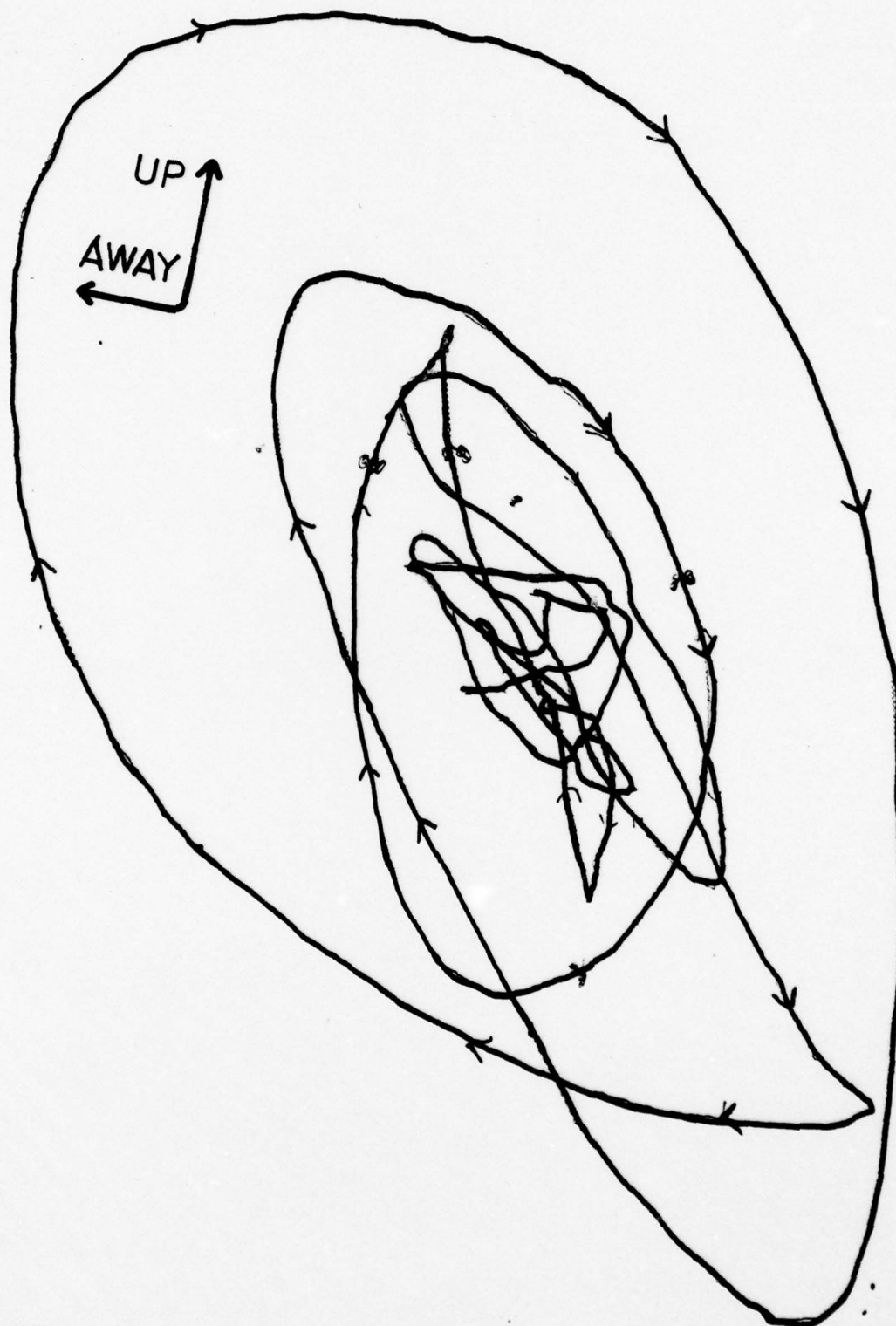


Figure 58. Particle motion of second surface wave group.
W-15000. September, 1975.

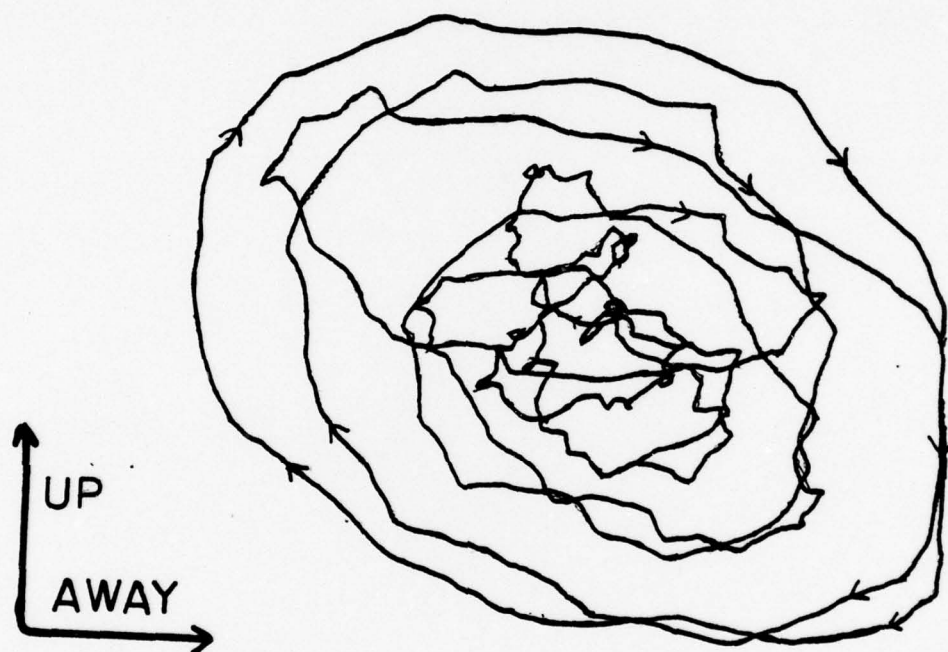


Figure 59. Particle motion of first surface wave group.
E-24000. August, 1975.



Figure 60. Particle motion of second surface wave group.
E-24000. August, 1975.

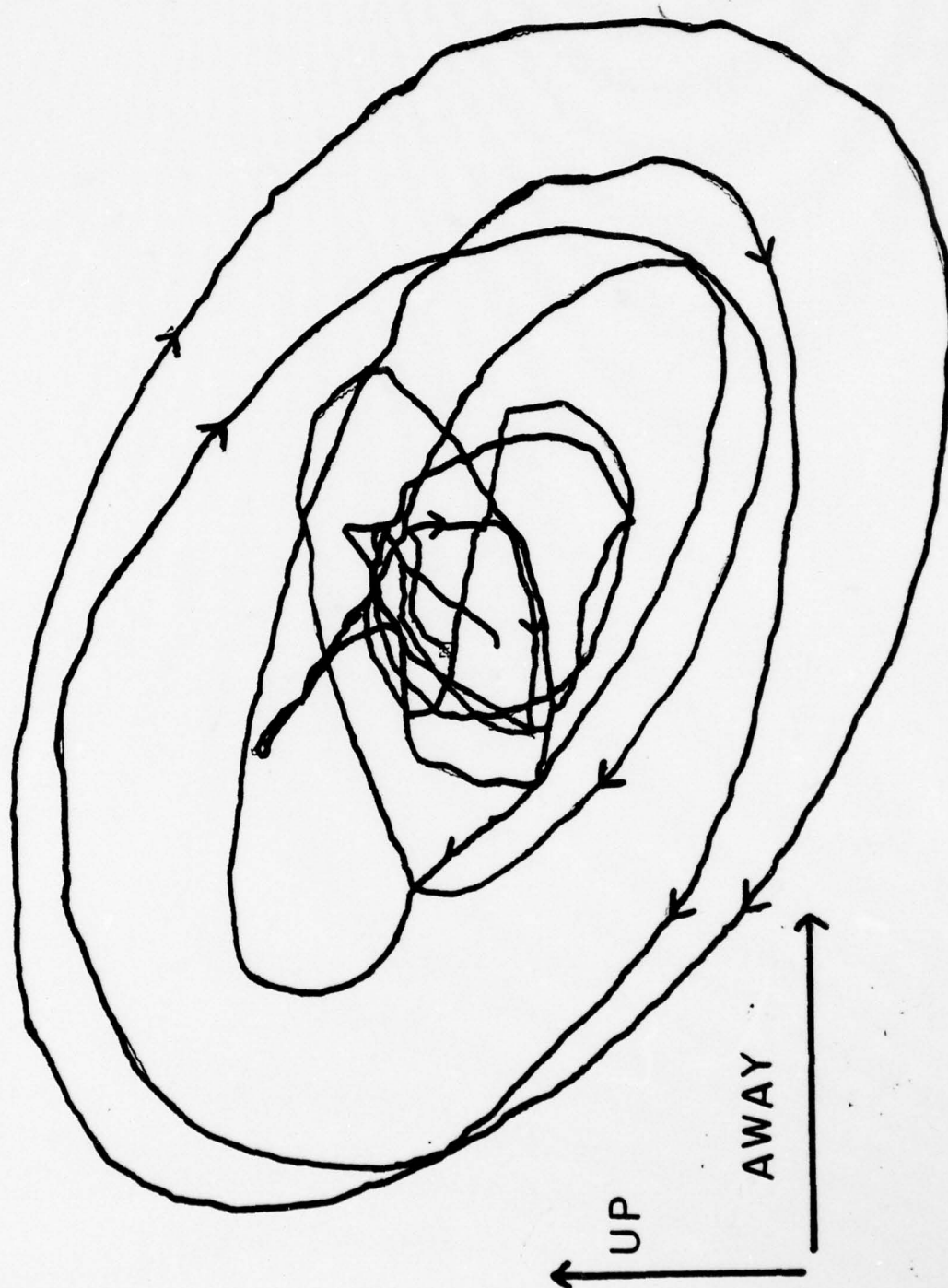


Figure 61. Particle motion of first surface wave group.
E-24000; September, 1975.

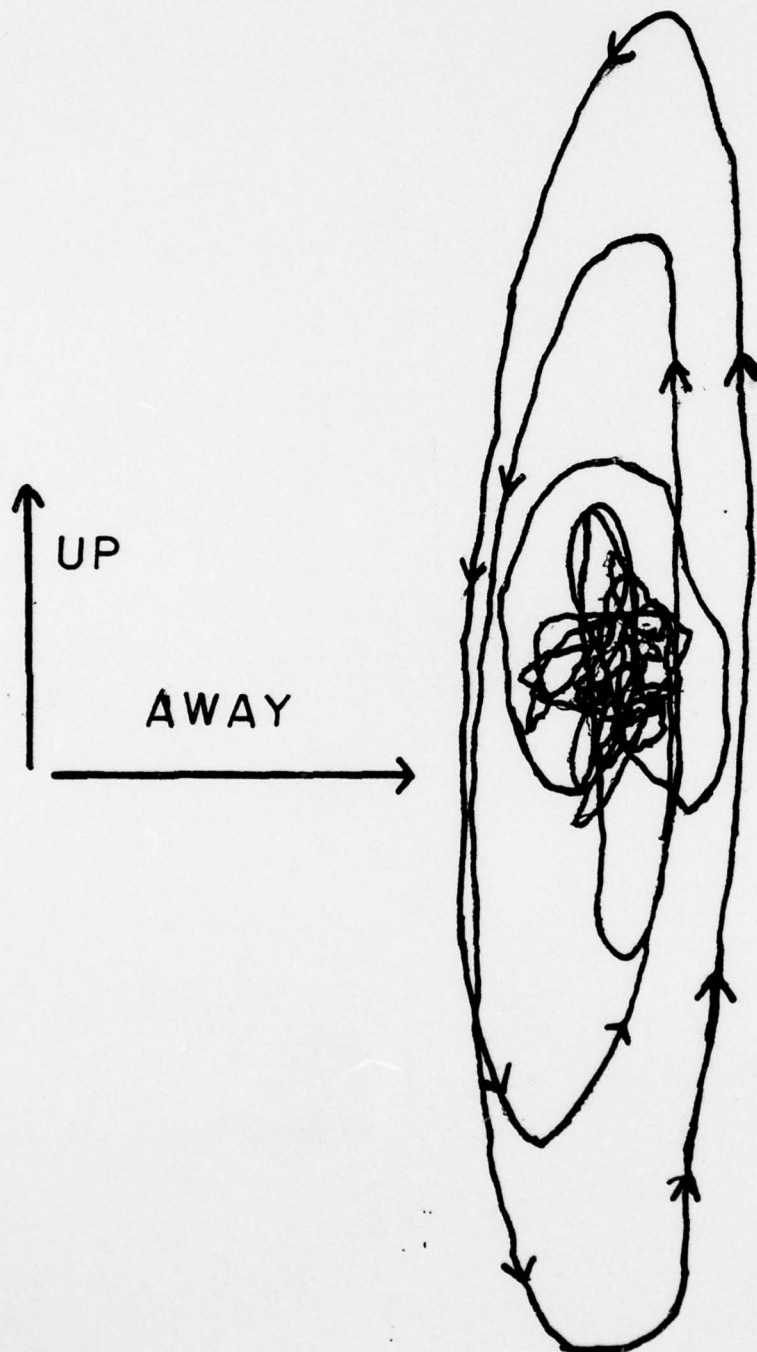


Figure 62. Particle motion of second surface wave group.
E-24000. September, 1975.

records of the radial and vertical components. Diagrams from the E-24000 station from the second shot (Figures 61 and 62) are perhaps the best examples of the characteristic particle motions of the two phases. The first wave group is a prograde phase with a stronger horizontal component than vertical. The second surface wave arrival is predominantly vertical and retrograde. On the basis of particle motion the second phase corresponds more closely to the motion expected for the fundamental mode Rayleigh wave.

Mooney and Bolt (1966) computed theoretical models of Rayleigh wave behavior for a number of simple one layer cases representing various geological situations. For a model consisting of alluvium over shale, prograde particle motion was predicted for a portion of the fundamental Rayleigh mode. They suggested that the prograde "hydrodynamic" wave reported by Leet (1946) at the Trinity test might be a prograde phase of the fundamental Rayleigh mode. Hasegawa (1968) identified a prograde phase produced by high explosive tests as a fundamental Rayleigh mode. However, since a velocity curve for a single mode cannot be a multiple-valued function of period, the similarity of the spectra of the two phases observed in the Tularosa Basin rules out the interpretation that the two wave groups are prograde and retrograde portions of the fundamental Rayleigh mode.

The results of the shear velocity refraction survey discussed previously provide a good input for models from which theoretical Rayleigh wave behavior in the Tularosa Basin may be calculated. Rayleigh wave characteristics depend primarily upon the SV velocity of each layer in the substratum. As discussed previously, the anisotropy factor is not thought to be large in the Tularosa Basin deposits so that the observed SH velocities are probably in fairly close correspondence with the true SV velocities.

The Haskell-Thomson (Haskell, 1953) method programmed for an XDS-925 digital computer was used to compute theoretical Rayleigh wave models for the Tularosa Basin. Initially, an attempt was made to correlate observed phase velocities for the two wave groups with theoretical phase velocity curves computed by the Haskell-Thomson program. The phase velocities were determined by Fourier analysis of the seismic records obtained from the two vertical seismometers in operation at the SMU station for the first Tularosa Basin shot. The two seismometers were separated by about 500 feet (152 meters) as determined by the time of air wave arrival. All other attempts at phase velocity measurements failed, apparently because of too large a distance between seismometers. The measured phase velocities at the SMU station are shown in Figure 63. The phase velocity determinations for the second

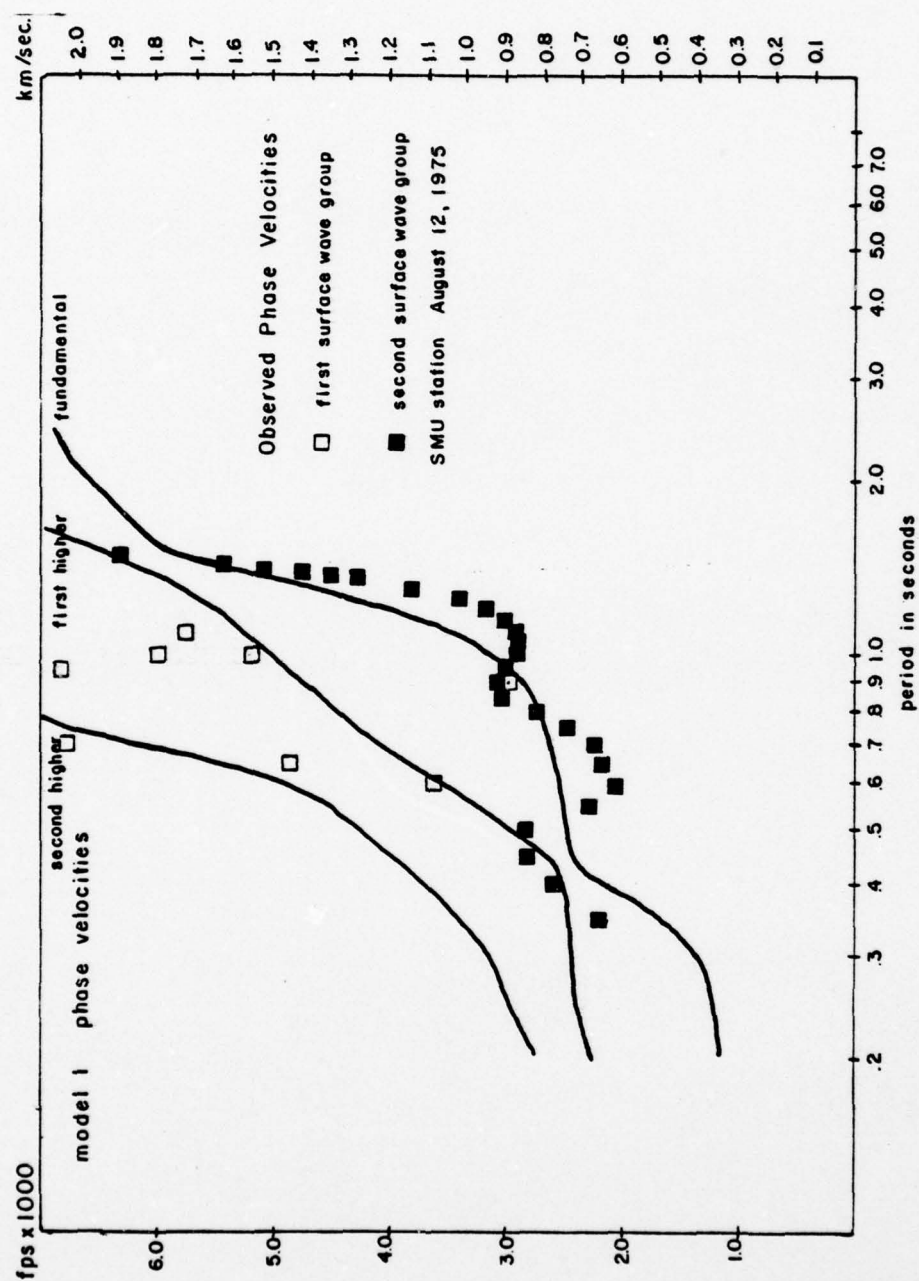


Figure 63. Comparison of observed phase velocities at SMU station with those computed for model 1.

surface wave arrival form a reasonably smooth curve with some undulations. Velocities determined for the first arrival exhibit a random variation with some of the points plotting off the scale of Figure 63. As a whole, all of the phase velocities for the first wave group are faster than the velocities determined for the second surface wave arrival. The undulations in the curve obtained for the second wave group and the random variations in the velocity determinations for the first wave are probably due to interference effects caused by the simultaneous propagation of several modes.

Trial and error variation of layer thicknesses of a model consisting of 4 layers over a half space provided the fit shown in Figure 63. between the theoretical fundamental and higher mode Rayleigh waves and the experimentally determined phase velocities of the second and first wave groups. The model providing the best fit (model 1) is shown in Figure 65. To obtain the fit the thicknesses of layers 2 and 4 were varied while the thicknesses of layers 1 and 3 were held constant. The SV velocities used corresponded to the SH velocities obtained from the ERIM refraction survey except for layer 3 and the half space. The velocity of layer 3 was rather arbitrarily set at 2600 feet per second (492 meters per second). (Calculations of Rayleigh wave characteristics for model 1 with various velocities for layer 3

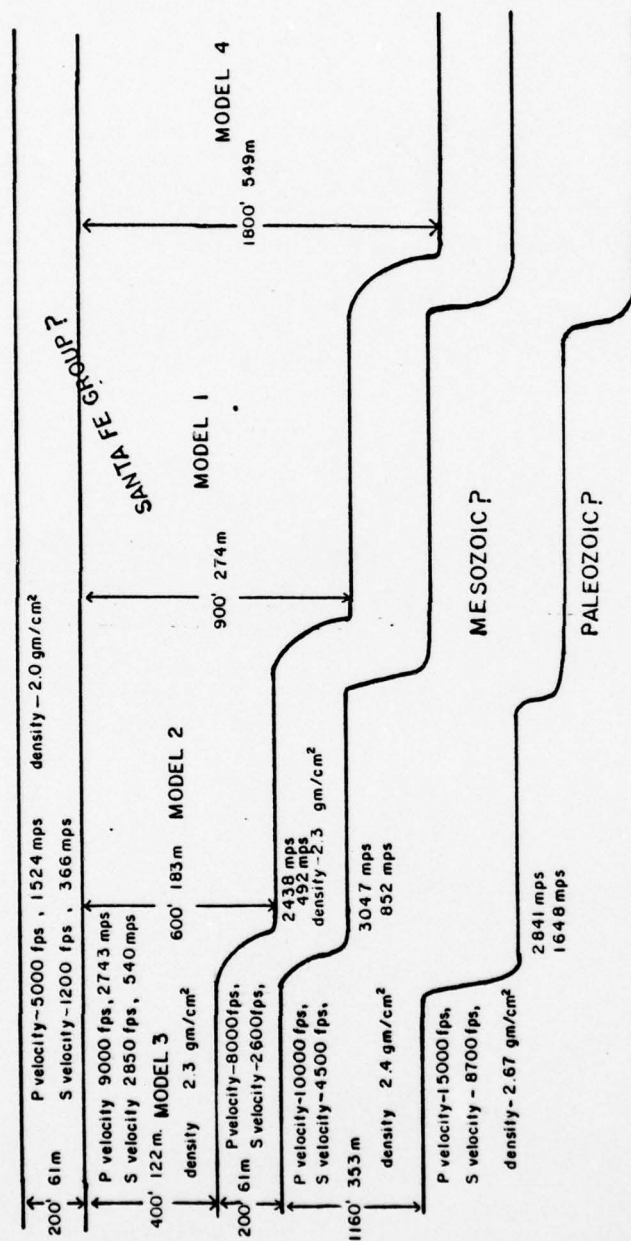


Figure 65. Layered models for Tularosa Basin.

show that it has little effect on Rayleigh wave behavior.) The half space velocity was estimated at 8700 feet per second (2651 meters per second). The half-space velocity does not have much effect on the shape of the dispersion curve in the period range of interest. P velocities for the lower layers and the half-space were estimated as were densities for all of the layers. As Mooney and Bolt (1966) have shown, compressional velocities and densities have a much smaller effect upon Rayleigh wave behavior than do shear velocities.

As seen in Figure 63., model 1 provides a good fit between the phase velocities determined for the second surface wave arrival and the theoretically predicted fundamental mode Rayleigh wave. The phase velocities determined for the first surface wave arrival can be loosely correlated with the theoretical phase velocity curves computed for the first and second higher modes of the Rayleigh wave.

The experimentally determined group velocities from the SMU station do not fit well with the group velocities computed for model 1. The group velocities for the first and second surface wave groups, determined by the zero crossing method, along with the computed group velocity curves for model 1 are shown in Figure 64. The theoretical group velocity for the fundamental mode is considerably faster in the range of

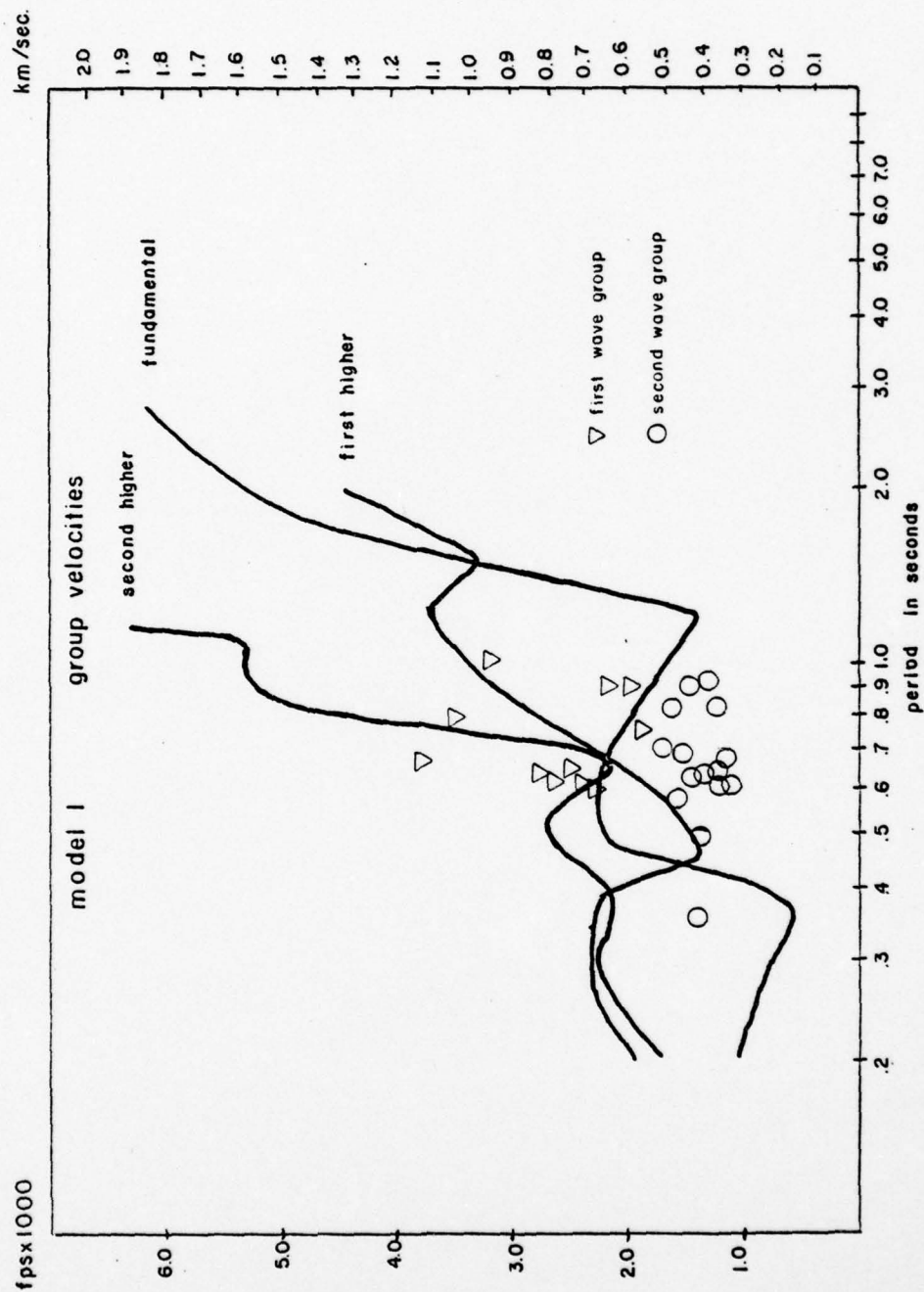


Figure 64. Comparison of observed group velocities at SMU station with those computed for model 1.

interest than the observed group velocities.

The group velocity as measured is determined by the geologic structure along the entire length of the travel path. The phase velocity as determined by Fourier analysis depends only on the properties of the layered substratum immediately below the two seismometers used in the phase velocity determination. This suggests that the structure in the immediate area of the SMU station is not the same as the average structure along the travel path.

The gravity studies of McLean (1970) and Healey (1976a,b) and the aeromagnetic survey interpretation of Bath (1977) all indicate that depth to bedrock varies considerably within the area occupied by the SMU and ASL seismic stations. Results of the ERIM refraction profile reveal that a considerable change in thickness of the unconsolidated fill, hereafter referred to as the Santa Fe Group (?), occurs within the extent of the refraction line. To determine the effect of varying thicknesses of the lower Santa Fe Group(?) upon Rayleigh wave behavior within the Tularosa Basin, dispersion curves for several theoretical models were computed using the Haskell-Thomson program. The four models shown in Figure 65 are thought to be representative of the structure traversed by the surface waves excited by the pre-Dice Throw tests and received at the SMU and ASL stations to the east and to the

south of the test site.

The pre-Dice Throw test site is probably near the transition point between high and low energy depositional environments of the bolson fill. A short distance to the west surface elevation begins to increase rapidly up to the San Andres Mountains. To the east and south, elevation varies little. It seems reasonable, then, to assume that to the east and south of the test site, facies changes within the Santa Fe Group(?) (and likely velocity changes) are relatively small and the predominant influence on surface wave characteristics in the period range of interest is the varying thickness of the Santa Fe(?) fill. Consequently in computation of the theoretical models the shear velocities obtained from the ERIM profile were held constant.

As mentioned previously, the phase velocity curve for model 1 fits fairly well with the experimental phase velocity curve obtained from the SMU station on the north side of the Malpais. A better fit to the group velocities measured at the SMU and ASL stations at the north edge of the Malpais is provided by models 2 and 3. As shown in Figure 66, model 2 provides a good fit to the group velocities measured at ASL stations E-35000 and E-LAVA. Model 3, shown in Figure 67., provides a slightly better fit than model 2 to the observed group velocities at the SMU station. Because the

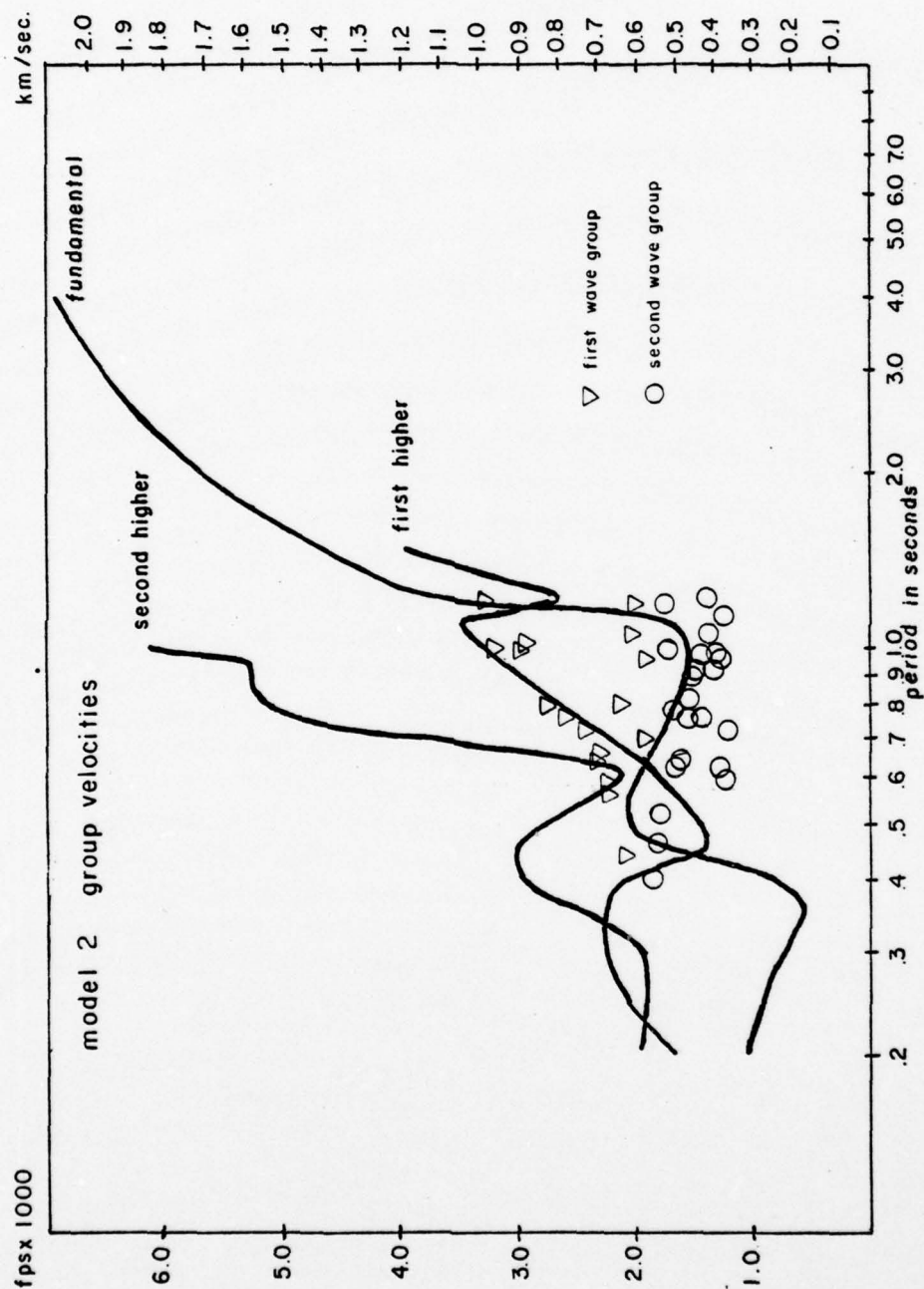


Figure 66. Comparison of observed group velocities at E-35000 and E-LAVA with those computed for model 2.

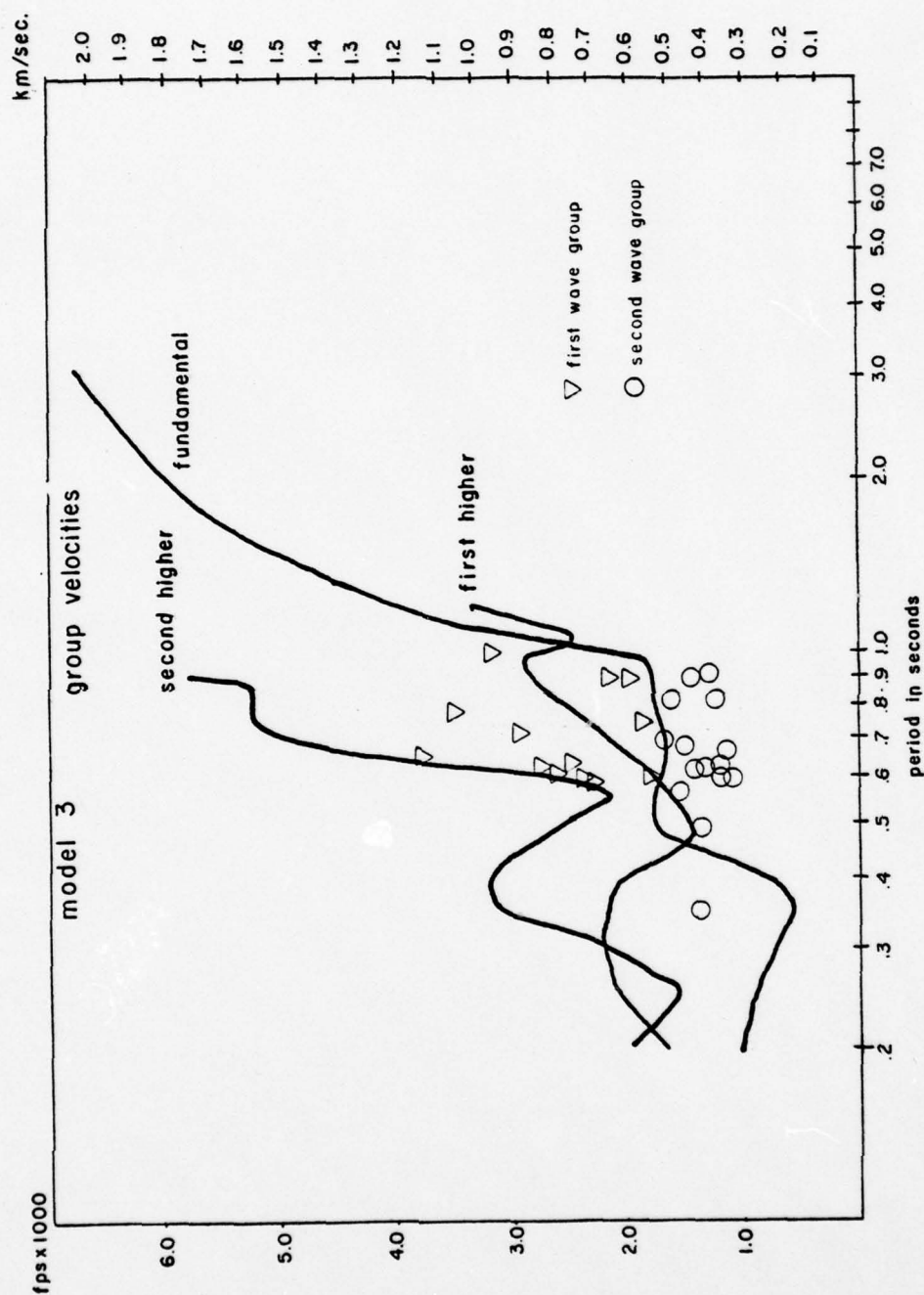


Figure 67. Comparison of observed group velocities at SMU station with those computed for model 3.

group velocity as measured depends on the subsurface properties along the entire path of the surface waves, model 2 is therefore thought to be a good approximation to the average structure along the travel path for the waves received at stations E-35000 and E-LAVA. This interpretation is supported by the good agreement between model 2 and the layer thicknesses found at the east end of the refraction profile. The SMU station for the August 100 ton event was located slightly north of the ASL stations E-35000 and E-LAVA; thus, the surface waves received at the SMU stations traversed a path slightly to the north of those received at the ASL stations. The gravity maps of Healy (1976a,b) and the bedrock contour map of McLean (1970) as well as the magnetic interpretation of Bath (1977) all indicate a general northward decrease in depth to consolidated rock (Precambrian rock in the case of the magnetic survey) in this area of the basin. This may explain why a thinner layer of the lower Santa Fe Group(?) in model 3 fits the SMU group velocities better than model 2. (The Santa Fe(?) layer in model 3 has probably been made too thin. A model halfway between 2 and 3 is probably more realistic. The flattening of the group velocity curve in the 0.5 - 1.0 second region between model 2 and model 3 does illustrate the general trend.)

In contradiction with the surface wave structure models

of the area between the pre-Dice Throw test site and the Malpais is the interpretation of Reynolds (1976) of the reflection line in the same area. As shown in Figure 9, Reynolds has placed a normal fault with about 2000 feet (610 meters) of displacement near the east end of the ERIM refraction survey. Structure contours indicate almost 2000 feet more of Tertiary(?) deposits to the east of the fault zone in section 12 than to the west. The indicated fault coincides with an offset in the reflection line as shown in Figure 9. Field work for the portion of the line to the east of the offset was done almost one year after the survey of the line to the west of the offset. In addition, slightly different equipment was in use for the later survey, one of the modifications being an increase in thumper weight from 300 pounds to 700 pounds. Apparently the last good reflection observed was considered by Reynolds to originate from the base of the Tertiary. As discussed previously, this interpretation appears to be correct for the earlier survey line, but the increase in the intensity of the seismic source likely resulted in good reflections being received from deeper horizons than the base of the Tertiary(?) during the later survey. This coupled with the offset in the line location probably made correlation between horizons difficult if not impossible. Therefore, the indicated fault at the offset between lines is likely not real.

As shown in Figure 22 , the cross section interpreted by Healey (1975a) does indicate a depression about halfway between the pre-Dice Throw test site and the location of the E-35000, E-LAVA, and SMU stations on the edge of the Malpais. As discussed previously, the interface on the cross section is probably closer to the base of the Mesozoic section rather than the base of the Tertiary. An increase in thickness of the Mesozoic section could be the cause of the depression shown on the cross section. As shown in Figure 23 , the gravity interpretation is not controlled by any survey points near the proposed depression. In addition, no corresponding anomaly appears on the magnetic map of Bath (1977) in the area of the indicated depression. For these reasons the gravity interpretation of Healey does not necessarily contradict the structural models obtained from the surface wave behavior.

The interpreted magnetic map of Bath (1977) (Figure 28.) shows a small area of negative anomaly in the Malpais near the site of stations E-35000, E-LAVA, and the SMU station and directly north of the large negative anomaly centered at A. Bath indicates that the anomaly at A is due to an increase in the thickness of sediments over the Precambrian. It may be that the smaller anomaly is connected with the anomaly at A and indicates a depression extending from A to the center of

the Malpais. This would place the ASL and SMU stations near the edge of the depression, possibly explaining why model 1 with a greater thickness of Santa Fe(?) deposits best describes the structure directly below the SMU station, while models 2 and 3 with lesser Santa Fe(?) thicknesses best describe the average structure between the ASL and SMU stations and the pre-Dice Throw test site.

Theoretical horizontal to vertical particle velocity ratios are easily obtained during the computation of dispersion curves by the Haskell-Thomson method. Theoretical particle velocity ratios for models 1, 2, 3, and 4 are shown in Figures 68, 69, 70, and 71. In the period range of the surface waves observed the theoretical particle motion for all models is retrograde for the fundamental mode and prograde for the higher modes. This agrees with the observed particle motions for the two wave groups presented in Figures 47 to 62. Without obtaining spectral ratios of the vertical and radial components it is not possible to make a strict quantitative comparison between the observed wave motion and the theoretical ellipticity. A good qualitative comparison can be made between the computed ellipticity curves and the particle velocity diagrams obtained from ASL station E-24000 at which radial and vertical gains were set at the same level. The E-24000 diagrams for both shots (Figures 59, 60, 61, and 62) reveal that the first surface wave arrival is predominantly

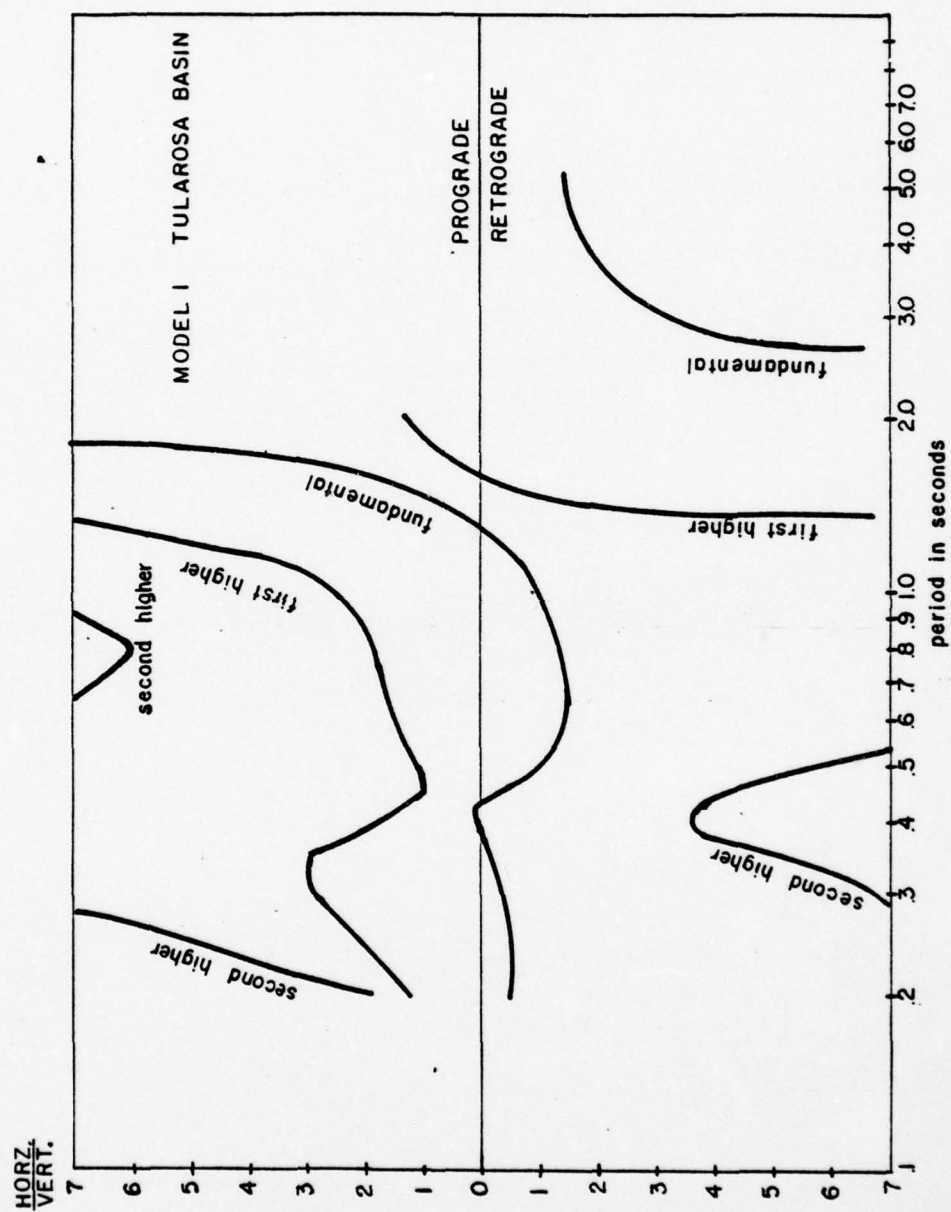


Figure 68. Theoretical ellipticity for model 1.

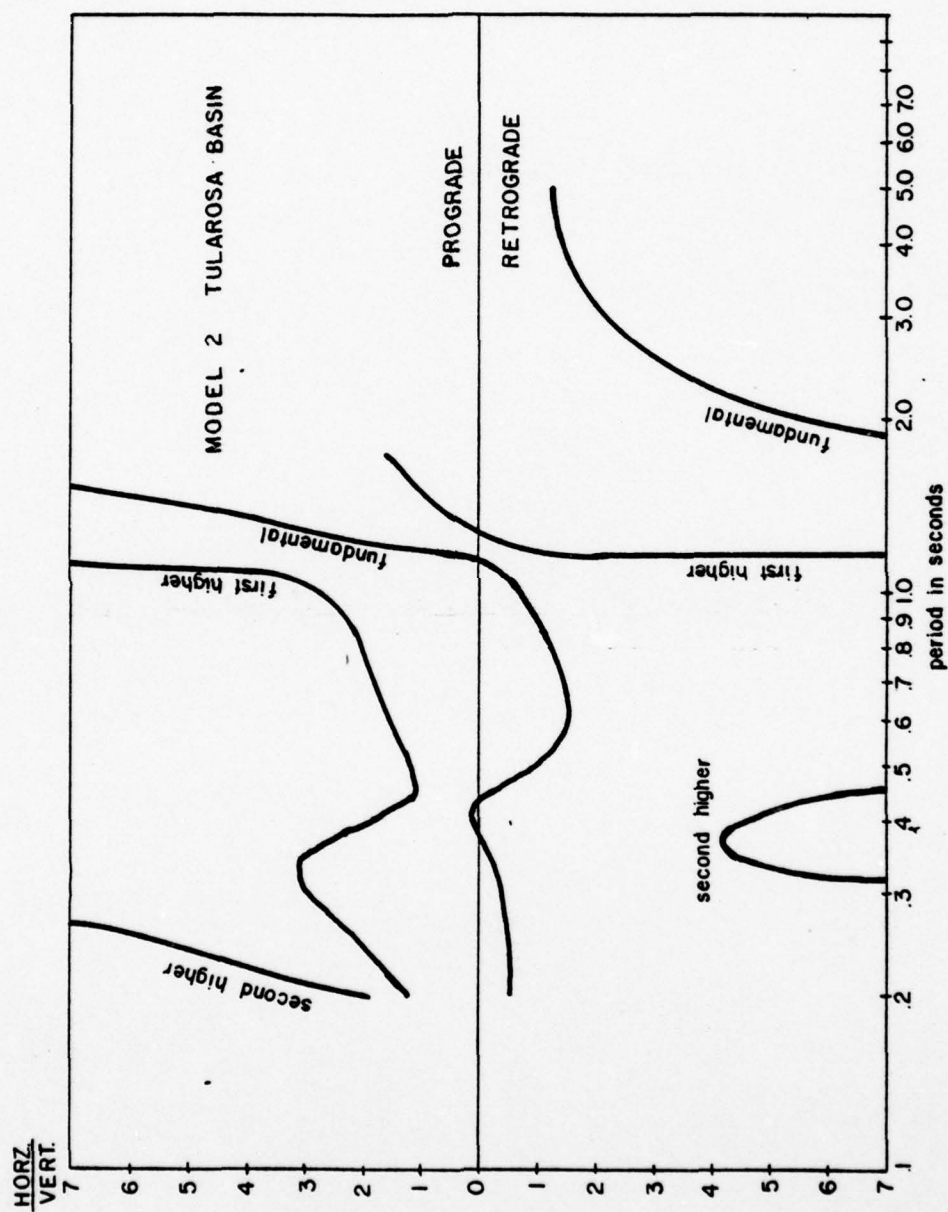


Figure 69. Theoretical ellipticity for model 2.

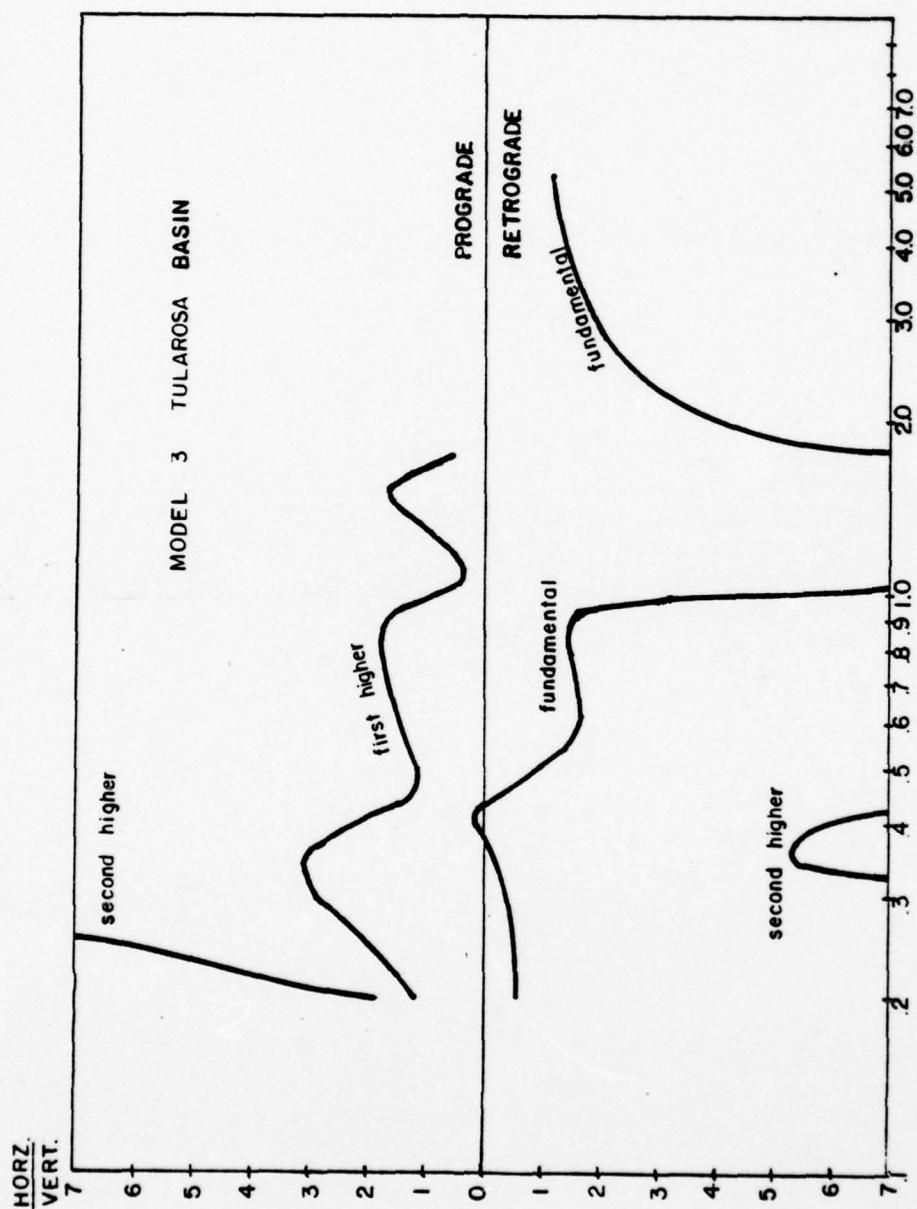


Figure 70.. Theoretical ellipticity for model 3.

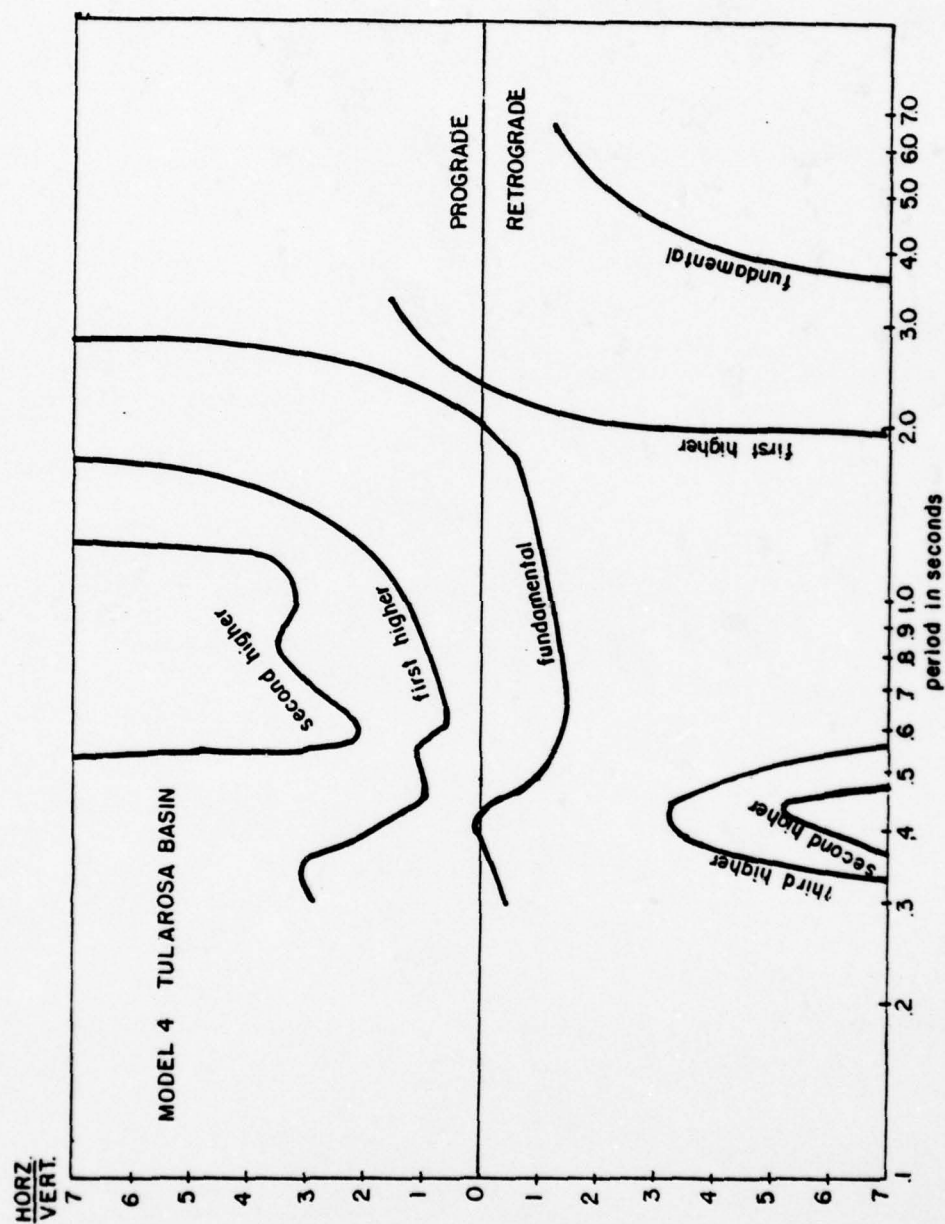


Figure 71. Theoretical ellipticity for model 4.

horizontal and prograde, while the second retrograde wave group has a horizontal to vertical ratio of 0.5 or less. Model 2 is the only one of the four theoretical models which predicts a horizontal to vertical velocity ratio of less than 1.0 in the 0.5 - 1.0 second region of the fundamental model. Since the ellipticity, like phase velocity, depends only on the properties of the substratum immediately below the seismometers, and considering the location of station E-24000 (Figure 29), the correspondence between the predicted ellipticity for model 2 and the observed particle motion at E-24000 lends further support to the proposal that model 2 best represents the average structure between the pre-Dice Throw test site and the E-35000 and E-LAVA stations.

Surface Waves observed to the Northeast, South, and West of the Shotpoint

Three of the ASL stations were deployed to the northeast of the September, 1975, detonation (Figure 37). The surface waves received at these stations are quite complex when compared to the two relatively "clean" wave groups received by stations on the southeast line. Characteristic particle motion in the vertical-radial plane is also quite complicated as illustrated in Figure 72. Paleozoic rocks crop out a short distance to the north of the seismic line (Figure 4), and structure in this area is likely quite complex relative to

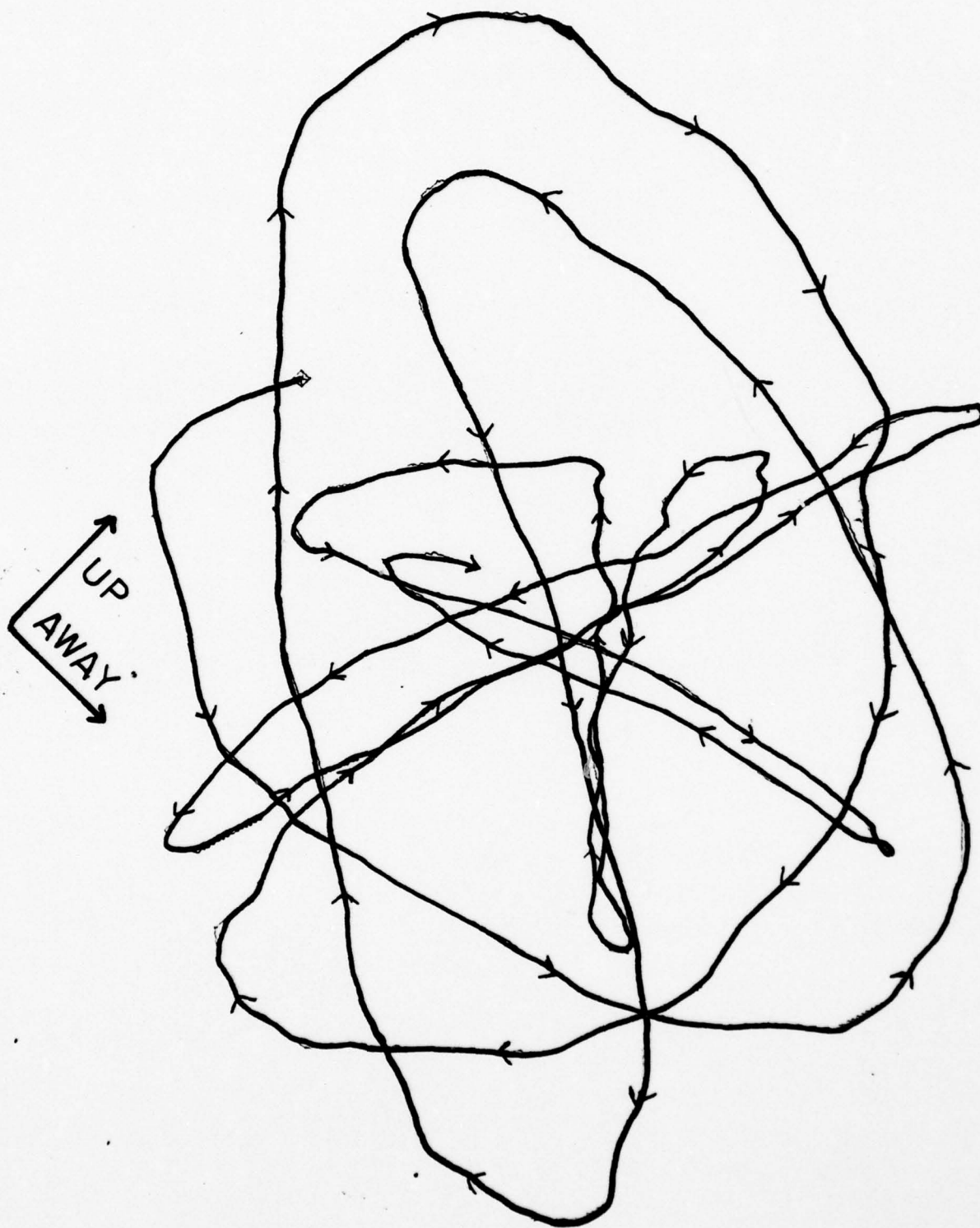


Figure 72. Characteristic particle motion from OR-1.

that southeast of the test site. The confused character of the surface waves received at these stations is perhaps indicative of multipathing and reflection caused by the complex structural nature of the area.

The ASL stations to the west of the test site received waves quite similar to the two characteristic waveforms received to the east of the shotpoint (Figures 35 , 36 , and 43 , 44). Since layer velocity changes likely occur to the west of the shotpoint, no attempt has been made to fit theoretical models to their observed characteristics.

The seismogram from the SMU station located south of the Malpais for the second shot (Figure 45 .) presents a puzzle. A fairly well defined "clean" waveform with two apparent beats arrives with a group velocity roughly corresponding to that of the first surface wave group received at the ASL and SMU stations to the east of the shotpoint. No other surface wave of any consequence, except the air coupled Rayleigh wave near the end of the record, is visible.

Vertical-radial particle motion diagrams for the two beats in the surface wave group received at the SMU station are shown in Figures 73 and 74. Both beats are prograde, predominantly horizontal and very similar in appearance to the observed motion of the first wave group received at the



Figure 73. Particle motion of first beat in surface wave group. SMU station south of the Malpais.

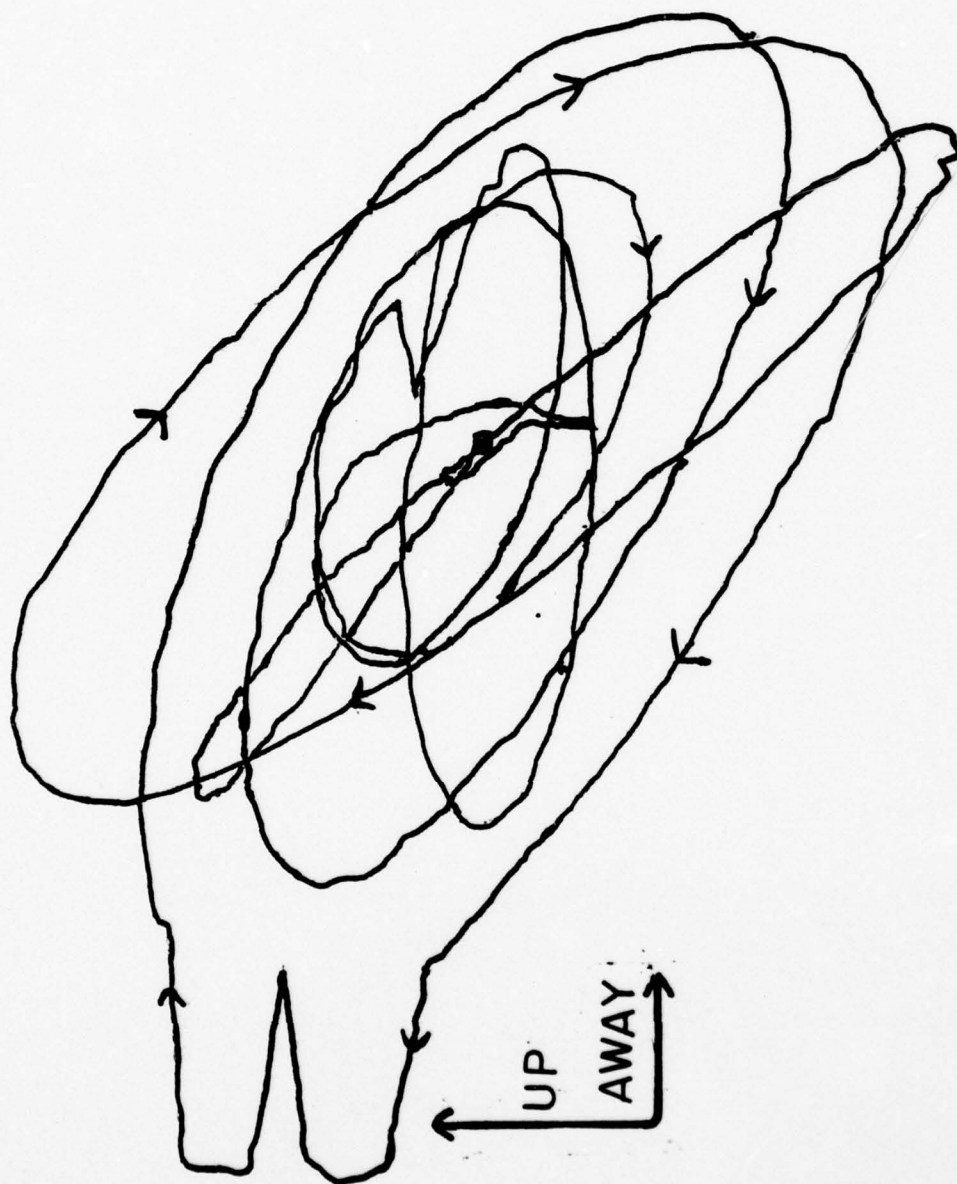


Figure 74. Particle motion of second beat in surface wave group. SMU station south of the Malpais.

stations to the east of the pre-Dice Throw test site. If the surface wave group received is indeed of the same nature as the first wave group observed to the east of the test site, and composed of one or more higher modes of the Rayleigh wave, what happened to the fundamental mode? One obvious explanation is, of course, severe attenuation; however, severe attenuation of the fundamental mode was not evident at the seismic stations to the east of the shot point. A better answer can be obtained by considering the structure of the path between the test site and the SMU station south of the Malpais.

The gravity interpretation of McLean (1970), the gravity map of Healey (1976a,b), and the magnetic interpretation of Bath (1977) all suggest that depth to bedrock increases to the south in this area of the basin. This implies that surface waves received south of the Malpais traversed a path with a greater thickness of unconsolidated rock than did those observed to the north of the Malpais and east of the shotpoint. McLean's map suggests that a travel path with an average Santa Fe(?) thickness of roughly 2000 feet (610 meters) is appropriate for waves arriving at the south Malpais station. Healey's residual map would indicate somewhat less depending on the density contrast assumed. Theoretical Rayleigh wave characteristics have been computed for model 4

(Figure 64.) with a Santa Fe(?) thickness of 1800 feet (549 meters).

Group velocities for model 4 are shown in Figure 75.

Let us consider the shape of the curve for each mode.

Remembering that almost all of the surface wave energy is in the 0.5 - 1.0 second region (Hoffman and Harding (1977) show that the spectral shape changes little from station to station), an idea of the appearance of the waveforms predicted by the dispersion curve can be obtained. The fundamental mode curve is flat in the spectral region of interest, while Airy phases of the first, second, and third higher modes are present. The wave groups corresponding to the higher modes should actually arrive after the fundamental mode. We would expect the fundamental mode to be a pulse of very short duration. The higher modes would produce wave forms of much longer duration in comparison to the fundamental mode. A wave group corresponding to the Airy phases of the second and third higher modes should arrive shortly before the wave group corresponding to the Airy phase of the first higher mode.

The observed wave forms correspond closely to those expected from the shapes of the dispersion curves. Two closely spaced beats are visible. Both are predominantly horizontal and prograde with the earlier arrival being more

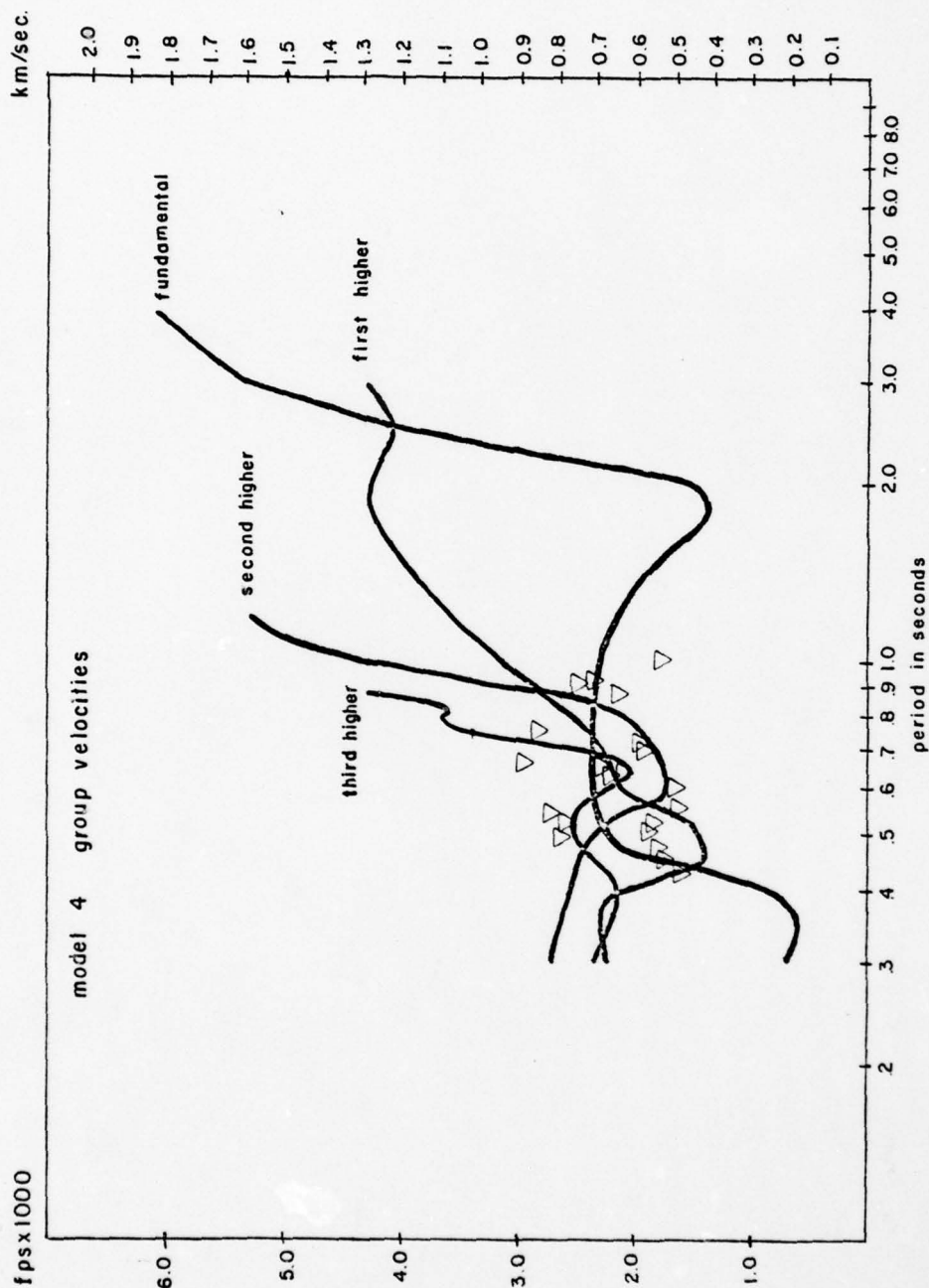


Figure 75. Comparison of group velocities observed at SMU station south of the Malpais with those computed for model 4.

strongly horizontal than the second as predicted by the theoretical ellipticity for model 4 (Figures 71, 73, 74). The observed group velocities correspond fairly well to the theoretical group velocity curves (Figure 75). If the first and second arriving beats correspond to the Airy phases of the second (and third ?) and first higher modes, respectively, the peak amplitude should undergo a frequency shift from the first beat to the second. Fourier spectra of the two beats (Figure 76) show a definite shift. The peak amplitude of the first beat occurs between 0.7 - 0.8 seconds which is near the period range of the bottoms of the Airy phases of the second and third higher modes. The second beat peaks between 0.5 - 0.6 seconds, roughly corresponding to the bottom of the first higher mode Airy phase.

There is solid evidence, then, for identifying the wave group received as composed of the first two or three higher modes. If this is so, why is the fundamental mode not apparent? The model 4 group velocity curve in the 0.5 - 1.0 second region confines it to a very narrow pulse of 1 second duration or less, at the station range (50000 feet, 1.5 kilometers), coming in near the beginning of the higher mode arrivals. Intuitively we might expect a large amount of energy to be funneled into this short pulse, but its presence is not apparent on the vertical component. The theoretical

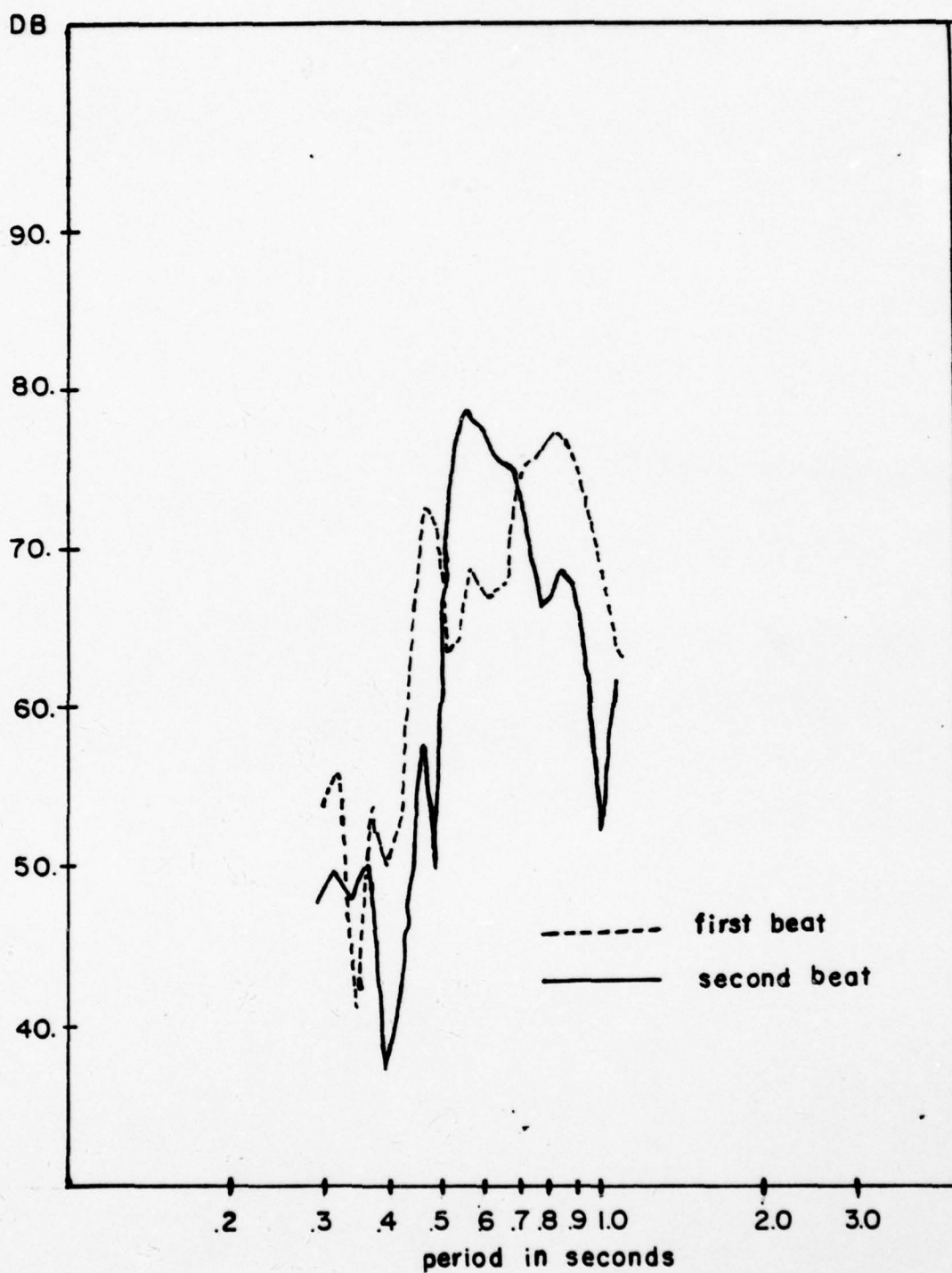


Figure 76. Comparison of spectra of first and second beats in surface wave group. SMU station south of the Malpais.

ellipticity (Figure 71) for model 4 shows that the horizontal to vertical velocity ratio is between 1 and 2 for the fundamental mode in the 0.5 - 1.0 second period range. The first beat is very strongly horizontal. Severe clipping occurred on the radial component. Perhaps this extremely strong radial motion is partially a result of a strongly horizontal fundamental mode pulse, although the theoretical ellipticity also predicts a very strong horizontal component for the second higher mode. Perhaps fundamental to higher mode conversion has occurred. No firm explanation can be offered at this time.

SURFACE WAVE PROPAGATION IN THE JORNADA DEL MUERTO

Description of Explosion and Seismic Array

In October of 1976, 620 tons of ANFO, roughly equivalent to 500 tons of TNT, were detonated on the surface of the Jornada del Muerto Valley north of Mockingbird Gap. The seismic array shown in Figure 3 fielded by the Environmental Research Institute of Michigan and Southern Methodist University recorded the farfield seismic waves excited by the explosion.

The SMU station recorded 3 vertical components and one radial component. In an attempt to obtain good phase velocity measurements, the 3 vertical components were positioned about 500 feet apart in increasing distance from the shotpoint. The seismometers utilized were the Geotech S-13 models recorded by analog magnetic tape.

The ERIM stations discussed in this paper (16000 feet, 4.9 kilometers, and out) employed three component Hall-Sears seismometers with a natural frequency of 2 hertz recorded on analog tape.

Discussion of Observed Surface Waves

Surface waves received at the SMU and ERIM stations in the range between 16,000 and 35,000 feet (4.88 - 10.67 kilometers) are very similar in appearance to those excited by the Tularosa Basin shots and recorded at similar ranges. The record from one of the SMU vertical components is shown in Figure 6. Records from the ERIM stations are shown in Figures 77-82.

Trinity site, where the first atomic bomb was tested in July of 1945, is located a short distance to the east of the October 1976 Dice Throw test site. Leet (1946) presented a seismic recording of the Trinity test (Figure 7) in which two surface wave groups were apparent on the radial and vertical components. The first surface wave arrival was prograde, the later arrival, retrograde. Because the motion of the first arrival was similar to that of a water wave, Leet attributed its existence to the properties of the materials near the surface of the Jornada del Muerto and named it the "Hydrodynamic" wave. The second arrival, because of its characteristic retrograde motion, was identified as the fundamental mode Rayleigh wave.

In a later article (Leet, 1962), Leet stated that the "Hydrodynamic" wave was recorded at a distance of 8 kilometers from the Trinity explosion. The exact location of

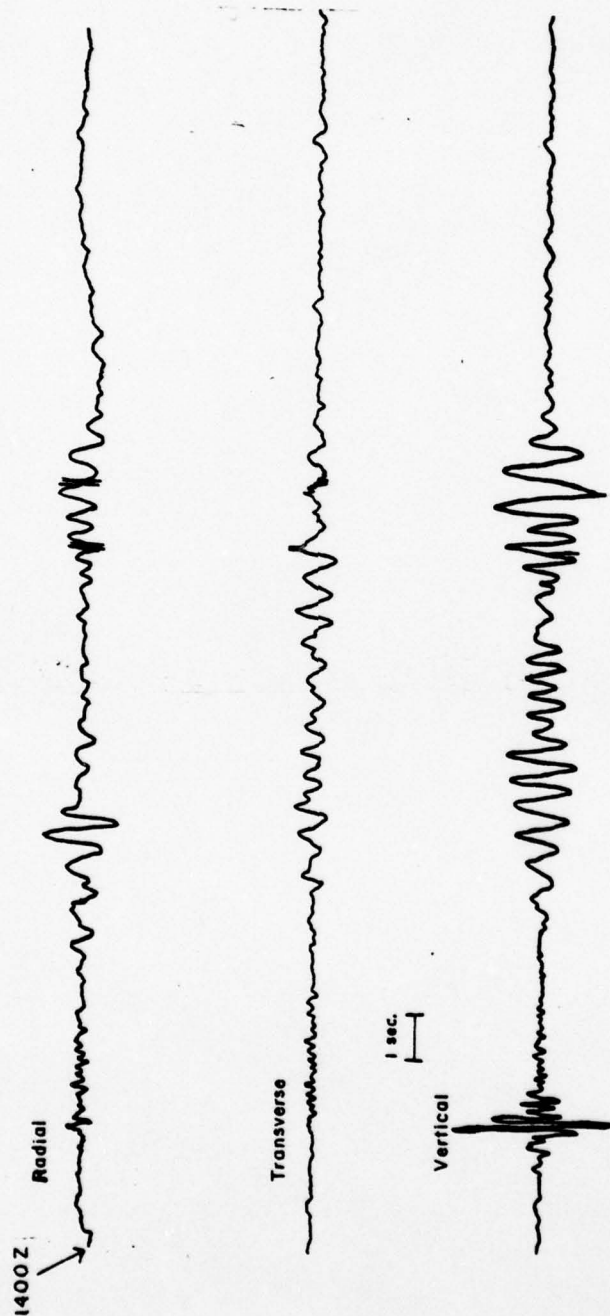


Figure 77. Recording from ERIM 16000 station.

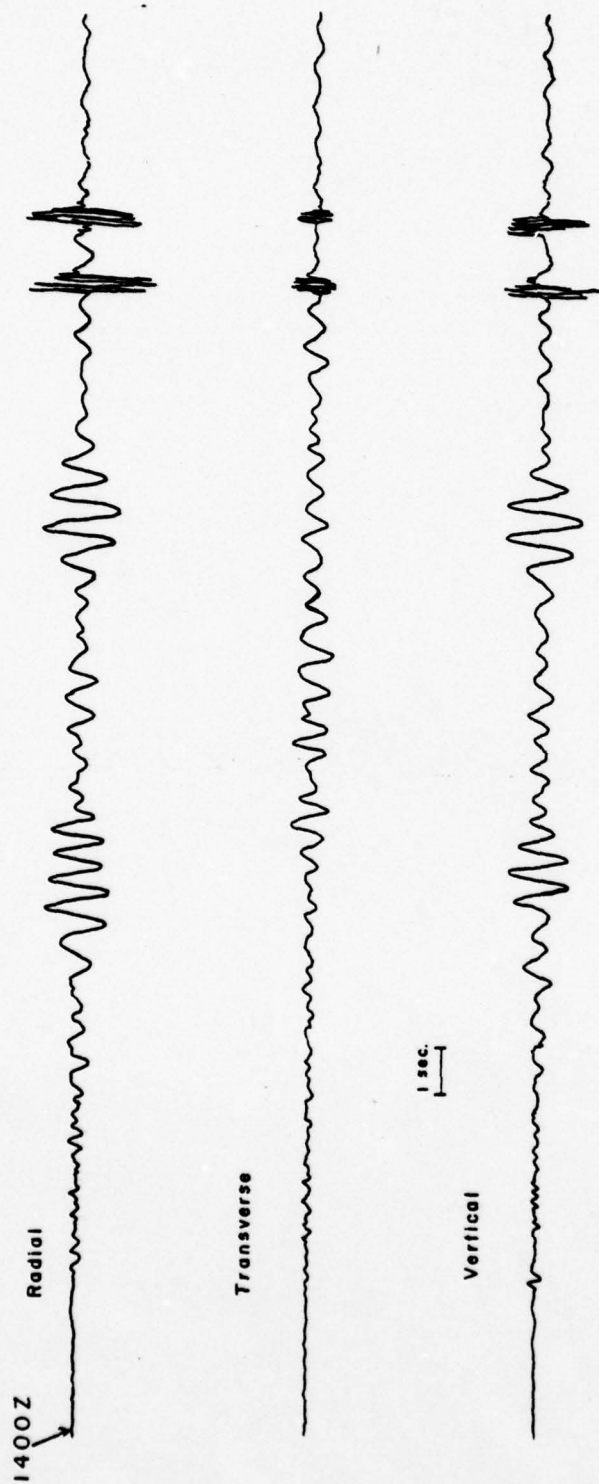


Figure 78. Recording from ERM 25000 East station.

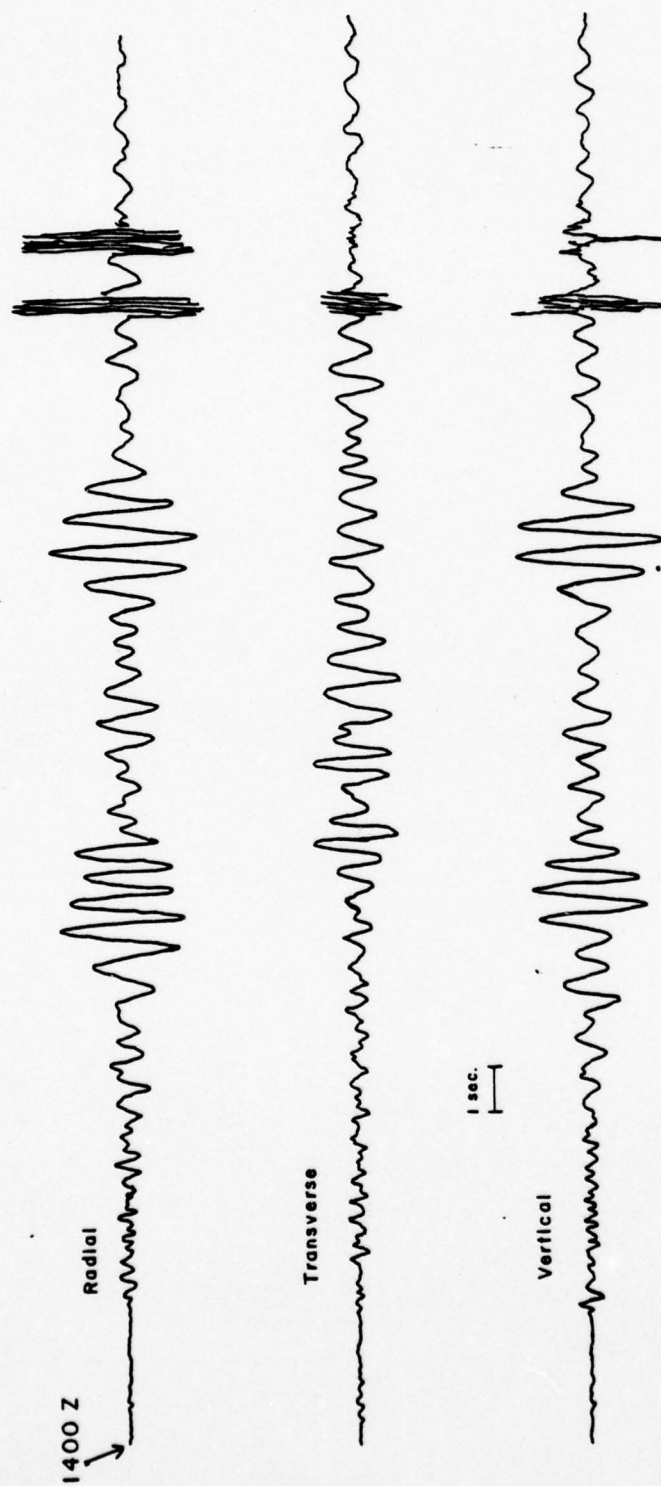


Figure 79. Recording from ERIM 25000 South station.

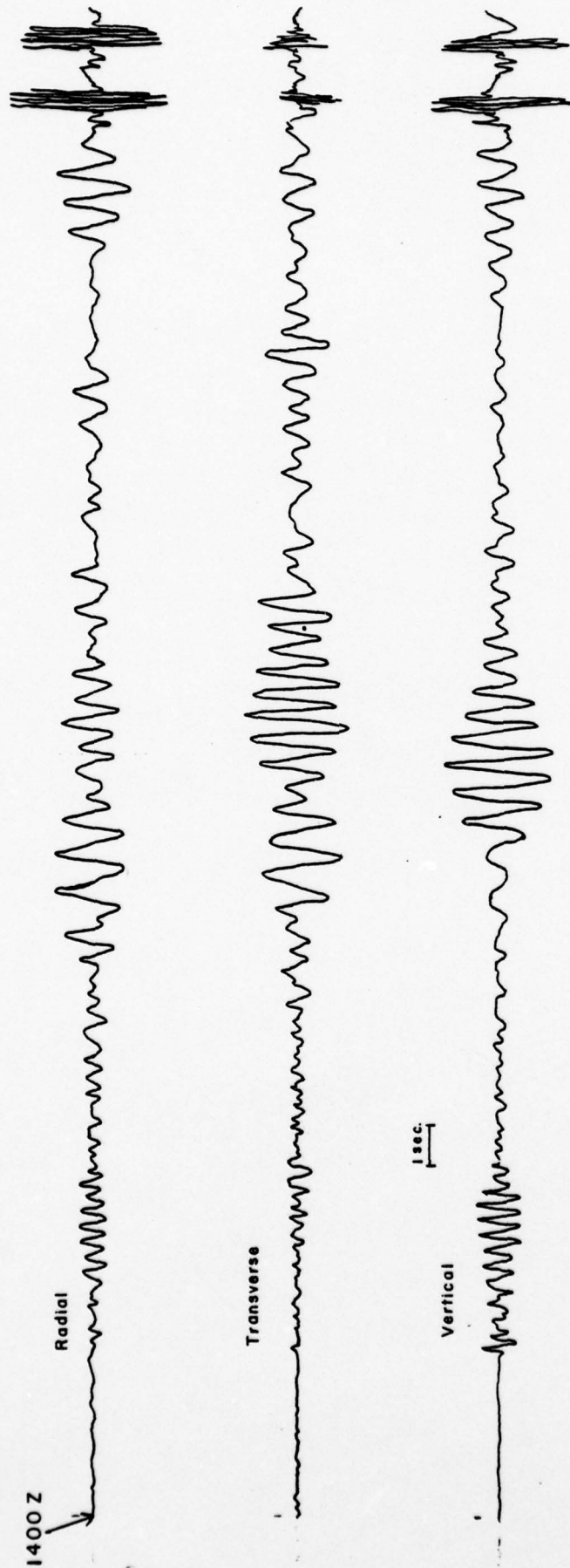


Figure 80. Recording from ERIM 35000 station.

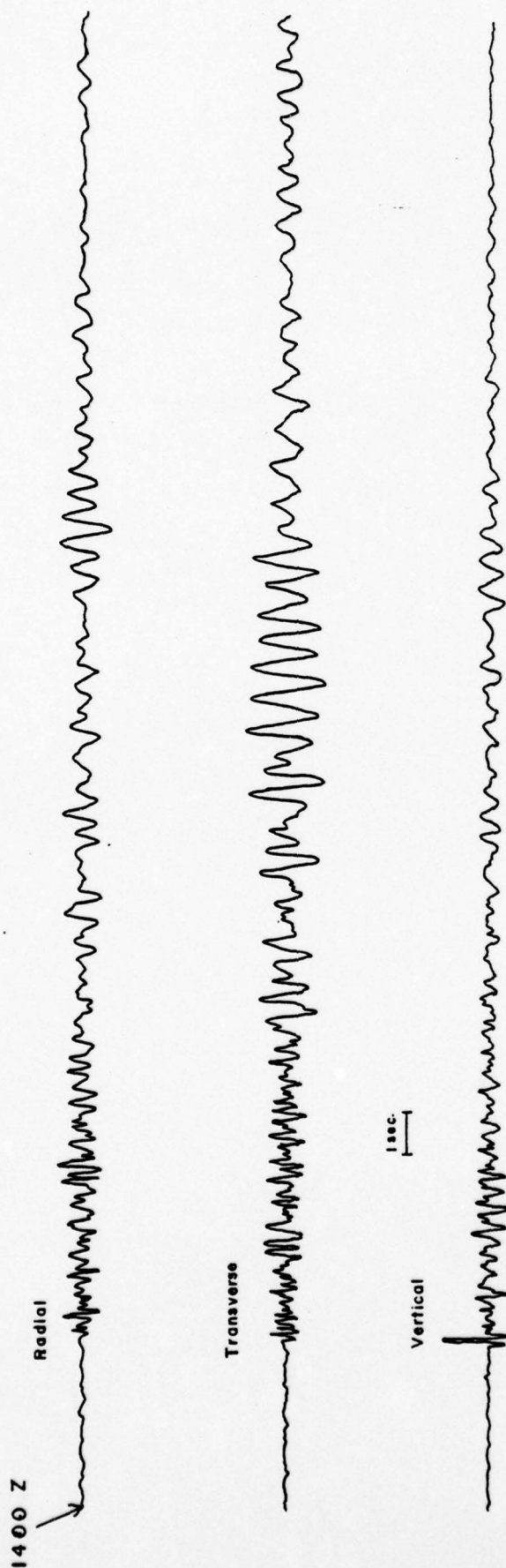


Figure 81. Recording from ERIM 43000 station.

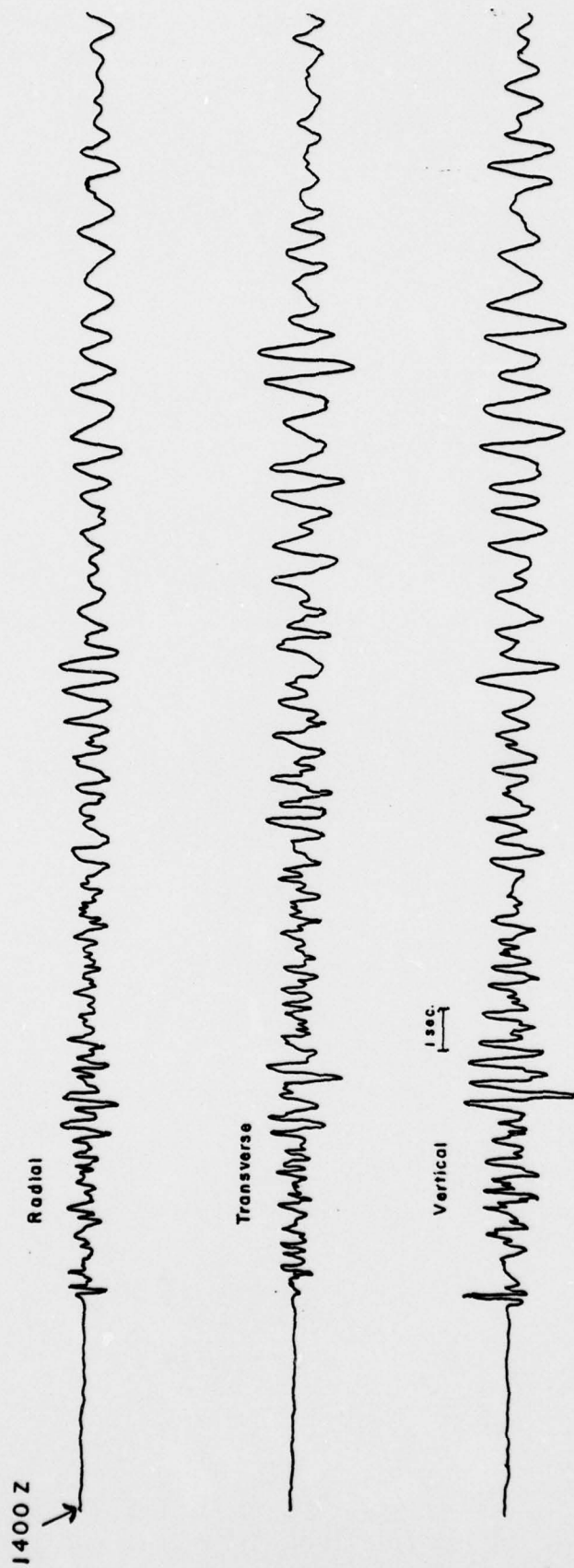


Figure 82. Recording from ERM 62000 station.

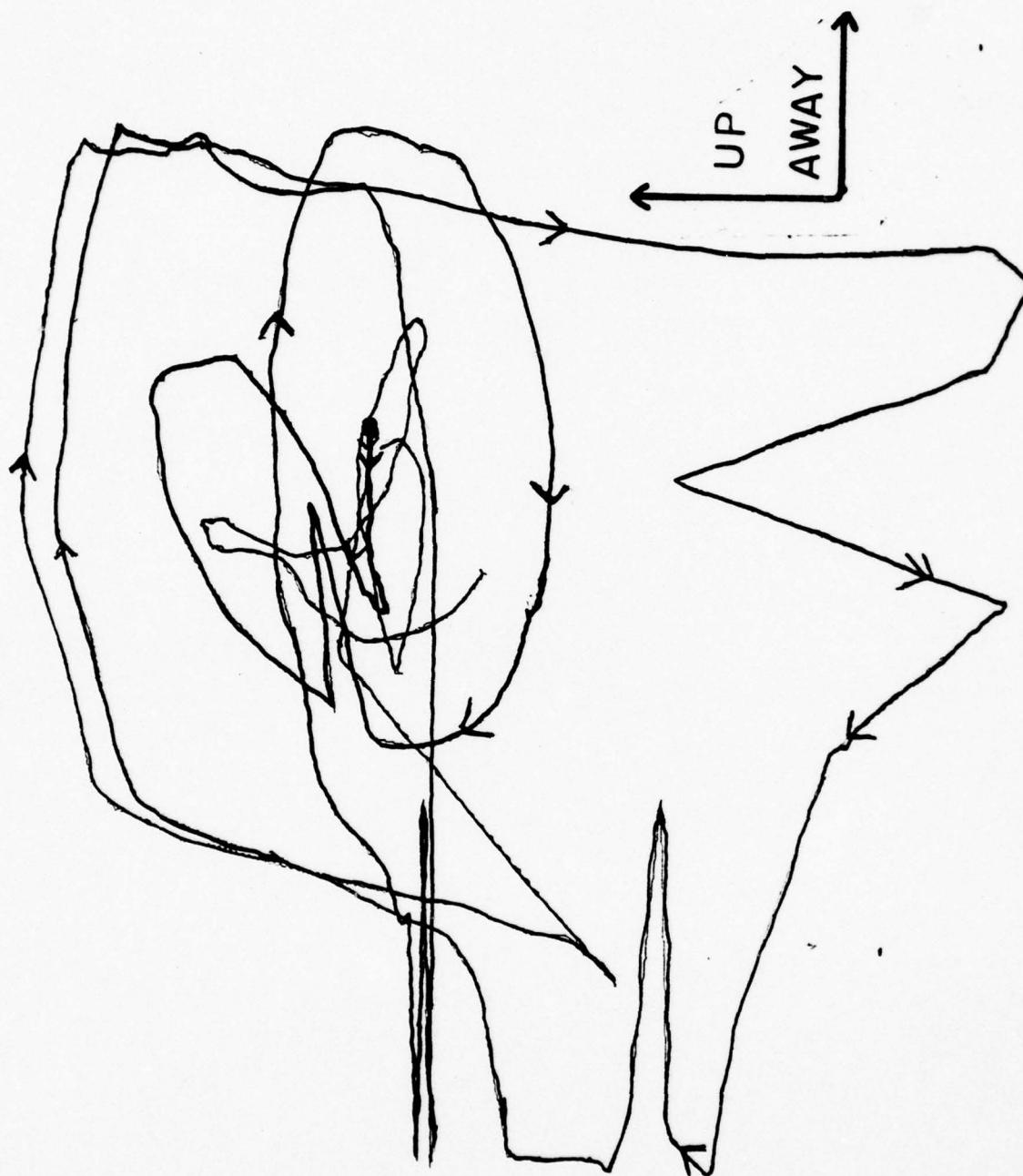


Figure 83. Particle motion of first surface wave group.
SMU station. October, 1976.

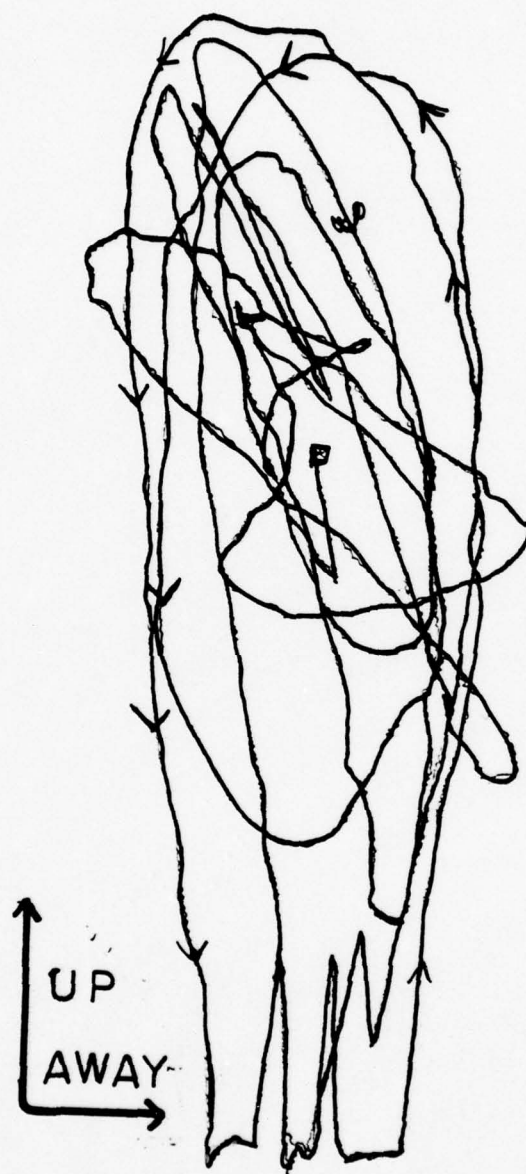


Figure 84. Particle motion of second surface wave group.
SMU station. October 1976.

the seismometer was not specified. Partially in an effort to duplicate the recording Leet obtained from the Trinity test, three of the seismic stations were positioned to the north, south, and east of the Dice Throw test at a range of 25,000 feet (7.62 kilometers). The records from all three stations (Figures 6, 78, and 79) were very similar in appearance to Leet's seismogram. Particle motion diagrams from the SMU station (Figures 3 and 4) reveal that the first and second wave groups excited by the Dice Throw test are indeed prograde and retrograde respectively, making it likely that the waves excited by the Dice Throw test were the same as those recorded by Leet at the Trinity test.

In an effort to obtain good phase velocity measurements, the SMU station operated 3 vertical component seismometers spaced about 500 feet (152 meters) apart in increasing distance from the shotpoint. Unfortunately, due to much higher than expected surface wave amplitudes, two of the verticals clipped, one so severely as to be unuseable. Phase velocity determinations for the two wave groups obtained from the remaining pair of seismometers, spaced about 500 feet (152 meters) apart, are shown in Figure 85. Phase velocity measurements made by Fourier analysis yield points with considerable scatter and some unrealistic values. This is likely a result of the distortion introduced by the clipping.

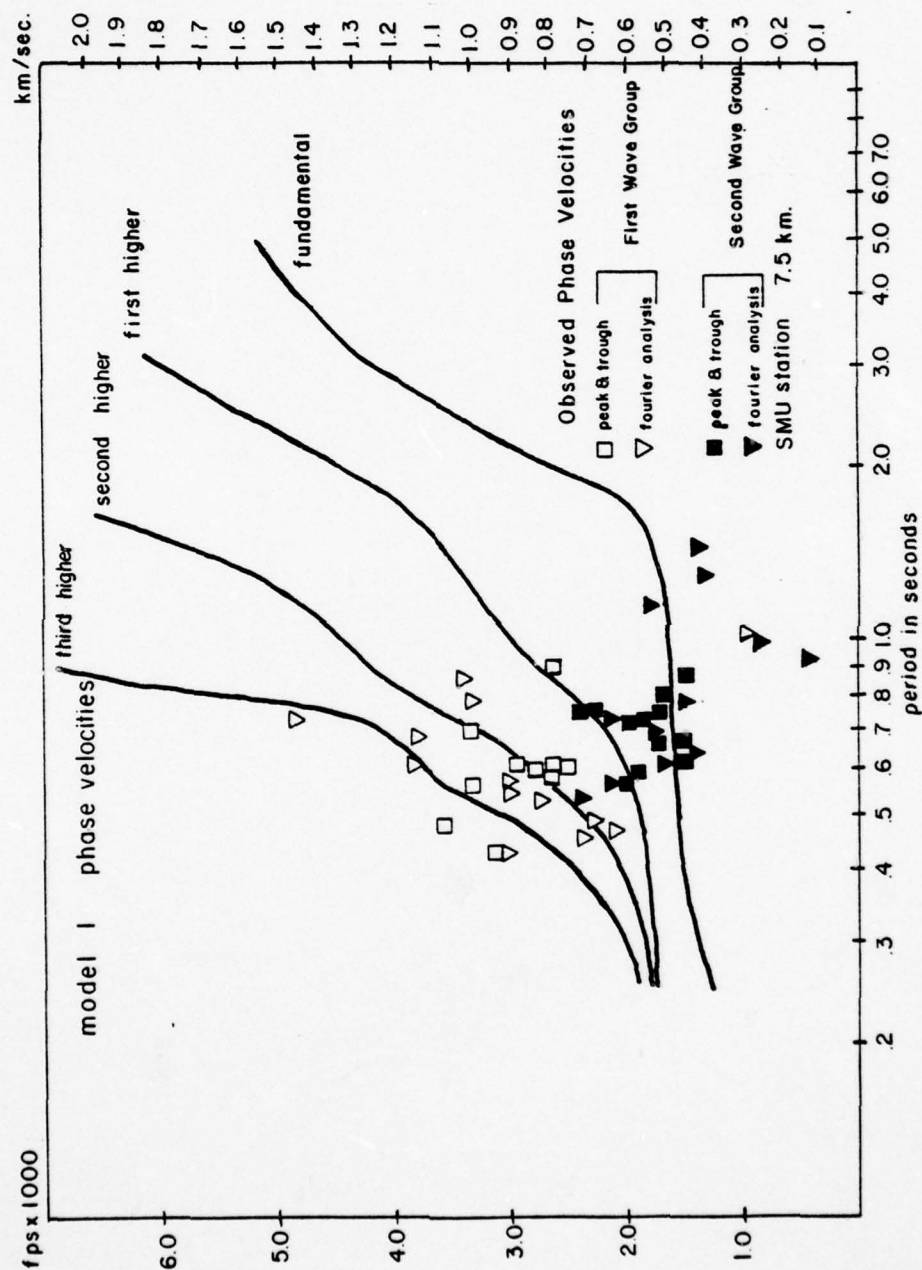


Figure 85. Comparison of observed phase velocities at SMU station with Jornada model.

Because of this, phase velocities were also determined by visual peak and trough correlation.

In an attempt to fit a higher mode-fundamental mode Rayleigh wave model, after the fashion of the Tularosa models, to the Jornada waves, phase velocities of theoretical models were compared with the observed values. The measured phase velocities of the first wave group seem to indicate that the fundamental mode curve should be relatively flat in the 0.5 - 1.0 second region. (Surface wave spectra for the Jornada shot were almost identical to that observed at the Tularosa explosions.) In fitting the theoretical curves, the lower Santa Fe(?) thickness was chosen large enough to make the fundamental mode curve flat in the region of the observed phase velocities. The lower Santa Fe(?) shear velocity was selected so that the fundamental mode phase velocity curve passed through the lower portion of the cluster of phase velocities obtained from the second surface wave arrival. Shear velocity of the third layer (Mesozoic?) was set equal to that observed for the Mesozoic(?) layer in the Tularosa Basin. The thickness of the first layer (Quaternary?) was estimated from shallow reflection work in the area (Reynolds, 1976), and its shear velocity was assumed to be the same as that observed in the Tularosa Basin. The first and second layer P velocities were obtained from shallow refraction

profiles of the area carried out by the Air Force Weapons Laboratory (L. S. Karably, personal communication, 1976). All other velocities and densities were estimated. The resultant model is shown in Figure 86. (The model would probably be intuitively more attractive if the P and S velocities and the densities of the lowest layer and halfspace had been made the same as those in the Tularosa models, but these parameters have little effect on the shape of the dispersion curve within the period range of interest.)

The fundamental and first three higher modes of the Rayleigh wave calculated for model 1 all pass through the region of phase velocities observed for the first and second surface wave arrivals. The fit is as good as can be expected considering the scatter of the observed points.

Group velocity curves for the Jornada model are shown in Figure 87 along with the group velocities observed at the three stations at the range of 25000 feet (7.62 kilometers). As in the case of the phase velocities, considerable scatter is present in the group velocities also. Group velocities from the three stations for the most part all fall within the same range and again correlate fairly well with the theoretical curves considering the degree of scatter present. A number of the points plot to the left and above the third higher mode curve, suggesting that perhaps still

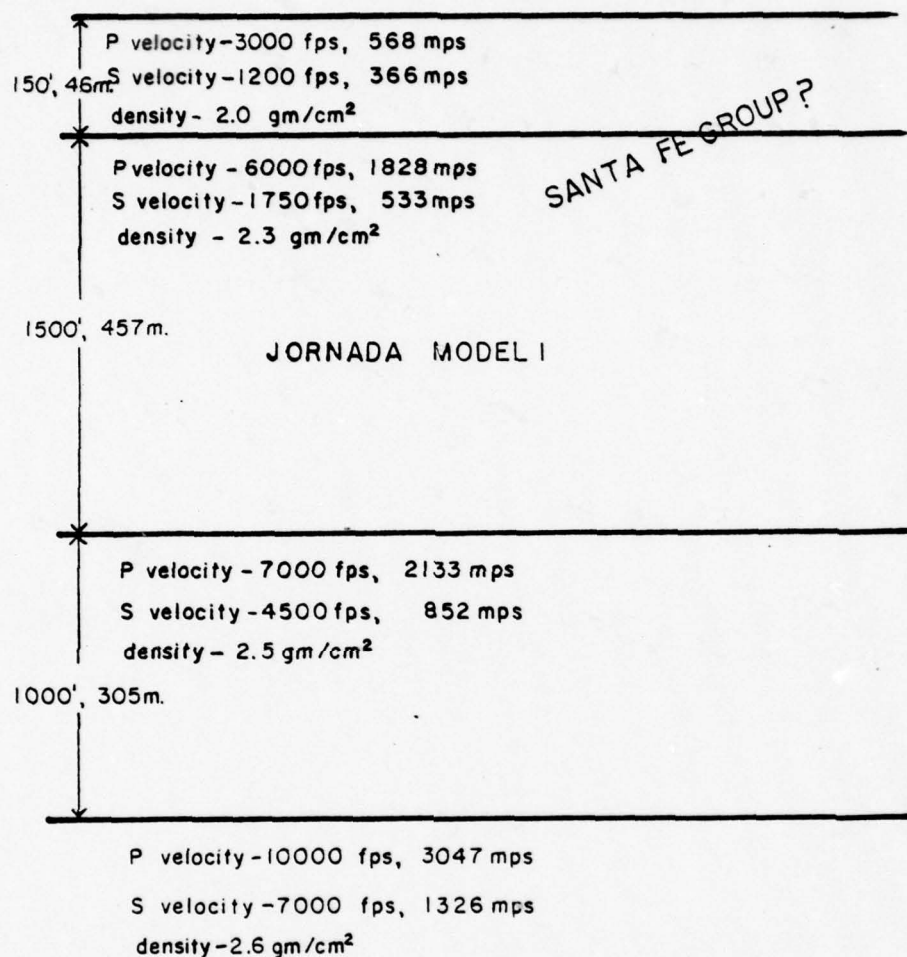


Figure 86. Layered model for Jornada del Muerto.

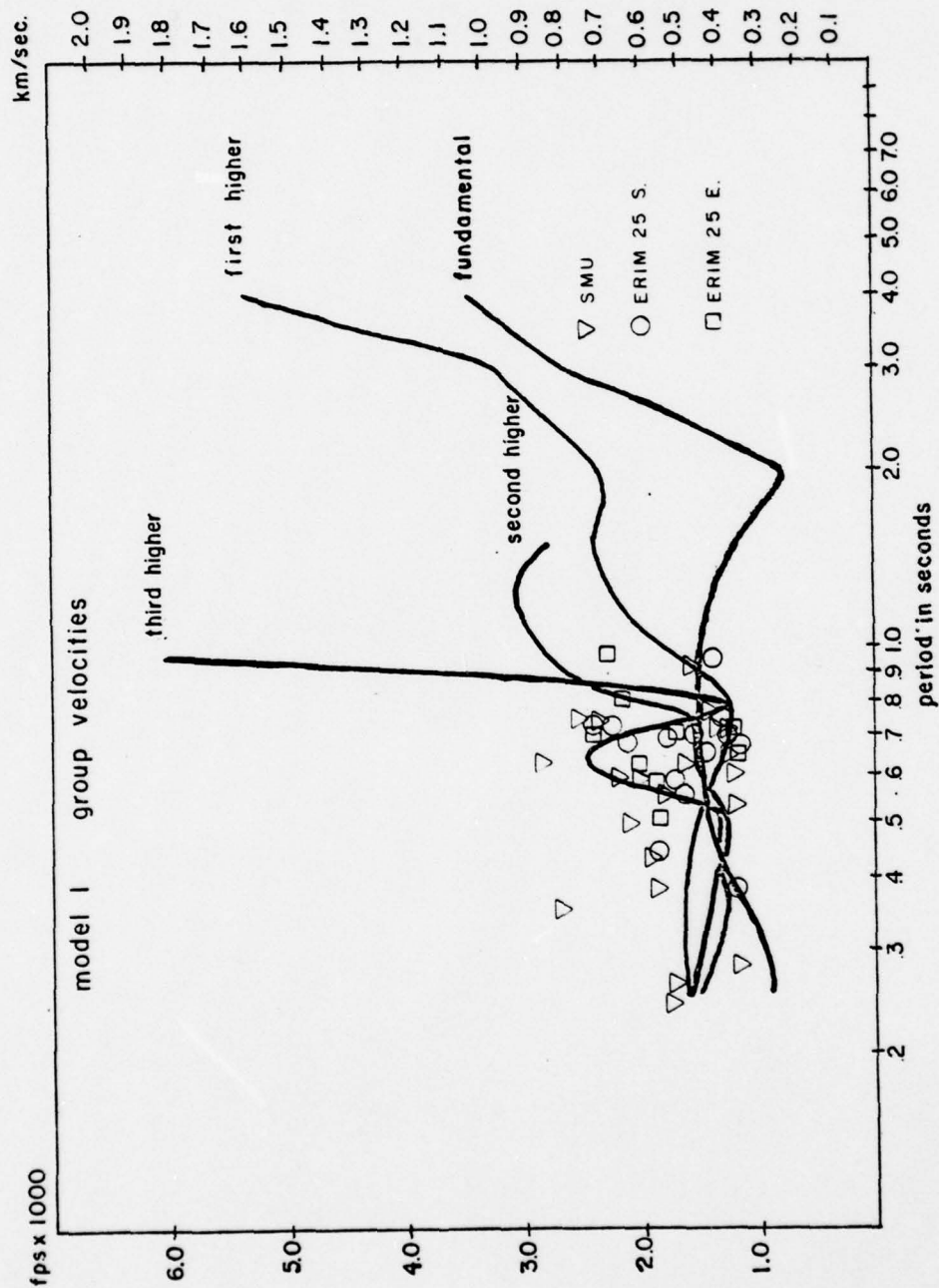


Figure 87. Comparison of observed group velocities with those computed for Jornada model.

higher modes might be important here. The fundamental mode curve is relatively flat in the 0.5 - 1.0 second region, while a shallow Airy phase of the first higher mode, somewhat slower than the fundamental, is present in the same area. This suggests that the first higher mode, in addition to the fundamental mode, may be important in explaining the slowest surface wave group. The theoretical ellipticity (Figure 88) of the Jornada model verifies that this could indeed be possible because the first higher mode as well as the fundamental mode is predominantly vertical and retrograde in the spectral region of interest. The second and third higher modes are prograde and strongly horizontal in the same area.

As discussed previously, gravity data suggest that the thickness of Santa Fe(?) fill near the Dice Throw 500 ton site is considerably greater than that in the immediate pre-Dice Throw test site area. According to Reynolds' (1976) reflection interpretation of the area, a north-south trending normal fault lies just to the west of the Dice Throw test site (Figure 28). The base of the Tertiary(?) is thought to be near 2500 feet (762 meters) in thickness to the west of the fault and roughly 2000 feet (610 meters) to the east of it. The residual Bouguer anomalies (Figure 3) suggest that the thickness of the Santa Fe(?) Group remains roughly

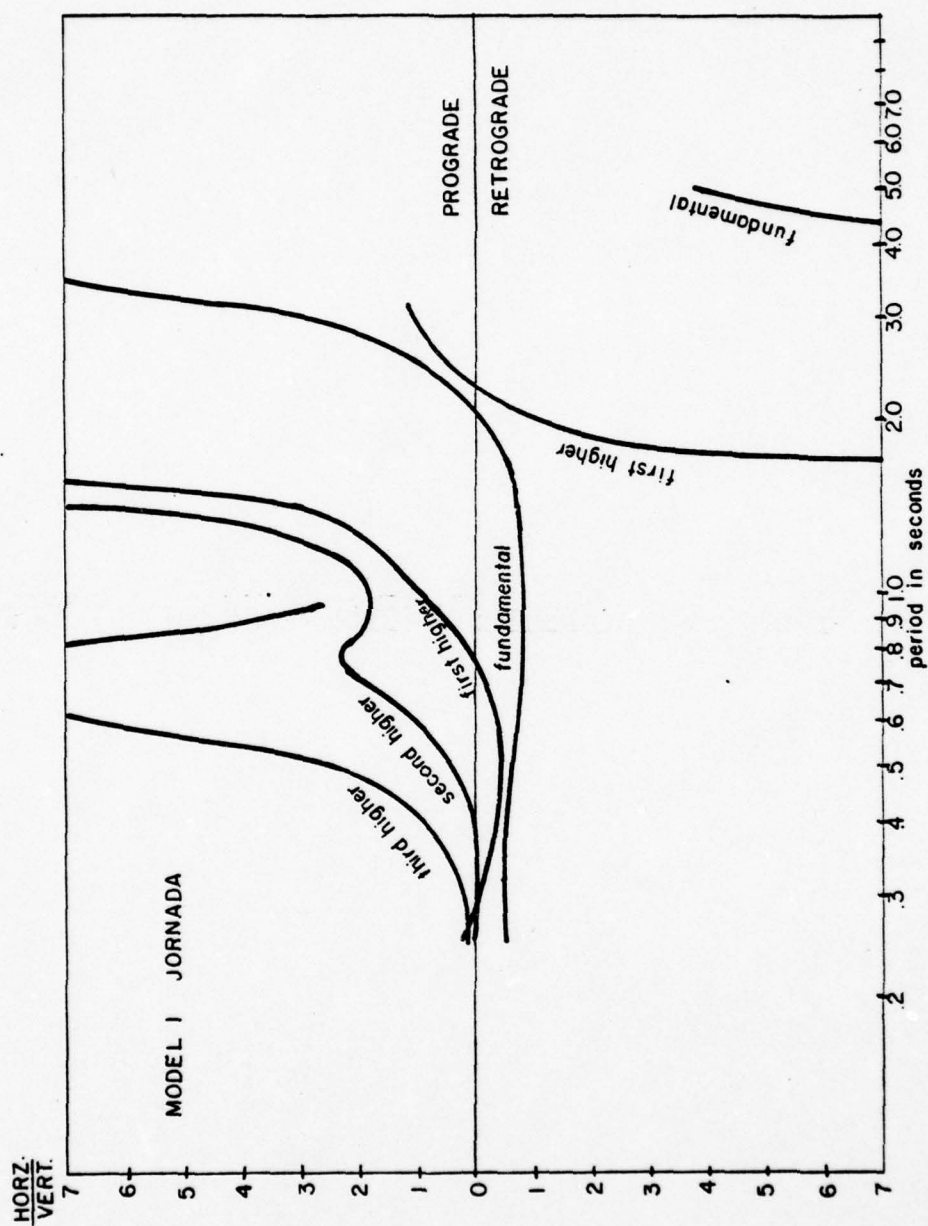


Figure 88. Theoretical ellipticity computed for Jornada model.

the same between the test site and the SMU station. If this is true, then the theoretical model from which the dispersion curves were calculated has a Santa Fe(?) thickness that is somewhat too thin. An increase in the thickness of layer 2 of the model will, however, have little effect on the shape of the fundamental mode in the 0.5 - 1.0 second range. The effect would be primarily one of flattening of the higher mode phase and group velocity curves and more of the higher mode curves would fall within the range of the observed group and phase velocities. It is likely that as long as a certain minimum thickness of the Santa Fe Group(?) is present in the subsurface of the Jornada, the appearance of the lower modes of the Rayleigh wave will be changed little. This could explain why the appearance and group velocities of the two surface wave groups are very similar even though gravity data suggests that the subsurface structure along the paths travelled by the surface waves received at these stations varies considerably.

The transverse record from the ERIM 35000 station (Figure 80) is interesting in that surface waves seen on the transverse component are very similar to the waves on the radial component except that the entire surface wave train on the transverse component appears shifted in time relative to the wave train on the radial component. The wave train

seen on the transverse component may be a reflected or multipathed version of the higher-fundamental mode Rayleigh wave train.

The ERIM 16000 record (Figure 77) shows that the second surface wave group arrives after the air wave, suggesting that the fundamental mode here may be air induced. At the periods observed on the 16000 station record, this would necessitate a considerably increase in thickness of the surface Quaternary(?) low velocity layer because, as is well known, Rayleigh waves may be of air coupled origin only when the phase velocity of the wave is equal to the speed of sound in air. ERIM stations 43000 and 62000 are located on outcrops of Paleozoic rock. The records from these stations (Figures 81 and 82) are quite similar to those recorded at the OR-1, 2, and 3 stations in the Tularosa Basin and discussed previously.

Characteristics of the fundamental and higher mode Rayleigh waves calculated for reasonable theoretical models correlate fairly well with the characteristics of the two wave groups observed at three stations 25000 feet (7.62 kilometers) to the northwest, east, and southwest of the Dice Throw detonation. Waves essentially similar to Leet's recording of the Trinity test were observed at these three stations at roughly the same range as at the Trinity test.

Therefore, the explanation of the two wave groups excited by the Dice Throw explosion likely applies to the waves excited by the Trinity explosion as well. The first prograde wave group is not a "hydrodynamic wave" associated only with explosions as interpreted by Leet, nor is it a prograde portion of the fundamental mode Rayleigh wave as suggested by Mooney and Bolt (1966). It is instead probably a result of the propagation of several of the higher modes of the Rayleigh wave. The second wave group may be partially explained as a retrograde portion of the first higher mode as well as the fundamental mode of the Rayleigh wave.

CONSIDERATIONS FOR PREDICTION OF SURFACE WAVE GROUND
MOTION LEVELS IN ALLUVIAL VALLEYS

The work of Murphy and Hewlett (1975) holds important consequences for any attempt to predict levels of surface wave ground motion in typical intermontane valleys of the western United States. They showed that the high variability in levels of ground motion recorded within a short distance in the Las Vegas Valley from explosions at the Nevada Test Site can be at least partially explained in terms of the variation in thickness of Cenozoic alluvium present beneath the recording sites. Simple surface wave propagation models account for much of the variability in response.

Murphy and Hewlett demonstrate that the ratio of expected surface particle velocity between two recording sites (assuming equal energy flux) is equivalent to the ratio of the surface particle velocity values computed from the Haskell-Thomson (Haskell, 1953) layered model representation of the geology beneath the recording sites. Thus, the expected vertical velocity spectral ratio between recording sites 1 and 2 is simply equal to $|\dot{w}_o|_1 / |\dot{w}_o|_2$ where \dot{w}_{o1} and \dot{w}_{o2} are the vertical velocity components obtained from the Haskell-Thomson matrix formulation of the layered sequence

beneath each station. If there is a change in energy flux between the two stations the expected ratio can be written as $\sqrt{K} \left| \dot{w}_o \right|_1 / \left| \dot{w}_o \right|_2$ where $K = E_1/E_2$, E_1 and E_2 being the values of energy flux beneath station 1 and station 2.

Murphy and Hewlett demonstrated that in many cases PSRV (Pseudo Relative Velocity) spectral ratios between stations in the Las Vegas Valley correlated fairly well with the spectral ratios predicted by the Haskell matrix technique for Love and Rayleigh waves. Surface wave reflections were shown to be responsible for the discrepancy, in some cases, between predicted and observed spectral ratios.

In order to gain an insight as to the nature of the surface particle velocity effect in the Tularosa Basin, theoretical vertical spectral ratios have been computed for the Tularosa Basin models using model 1 as a reference. The predicted ratios are shown in Figures 89, 90, and 91. Without calibrated spectral ratios of the observed motion at different sites, no quantitative correlation is possible; however, the predicted spectral ratio between model 4 and model 1 may explain why the peak vertical velocity of the surface wave group observed at the SMU station on the south side of the Malpais at a range of 50000 feet (15 kilometers) was roughly 1.5 times the peak vertical velocity of the first surface wave group at the SMU station on the west edge of the

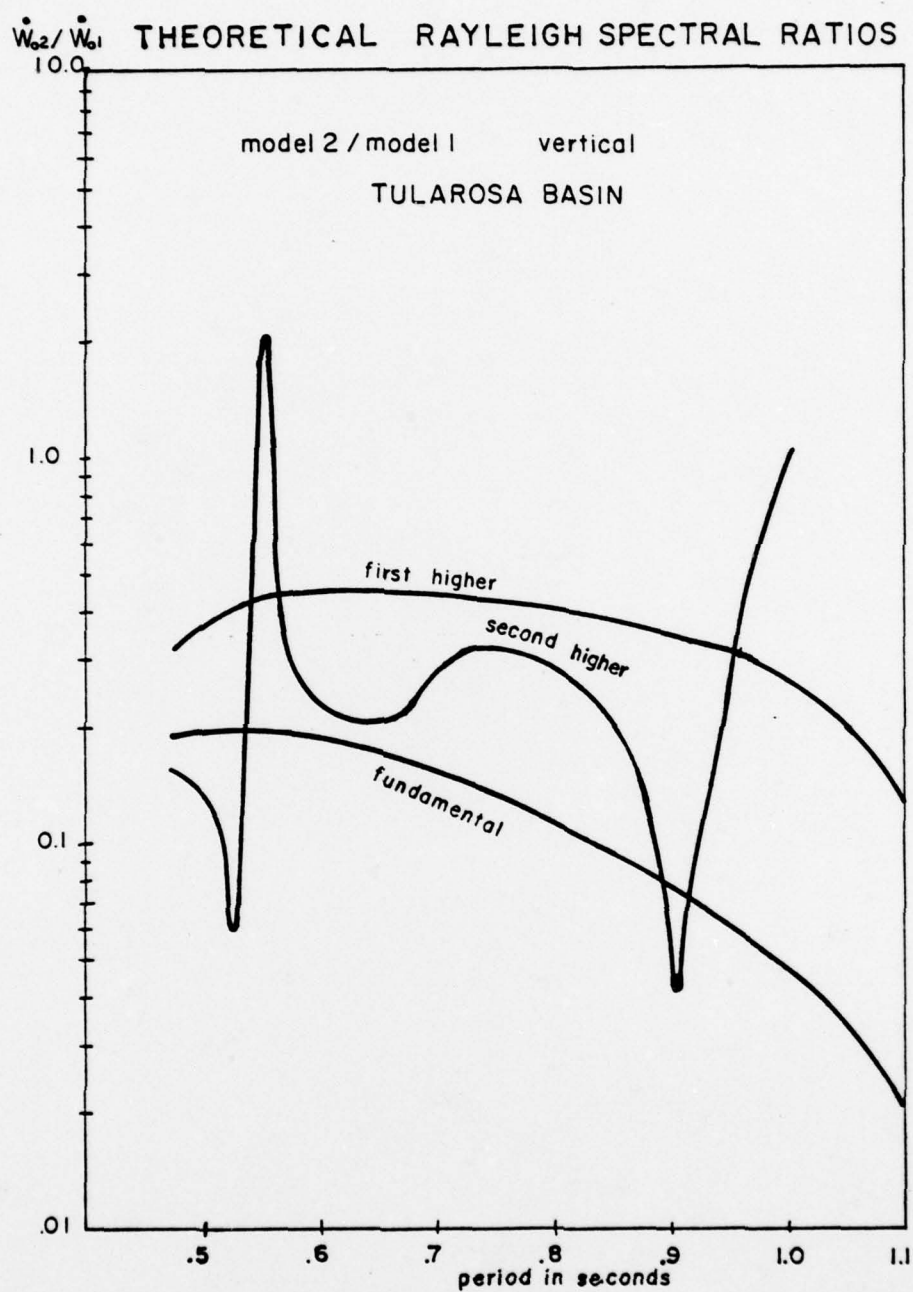


Figure 89. Theoretical spectral ratios. model 2/model 1.

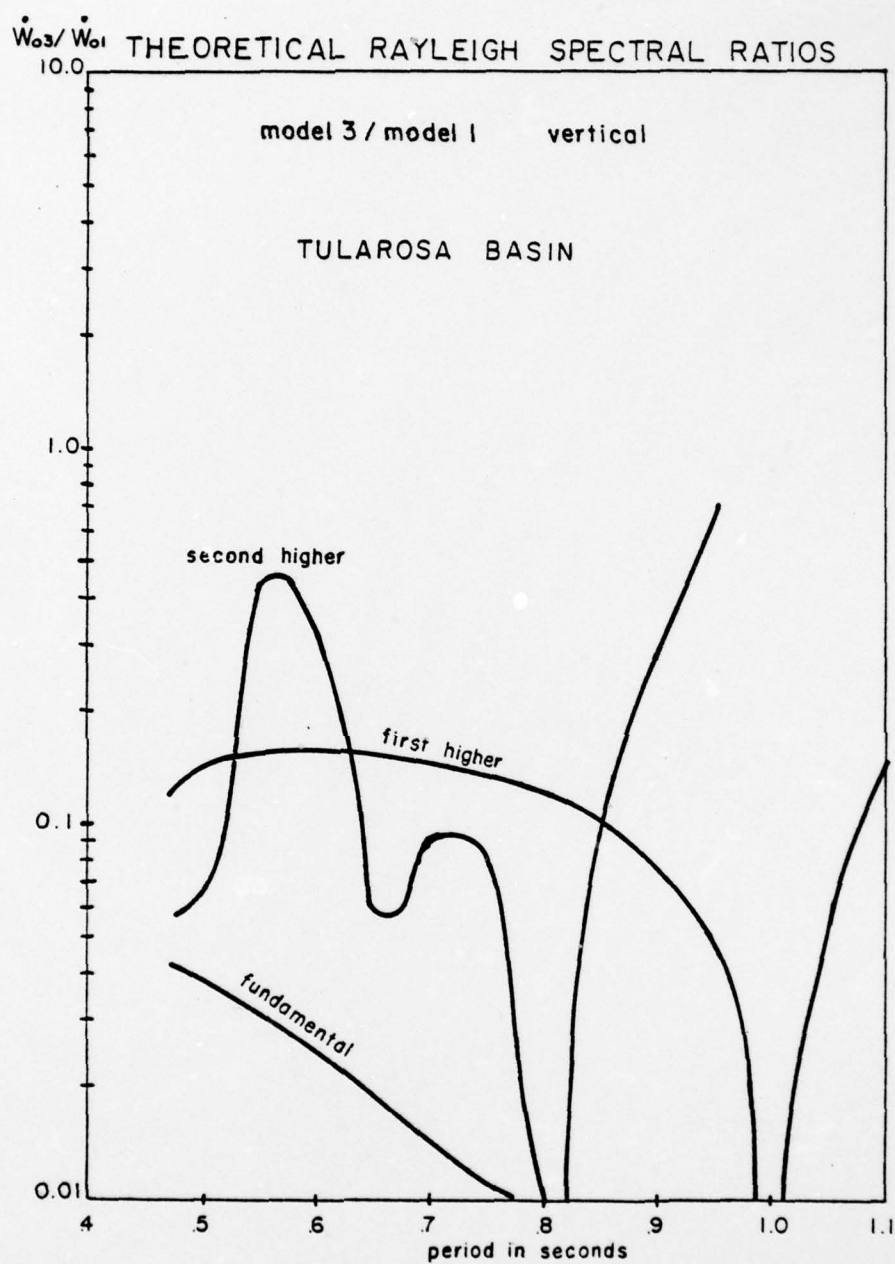


Figure 90. Theoretical spectral ratios. model 3/model 1.

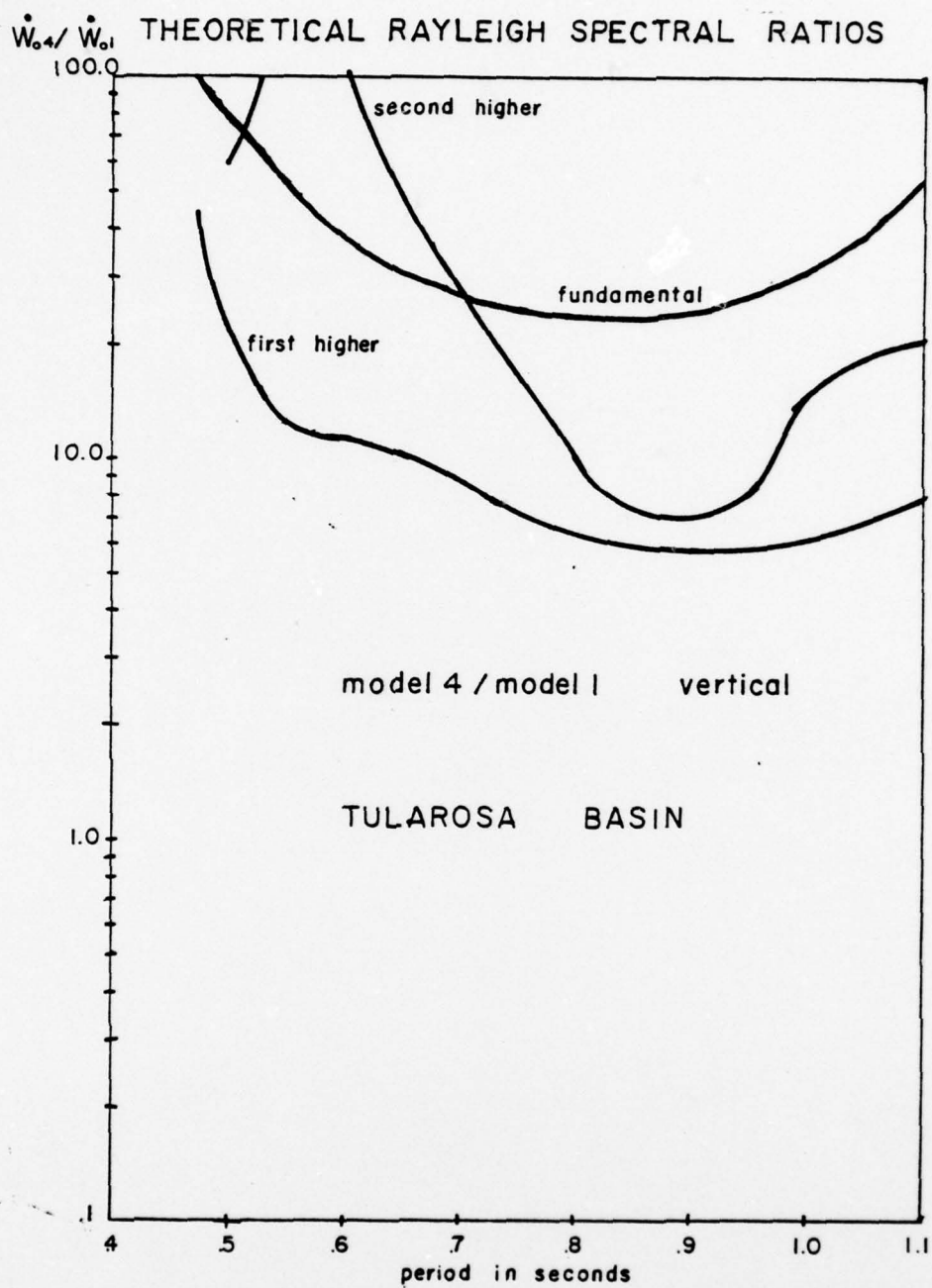


Figure 91. Theoretical spectral ratios. model 4/model 1.

Malpais at a range of only 33000 feet (10 kilometers).

Particle velocity amplitudes experienced at the SMU station in the Jornada del Muerto for the main Dice Throw event were much greater than expected resulting in the severe clipping of the wave forms on some of the SMU seismometers. Preliminary work indicates that this is to be expected from the spectral ratios between the Tularosa and Jornada models. Better evidence for the layer thicknesses and velocities in the Jornada is needed as well as an accurate estimate of the relative amount of surface wave energy generated by the Dice Throw explosion before a solid comparison can be made.

DISCUSSION AND CONCLUSIONS

Refraction Survey

The results of the SH wave refraction profile demonstrate that a cannon type generator is an effective source of shear waves for refraction studies in an alluvial geology. Good shear wave arrivals were received along the entire length of the refraction line 6000 feet (1828 meters) in length.

The presence of three subsurface layers with distinct SH velocities was revealed by the shear wave refraction profile. (Figure 92) Two layers were detected by the P wave refraction profile along the same line.

A low velocity layer or velocity reversal between the second and third layers is indicated by a time gap present between branches of the travel time curves.

Although the presence of the low velocity zone presents an interpretational problem, the depths to layer interfaces obtained from the SH wave data compare favorably with the depths indicated by a shallow P wave reflection profile. Thus it is thought that anisotropy is not severe within the Cenozoic bolson deposits of the Tularosa Basin.

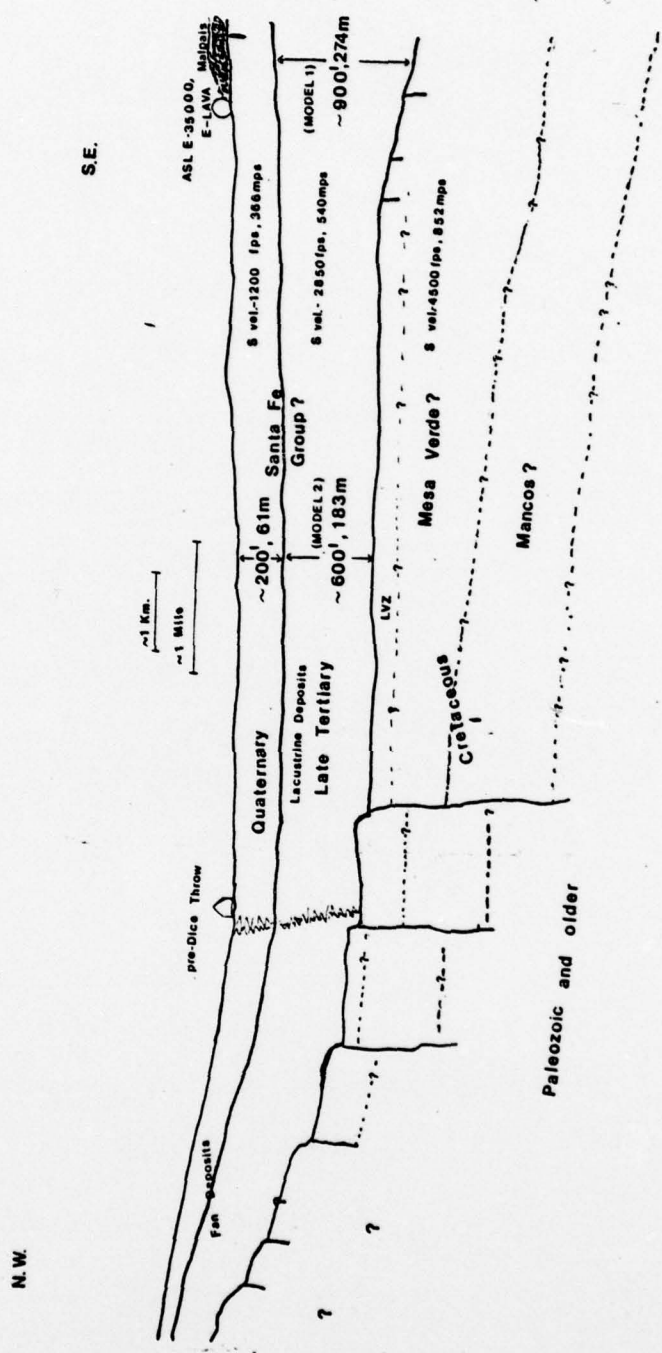


Figure 92. Generalized east-west cross section through the Tularosa Basin.

The upper two layers revealed by the shear wave survey are probably correlative with Quaternary and Late Tertiary members of the Santa Fe Group(?) present in the adjacent Jornada del Muerto Valley and basins of the Rio Grande Valley in New Mexico.

The deepest layer detected by the shear wave survey may be one of several Late Cretaceous-Early Tertiary formations found in and around the area. Because it is the youngest consolidated unit found in wells within the Tularosa Basin, the Mesa Verde formation of Late Cretaceous age is thought to be the most likely candidate.

The Surface Wave Studies

The subsurface shear velocities obtained from the ERIM refraction survey provided a good input for theoretical calculations of Rayleigh wave characteristics in the Tularosa Basin. The SH velocities obtained from the ERIM survey were held constant while the thickness of the layer representing the lower Santa Fe Group(?) was varied. Phase and group velocity curves computed for theoretical layered models were found to correlate well with velocities observed for the surface waves received at stations east of the shotpoint in the Tularosa Basin. Model 2 (Figure 92), with a Santa Fe thickness nearest to that obtained from the reflection and refraction data immediately east of the test site, provides the best

fit to the group velocities observed for the two wave groups received at the ASL stations southeast of the pre-Dice Throw explosions. Variations in the Santa Fe(?) thickness required to fit the observed phase and group velocities at the SMU station for the first 100 ton event (Figure 92) and the puzzling appearance of the surface wave received at the SMU station for the second shot can be explained in terms of the general structural character of the basin as revealed by gravity and magnetic surveys. Figure 92 shows a generalized east-west cross section of the basin which best fits the surface wave data as well as the gravity and magnetic data.

Although no shear velocity data were available for the Jornada del Muerto, reasonable higher-fundamental mode Rayleigh wave models can explain the surface waves excited by the Dice Throw 500 ton event as well as the "Hydrodynamic" wave recorded at the Trinity test in 1945.

The Haskell-Thomson method used in the theoretical calculations assumes a layered model in which the layers are elastic, horizontal, isotropic, and laterally homogenous. These conditions are obviously not strictly applicable in the Tularosa and Jornada del Muerto Basins. The purpose of the study was not, however, precise inversion of surface wave data, but rather identification of the type of surface wave propagation involved. The Haskell-Thomson approximation to the near subsurface structure of the two basins is thus thought to be quite adequate.

Although the general shape of the theoretical phase and group velocity curves fits well with observations, the observed velocities are overall slightly slower than the predicted values. This may indicate that SV layer velocities are a bit slower than the SH velocities obtained from the refraction survey, and used in the theoretical computations. As revealed by the particle motion diagrams the axes of the higher mode ellipses are strongly tilted. Haskell (1953) suggests that this is to be expected for Rayleigh waves propagating on the surface of a medium which is not purely elastic. Although it has not been studied here anelastic attenuation is probably an important factor for short period surface wave propagation in alluvial valleys.

As is well known the Haskell-Thomson method when programmed for a digital computer suffers from a lack of precision for short period surface wave computations. The problem becomes significant when the total thickness of the layers above the halfspace is greater than several wavelengths (Schwab, 1970). The XDS-925 computer utilizes a 24 bit word--halfway between IBM single and double precision. For the models discussed in this paper no problems with precision were evident at periods longer than 0.2 - 0.3 seconds (depending on the model). For shorter periods oscillations occur in the phase velocity curves and the two forms of the period equation presented by Haskell (1953) are

no longer in agreement. For precise inversion of surface wave data either a modified matrix formulation such as that discussed by Schwab (1970) or a layer dropping procedure should probably be employed.

A study of the relative excitation functions of the various surface wave modes for an alluvial geology, following the method described by Harkrider (1964, 1970), might be valuable in predicting total levels of surface wave response for a particular frequency.

An examination of the surface waves recorded on the transverse components combined with computation of Love wave characteristics for theoretical models might provide additional subsurface information.

Perhaps the most valuable addition to the study would be a borehole located east of the pre-Dice Throw test site penetrating at least to the depth of the proposed Mesozoic section with reliable velocity and density logs and good core samples from which positive stratigraphic identification could be made.

REFERENCES CITED

- Bachman, G. O. (1965). Geologic map of the Capital Peak NW Quadrangle, Socorro County, New Mexico, Misc. Geol. Inv., U. S. Geol. Surv., Map I-441.
- Bath, G. D. (1977). Aeromagnetic maps with geologic interpretations for the Tularosa Valley, South-Central New Mexico, U. S. Geol. Surv. Open-File Report 77-258, 16p.
- Bath, G. D., Healey, D. L., and Karably, L. S. (1977). Combined analysis of gravity and magnetic anomalies at Tularosa Valley, New Mexico (abs.), Geol. Soc. America, Abs. with Programs 9, 3-4.
- Burg, K. E. (1952). Exploration problems of the Williston Basin, Geophysics, 17, 465-480.
- Domzalski, W. (1956). Some problems of shallow refraction investigations, Geophysical Prospecting, 4, 140-166.
- Harkrider, D. G. (1964). Surface waves in multilayered elastic media, 1, Rayleigh and Love waves from buried sources in a multilayered elastic halfspace, Bull. Seismol. Soc. Am., 54, 627-679.
- Harkrider, D. G. (1970). Surface waves in multilayered elastic media, 2, Higher mode spectra and spectral ratios from point sources in plane layered Earth models, Bull. Seismol. Soc. Am., 60, 1937-1987.
- Hasegawa, H. S. (1968). Surface waves observed close to large chemical explosions at Suffield, Alberta, Canadian Jour. Earth Sci., 5, 185-198.
- Haskell, N. A. (1953). The dispersion of surface waves on multilayered media, Bull. Seismol. Soc. Amer. 43, 17-34.
- Healey, D. L. (1976a). Interpretation of gravity surveys in intermontane basins of Nevada and New Mexico, Report prepared by U. S. Geol. Surv., Special Projects Branch for the Air Force Weapons Laboratory.

- Healey, D. L. (1976b). Revised complete Bouguer anomaly map of Tularosa and Jornada del Muerto Basins, Map prepared by U. S. Geol. Surv., Special Projects Branch, for the Air Force Weapons Laboratory.
- Herrick, E. H., and L. V. Davis (1965). Availability of ground water in the Tularosa Basin and adjoining areas, New Mexico and Texas, U. S. Geol. Surv. Hydrologic Inv., Atlas HA-191.
- Hoffman, J. P., and S. T. Harding (1977). Strong ground motion in the Tularosa Basin, New Mexico, U. S. Geol. Surv., Open File Report 77-143.
- Jackson, P., R. Turpening, H. Bennett, A. Liskow, R. Shuchman, and L. Wilock (1976). Geophysical techniques applied to oil shale mining problems, Environmental Research Institute of Michigan Technical Report 114500-17-T, U. S. Bureau of Mines Contract No. H 0252062.
- Jolly, R. N. (1956). Investigation of shear waves, *Geophysics* 21, 905-939.
- Knox, W. A. (1967). Multilayer near surface refraction computations in Seismic Refraction Prospecting, Albert W. Musgrave, Editor, Society of Exploration Geophysicists, Tulsa, Oklahoma, 197-216.
- Kottlowski, F. E., R. H. Flower, M. L. Thompson, and R. W. Foster (1956). Stratigraphic studies of the San Andres Mountains, New Mexico, N. Mex. Bur. Mines Miner. Resourc., Memoir 1.
- Kottlowski, F. E. (1975). Stratigraphy of the San Andres Mountains in South-Central New Mexico in New Mexico Geol. Soc. Guidebook, 26th Field Conf., Las Cruces Country, 95-103.
- _____, and J. W. Hawley (1975). First day road log from Las Cruces to Southern San Andres Mountains, and Return in New Mexico Geol. Soc. Guidebook, 26th Field Conf., Las Cruces Country, 1-16.
- Leet, L. D. (1946). Earth motion from the atomic bomb test (New Mexico, July 16, 1945), *Am. Scientist.* 34, 198-211.
- Leet, L. D. (1962). The detection of underground explosions, *Sci. Am.* 206, 55-59.

- Levshin, A. L. (1962). Propagation of surface waves in unconsolidated formations, Bull. Acad. Sci. USSR, Geoph. Ser., 12, 1094-1104
- Mooney, H. M. and B. A. Bolt (1966). Dispersive characteristics of the first three Rayleigh modes for a single surface layer, Bull. Seismol. Soc. Am. 56, 43-67.
- Mota, L. (1954). Determination of dips and depths of geological layers by the seismic refraction method, Geophysics 19, 242-254.
- Murphy, J. R. and R. A. Hewlett (1975). Analysis of seismic response in the city of Las Vegas, Nevada: A preliminary microzonation, Bull. Seismol. Soc. Am. 65, 1575-1597.
- McLean, J. S. (1970). Saline ground-water resources of the Tularosa Basin, New Mexico, U. S. Geol. Surv. OSW Report 561, 128p.
- Press, F and M. Ewing (1948). Low speed layer in water-covered areas, Geophysics 13, 404-420.
- Press, F. and M. B. Dobrin (1956). Seismic wave studies over a high-speed surface layer, Geophysics 21, 285-298.
- Reynolds, C. B. (1976). 1975 Shallow seismic reflection survey, White Sands Missile Range, New Mexico, Final Report prepared for Air Force Weapons Laboratory.
- Sanford, A. R. (1968). Gravity survey in central Socorro County, New Mexico, N. Mex. Bur. Mines Miner. Resourc. Circular 91.
- Schwab, F. (1970). Surface wave dispersion computations: Knopoff's method, Bull. Seismol. Soc. Am. 60, 1491-1520.
- Seager, W. R. (1975). Cenozoic tectonic evolution of the Las Cruces area, New Mexico in New Mexico Geol. Soc. Guidebook, 26th Field Conf., Las Cruces Country, 241-250.